

**The molecular basis of pathogenicity of the glycoprotein of
typical South African canid and mongoose rabies biotypes**

Wonhyo Seo

The molecular basis of pathogenicity of the glycoprotein of typical South African canid and mongoose rabies biotypes

by

Wonhyo Seo

Submitted in partial fulfillment of the requirements

for the degree of

MASTER OF SCIENCE (Veterinary science)

in the

Department of Veterinary Tropical Diseases

Faculty of Veterinary Science, University of Pretoria

Dr Claude Sabeta

Dr Monique Lafon

Dr Christophe Prehaud

Dr Akinbowale Jenkins



UNIVERSITEIT VAN PRETORIA
UNIVERSITY OF PRETORIA
YUNIBESITHI YA PRETORIA
Denkleiers • Leading Minds • Dikgopolo tša Dihlalefi

I declare that the dissertation which I hereby submit for the degree MSc at the University of Pretoria, South Africa is my own work and has not been submitted for a degree at another university.

WONHYO SEO

MARCH 2012

ACKNOWLEDGEMENTS

I would like to thank the following people for the contribution towards the completion of this project:

Special thanks to my supervisor Dr C.T. Sabeta (Agricultural Research Council-Onderstepoort Veterinary Research Institute) and co-supervisor Dr A.O. Jenkins (Department of Veterinary Tropical Diseases, University of Pretoria) for their encouragement and unlimited supports during the course of this study.

Also special thanks to my French supervisors, Dr C. Prehaud and Dr M. Lafon (Unité de Neuroimmunologie Virale, Institut Pasteur), allowed me to perform the second part of this work. The knowledge of reverse genetics techniques employed in this study, financial support from Institut Pasteur during the training, a new insight of molecular biology and endless advice were given.

Many thanks to the Director, Prof T. Musoke and Staff of Agricultural Research Council-Onderstepoort Veterinary Institute for providing opportunities and the best environment for the research to achieve this academic goal.

I appreciate the support of Mr C.E. Ngoepe and Dr W. Shumba (Onderstepoort Veterinary Research Institute) for assistance in animal and laboratory experiments.

Appreciation go to Dr Z. Khan (Unité de Neuroimmunologie Virale, Institut Pasteur) for his assistance, guidance on laboratory experiments and for providing for plasmid for this project.

Students and colleagues at Agricultural Research Council-Onderstepoort Veterinary Institute and the Department of Veterinary Tropical Diseases, the Faculty of Veterinary Science (Onderstepoort, South Africa).

Colleagues at Unité de Neuroimmunologie Virale, Institut Pasteur (Paris, France).

Many thanks go to my family who always gave me support and love through my entire life.

Lastly,

I give special thanks to Ms. YoungShuk Yi who supported and gave me endless courage throughout the project.

Funding for this project was provided by:

The Poliomyelitis Research Foundation (#09/31), The Department of Veterinary Tropical Diseases, Unité de Neuroimmunologie Virale, Institut Pasteur, The University of Pretoria Postgraduate Study Abroad Bursary and The European Virus Archive (04/17/C215).

SUMMARY

The molecular basis of pathogenicity of the glycoprotein of typical South African canid and mongoose rabies biotypes

by

WONHYO SEO

Main supervisor: Dr C. T. Sabeta
OIE Rabies Reference Laboratory, Onderstepoort Veterinary Institute

Co-supervisors: Dr A. O. Jenkins
Department of Veterinary Tropical Diseases, University of Pretoria

Dr M. Lafon
Unité de Neuroimmunologie Virale, Institut Pasteur, France

Dr C. Prehaud
Unité de Neuroimmunologie Virale, Institut Pasteur, France

For the degree of Master of Science (Veterinary Science)

Rabies is an important public and veterinary health threat in South Africa. The genus Lyssavirus is composed of 12 species including classical rabies virus (RABV, genotype 1), Lagos bat virus (LBV, genotype 2), Mokola virus (MOKV, genotype 3), Duvenhage virus (DUVV, genotype 4), European bat lyssavirus type-1 and type-2 [EBLV-1 (genotype 5) and EBLV-2 (genotype 6), respectively] and Australian bat lyssavirus (ABLV, genotype 7). In addition, several lyssaviruses have been also recovered from Chiroptera including Aravan virus (ARAV), Khujand virus (KHUV), Irkut virus (IRKV), West Caucasian bat virus (WCBV) as well as Shimoni bat virus (SHIV). The unusual lyssaviruses (Lagos bat virus, Mokola virus and Duvenhage virus) have been identified exclusively on the African continent. The canid and mongoose rabies biotypes in genotype 1 are commonly diagnosed in the *Canidae* and

Herpestidae species, respectively. Dog rabies is responsible for at least 90% of the human death tolls rather than by mongoose rabies biotype through case surveillance data in South Africa and this has led to the notion that canid rabies biotype is more virulent rather than mongoose rabies biotype. Therefore, this study was proposed to the difference in virulence of two rabies biotypes prevalent in South Africa.

The rabies viral genome encodes five structural proteins, namely the nucleoprotein (N), phosphoprotein (P), matrix protein (M), glycoprotein (G) and RNA-dependent RNA polymerase (L). Amongst the proteins, the G-protein has been found to control entry, egress and pathogenicity of RABV, and is a critical factor for death of infected cells. Several amino acid residues which drive the pathogenicity of the RABV, known as pathogenic determinants, are found on the RABV G-protein. Furthermore, the interactions between PDZ domains and PDZ-binding site (PDZ-BS), located at the carboxyl terminus of the G-protein cytoplasmic domain (Cyto-G) could be pivotal role in the determination of phenotypes depending on cellular partners recruited by the PDZ-BS of its envelope G-protein.

The present study was undertaken to provide an insight into the pathogenicity of the South African RABV biotypes, namely canid and mongoose rabies biotypes. Moreover, mongoose rabies biotype recovered in a domestic dog (referred as *spill over*) was also included in this study. These viruses were selected to represent the two rabies biotypes based on their reactivity patterns to a panel of monoclonal antibodies (mAbs) and phylogenetic analysis using the cytoplasmic domain of the G-protein and the variable G-L intergenic region. In order to elucidate the pathogenicity of the selected RABV isolates, the nucleotide and amino acid homologies of the complete G-protein encoding gene and pathogenic determinants on the G-protein ectodomain were evaluated. Then, the chimeric G-protein constructs were generated by grafting the carboxyl terminal of the cytoplasmic domain in a virulent RABV CVS backbone (GenBank Acc. No: AF406694). These chimeric constructs were expressed in a recombinant lentivirus system and *in vitro* neuronal survival or death phenotypes were evaluated to determine the pathogenicity of South African RABV constructs.

The genetic analyses exhibited that the three RABV isolates in this study possessed identical amino acid residues at positions 194 (asparagine), 318 (phenylalanine), 352 (histidine) and 333 (arginine), which are highly involved in RABV pathogenicity. Therefore, the search for other pathogenicity determinants was required. Through phenotypic observations of neurite outgrowth and apoptosis assays in a recombinant lentivirus system, the G-canid chimeric construct demonstrated the highest neurite outgrowth followed by G-spill over and G-mongoose constructs, despite no significant G-protein expression level differences being observed in immunocytochemistry assays. On the other hand, the G-canid construct exhibited the lowest apoptotic/cell death level followed by G-spill over and G-mongoose. Through the phenotypic observations, the change of histidine (H) to tyrosine (Y) at position -8 from the 5' end of the cytoplasmic domain was demonstrated that histidine at -8 may play an important role in apoptotic phenotype in the ETRL-COOH chimeric construct.

Overall, these findings suggest that amino acids outside of the canonical PDZ-BS (4 amino acids) can also influence the virulence/attenuation phenotype. This may possibly explain why some rabies strains such as PDZ-BS ETRL can be considered as virulent, since amino acids out of last 4 amino acids of carboxyl terminus may further modulate the PDZ BS/PDZ interaction and phenotypes.

LIST OF TABLES

Table number		Page
2.1	Epidemiological information of RABV isolates from various localities of South Africa used in this study.	25
2.2	Panel of 15 anti-nucleocapsid monoclonal antibodies (N-mAbs) for antigenic typing of southern African lyssaviruses and reactivity pattern of South African rabies isolates used in this study.	27
2.3	Primers used in cDNA synthesis, PCR and sequences.	28
2.4	Epidemiological information of previously characterized mongoose and canid rabies biotypes from different localities in South Africa and Zimbabwe.	31
2.5	Percentage nucleotide and amino acid identity of the complete G-protein gene of South African rabies isolates used in this study.	35
2.6	Comparisons of amino acid residues of the pathogenic determinants in the G-protein of the South African RABV and fixed laboratory strains (CVS and ERA).	36
3.1	Last 12 amino acid residues and nucleotide sequences of the cytoplasmic domain of laboratory RABV strains (CVS-NIV and ERA-NIV) and South African RABV isolates (canid, mongoose and spill over).	41
3.2	Sequences of two complementary oligonucleotide primers containing the desired mutation for mutagenesis. The underlined and bold sequences (letters) represent the target region to be mutated.	41
3.3	Gene-specific primers for lentivirus vectors transcription analysis.	45
3.4	Antibodies specific for peptides encoded by the cytoplasmic domain of G-protein used in Western blotting.	46
3.5	Pairwise comparisons and statistical analysis of neurite outgrowth of G-constructs.	54
3.6	Significant differences by GraphPad™ Prism 5 and the percentage value of apoptosis and cell death by Annexin V and Propidium Iodide (PI) analyses to indicate the level of cell surface changes during the apoptotic process. Statistical significance (P value < 0.05) is denoted as (+) and 'not statistical significance' is shown as (-) (P value > 0.05).	56

LIST OF FIGURES

Figure number		Page
1.1	A structure of the RABV particle illustrating the arrangement of the structural proteins and the nucleocapsid with the RNA genome.	5
1.2	A schematic illustration of rabies virus genome. Nucleoprotein (N), phosphoprotein (P), matrix protein (M), glycoprotein (G) and RNA-dependent RNA polymerase protein (L) genes are separated by non-coding intergenic sequences including the pseudogene (ψ). Short (58 and 70 nucleotides) non-coding sequences at the 3' and 5' ends of the genome, called leader (<i>Le</i>) and trailer (<i>Tr</i>) sequences, respectively.	6
1.3	A schematic overview of RABV life cycle in host cells.	15
1.4	Structural diagrams of PDZ3 domain of PSD-95. (A) Ribbon representation of the PDZ3 domain; 6 β -sheets and 2 α -helices consists of the modular structure characteristic for PDZ domains. The carboxylate-binding loop involved in ligand binding is indicated. (B) Chemical interactions involved in peptide binding. Hydrogen bonds are depicted (dashed white line) between residues of the PDZ domain (blue) and the peptide ligand (orange).	19
2.1	Two well-characterized RABV biotypes in South Africa, the canid and mongoose, circulate independently. The canid biotype infects carnivores of the <i>Canidae</i> family such as domestic dogs (<i>Canis familiaris</i>), jackal species (<i>Canis mesomelas</i> and <i>Canis adustus</i>) and bat-eared foxes (<i>Otocyon megalotis</i>), whereas the yellow mongoose (<i>Cynictis penicillata</i>) is the principal vector species of the mongoose rabies biotype. Occasionally, host switch events have happened between two families and are referred as spill over.	24
2.2	Representative map indicating geographical origins where the RABV isolates were recovered.	26
2.3	Mice mortality pattern of canid, mongoose and spill over isolates of 3-day-old outbred suckling BALB/c mice (n=8 per group) injected intracerebrally with 10% brain suspensions. Mortality was recorded daily basis and the Kaplan-Meier survival curves were established.	32
2.4	One per cent agarose gel stained with ethidium bromide and visualized by UV light. Lanes 1, 3 and 5 are hemi-nested PCR products (~ 1000 bp), whereas lane 2, 4 and 6 are the PCR products of the complete G genes (lane 7 and 8; positive controls and lane 9; negative control). Canid rabies biotype (lab reference number 77/10) and nuclease free water were used as positive and negative controls, respectively. A 100 bp DNA ladder was used for molecular weight marker (M) in lane 1.	33
2.5	A neighbour-joining tree constructed from an alignment of 592 bp nucleotide sequences encompassing the cytoplasmic domain of the G-protein gene and the G-L intergenic region of canid and mongoose rabies biotypes from Zimbabwe and South Africa. Bootstrapping of 1,000 trials was applied and only node confidence limits of $\geq 70\%$ were considered significant. The scale	34

bar indicates nucleotide substitutions per site. **Key**–LP-Limpopo, NW-Northwest, MP-Mpumalanga.

- 3.1 Schematic diagrams of the complete G-protein and RABV G gene construct. (A) Complete G-protein (524 amino acids are translated including signal peptide domain) of RABV CVS strain which contains the signal peptide domain, ectodomain, transmembrane domain and cytoplasmic domain. (B) The structure of G survival Δ EC, derived from complete G-protein, 437 amino acid residues of ectodomain were deleted and the cytoplasmic tail of the G-protein is the neurovirulent RABV (CVS strain) genetic back ground. (C) pLenti expression construct containing G-survival Δ EC, based on pLenti6.3/V5-TOPO vector (Invitrogen, USA). 40
- 3.2 A representative of a typical neuron indicating the basic part; including soma, dendrites and axon. Neurite refers to any filamentous or pointed outgrowth, which is either an axon or a dendrite, from the cell body of neurons. Neurite outgrowth is a fundamental process in the differentiation of neurons. 47
- 3.3 Variations in the relative abundance of mRNA transcription level in a recombinant lentivirus system by relative RT quantitative PCR at 48 hours post infection. 49
- 3.4 Concentrations of total protein determined using Micro BCA Protein assay Kit, which is a detergent-compatible bicinchoninic acid formulation for the colorimetric detection and evaluation of total protein. Representative results of protein contents of cellular lysates. N.I., not infected. 50
- 3.5 Immunoblotting analysis of G-constructs expressing recombinant lentiviruses. Proteins were separated electrophoretically on a 4~20% gel SDS-polyacrylamide gel, transferred to a PVDF membrane and detected with a specific anti-RABV G cytoplasmic domain antibody (V9). (A) Peptides which antibodies were recognized to express proteins. Polyclonal antibody (V9) recognizes NH₂-TGREVSVTPQSGKI-COOH and monoclonal antibodies (V17 and V18) recognize NH₂-GKIISWESHKS-COOH. No amino acid residue mutations in G-ERA-NIV and G-CVS-NIV on the peptides against monoclonal antibodies (V17 or V18). (B) Detection by Western blotting of cytoplasmic domain, RABV G-protein with polyclonal antibody (V9). The signal obtained for G-CVS-NIV was at saturated level. N.I., not infected. 51
- 3.6 Expression of G-protein distribution of a recombinant lentivirus expressing each G-construct was detected after the infection of recombinant viruses. The cellular RABV G distribution (green) was detected by UV microscopy. The nucleus was shown in blue by Hoescht 33342 staining. N.I., not infected. Scale bars, 20 μ m. 52
- 3.7 Neurite outgrowth of RABV infected cells. Neuroscreen-1 cells (72 hour post infection). (A) Variable different patterns of neurite outgrowth depending on the expression of the different G constructs. (B) Sustained neurite outgrowth was measured for average length of neurite with ImageJ 1.44p, Neuron J plug in. (C) The mean value of neurite length. The data shown are representative of duplicate experiments. N.I., not infected. 54

- 3.8 Analysis of the level of apoptosis using Annexin V-FITC (A) and membrane permeability using propidium Iodide (B) were analyzed at 96 hours post infection and the relative percentage values of apoptosis/cell death levels N.I., not infected. ns, not significant. 55
- 3.9 Summary of the phenotypic observation through the level of apoptosis and neurite outgrowth and hypothetical virulence of recombinant viruses. The mutations of amino acid residues are indicated as underlined bold letters. 57

LIST OF ABBREVIATIONS

ABLV	Australian bat lyssavirus
ARAV	Aravan virus
BBLV	Bokeloh bat lyssavirus
B.C.	Before Christ
BCA	Bicinchoninic acid
BHK	Baby Hamster Kidney cell
bp	Base pair
BSA	Bovine serum albumin
cDNA	Complementary DNA
Clustal	Cluster analysis
CNS	Central nervous system
COOH	Carboxyl
CSF	Cerebrospinal fluid
Ct	Threshold cycle
CVS	Challenge virus standard
Cyto-G	The C-terminal of the cytoplasmic domain
°C	degree Celsius
ΔEC	delta EC: Plasmids with the ectodomain deleted
DMEM	Dulbecco's Modified Eagle's Medium
DNA	Deoxyribonucleic acid
dNTP	Deoxynucleotide triphosphate
DPI	Day post infection
DTT	Dithiothreitol
DUVV	Duvenhage virus
EBLV	European bat lyssavirus
EM	Electron microscopy
ERA	Evelyn-Rokitnicki-Abelseth strain
<i>et al.</i>	and others
FACS	Fluorescence activated cell sorting
FAT	Fluorescent antibody test
FCS	Fetal calf serum
FITC	Fluorescein isothiocyanate
GFP	Green fluorescent protein
G-protein	Glycoprotein
ICTV	International Committee on Taxonomy Viruses
i.e.	that is

IKOV	Ikoma lyssavirus
IRF	Interferon regulatory factor
IRKV	Irkut virus
IU	International Unit
kb	Kilobase
kDa	Kilodalton
KHUV	Khujand virus
LBV	Lagos bat virus
L-protein	RNA-dependent RNA polymerase or large protein
mAbs	Monoclonal antibodies
MAST2	Microtubule Associated Serine-Threonine kinases 2
MIT	Mouse inoculation test
MNA	Mouse neuroblastoma cell
mRNA	Messenger RNA
ml	Milliliter
mM	Millimolar
µg	Microgram
µl	Microliter
MOKV	Mokola virus
M-protein	Matrix protein
MW	Molecular Weight
nAChR	Nicotinic acetylcholine receptor
NC	Nucleocapsid
NCAM	Neuronal cell adhesion molecule
ng	Nanogram
NGF	Neuronal growth factor
NIV	Neuroimmunologie Virale
nm	Nanometer
NJ	Neighbour-joining
N-protein	Nucleoprotein
NS	Nervous system
OIE	Office International des Epizooties
OVI	Onderstepoort Veterinary Institute
PBS	Phosphate buffered saline
PCR	Polymerase chain reaction
PDZ	derives from the first three proteins: <u>P</u> SD-95, <u>D</u> LG and <u>Z</u> O-1
PDZ-BS	PDZ - binding site
PEP	Post-exposure prophylaxis

PML	Promyelocytic leukemia
pmol	Picomole
P-protein	Phosphoprotein
PV	Pasteur virus
p75NTR	p75 neurotrophin receptor
RABV	Rabies virus
RNA	Ribonucleic acid
RNase	Ribonuclease
RNP	Ribonucleoprotein
RTCIT	Rabies tissue culture infection test
SHIV	Shimoni bat virus
S.O.C	Super optimal broth
STAT	Signal Transducer and Activator of Transcription
TLR	Toll-like receptor
TRAIL	Tumor necrosis factor-related apoptosis-inducing ligand
T.Y.M	Trypticase-yeast extract-maltose
U	Units of enzyme activity
UV	Ultraviolet
VSV	Vesicular stomatitis virus
WCBV	West Caucasian bat virus
WHO	World Health Organization

Abbreviations for the amino acids are as follows :

Amino acid	Single-letter data code	Amino acid	Single-letter data code
Isoleucine (Ile)	I	Serine (Ser)	S
Leucine (Leu)	L	Tyrosine (Tyr)	Y
Valine (Val)	V	Tryptophan (Trp)	W
Phenylalanine (Phe)	F	Glutamine (Gln)	Q
Methionine (Met)	M	Asparagine (Asn)	N
Cysteine (Cys)	C	Histidine (His)	H
Alanine (Ala)	A	Glutamic acid (Glu)	E
Glycine (Gly)	G	Aspartic acid (Asp)	D
Proline (Pro)	P	Lysine (Lys)	K
Threonine (Thr)	T	Arginine (Arg)	R

TABLE OF CONTENTS

ACKNOWLEDGEMENTS

SUMMARY

LIST OF TABLES

LIST OF FIGURES

LIST OF ABBREVIATIONS

	PAGE
Chapter 1. General introduction and objectives of the study	
1.1 The history of rabies	2
1.2 Classification of lyssaviruses	2
1.3 Rabies virus structure	4
1.4 Functions of rabies virus proteins	6
1.4.1 Nucleocapsid	6
1.4.1.1 RNA-dependent RNA polymerase/ large protein	6
1.4.1.2 Nucleoprotein	7
1.4.1.3 Phosphoprotein	8
1.4.2 Envelope proteins	9
1.4.2.1 Matrix protein	9
1.4.2.2 Glycoprotein	10
1.4.3 Non-coding regions of rabies virus	11
1.5 Host species, the route of infection and life cycle	11
1.5.1 Host species of rabies virus and the route of infection	11
1.5.2 The life cycle of rabies virus	12
1.5.2.1 The first phase (attachment and entry)	12
1.5.2.2 The second phase (virus replication)	13
1.5.2.3 The third phase (virus assembly and budding)	14
1.6 Infection of the nervous system by rabies virus	15
1.6.1 Entry into the central nervous system	15
1.6.2 Spread from the central nervous system	16

1.7	Diagnosis of rabies	16
1.8	Role of glycoprotein in pathogenicity and neuroinvasiveness	17
1.8.1	Pathogenic determinants in ectodomain	17
1.8.2	Protein interaction domains in cytoplasmic domain	18
1.9	Objectives of the study	20

Chapter 2. Genetic characterization and identification of pathogenic determinants of genotype 1South African rabies biotypes

2.1	Literature review	23
2.1.1	Host species of rabies in South Africa	23
2.1.2	Objective	25
2.2	Materials and methods	25
2.2.1	Selection of rabies virus isolates and diagnostic tests	25
2.2.1.1	Selection of rabies viruses	25
2.2.1.2	Fluorescent antibody test	26
2.2.1.3	Monoclonal antibody typing	26
2.2.1.4	Mouse inoculation test	27
2.2.2	Recovery of viral RNA and sequences	28
2.2.2.1	Total viral RNA extractions	28
2.2.2.2	Primer sequences	28
2.2.2.3	Complementary DNA synthesis	29
2.2.2.4	Polymerase chain reaction	29
2.2.2.5	DNA sequencing and analysis	29
2.2.2.6	Phylogenetic analysis	30
2.3	Results	32
2.3.1	Viral isolation and monoclonal antibody typing	32
2.3.2	PCR and phylogenetic analysis	33
2.3.3	Comparison of pathogenic domains on glycoprotein	35
2.4	Discussion	36

Chapter 3. *In vitro* neurosurvival/apoptotic properties of COOH terminus of G-protein of South African RABV isolates as assessed in a recombinant lentiviral system

3.1	Objective	39
3.2	Materials and methods	39
3.2.1	Design of plasmid and oligonucleotides	39
3.2.1.1	Plasmid	39
3.2.1.2	Oligonucleotides for mutagenesis	40
3.2.2	Recovery of recombinant viruses and viral characterization	42
3.2.2.1	Mutagenesis	42
3.2.2.2	Re-transformation	43
3.2.2.3	Lentiviral vectors and expression of the chimeric glycoprotein	43
3.2.3	Characterization of the expressed chimeric genes	44
3.2.3.1	Quantitative real-time polymerase chain reaction	44
3.2.3.2	Protein concentration and Western blotting	45
3.2.3.3	Immunocytochemistry assay	46
3.2.4	Neuroprotection assay	47
3.2.4.1	Neurite outgrowth assay	47
3.2.4.2	Measurement of apoptosis	48
3.3	Results	49
	Part 1 : Chracterization of recombinant rabies viruses	49
3.3.1	Quantitative monitoring of gene expression level	49
3.3.2	Concentration of total protein	50
3.3.3	Western blotting for protein expression	50
3.3.4	Immunocytochemistry	52
	Part 2 : Neuroprotection of G constructs delivered by recombinant lentivirus	53
3.3.5	Neurite outgrowth assay	53
3.3.6	Apoptosis assay	55
	Part 3 : summary of phenotypes observed	56
3.4	Discussion	57

Chapter 4. Concluding remarks and future directions	60
--	-----------

Chapter 5. References	63
Appendices	
Appendix 1	86
Appendix 2	90
Appendix 3	92
Appendix 4	93
Communications	94

CHAPTER 1

General introduction and objectives of the study

1.1 The history of rabies

Rabies is one of the oldest zoonotic diseases known to medical history. This disease is very closely associated with animal bites and still continues to be a public and veterinary health threat to date (Wilkinson, 1988). It was first described in the 23rd century B.C. from the Eshnunna Laws code (Babylon civilization). In this apt description of the disease, authorities would ask the owner of a mad dog to pay two thirds of a mine of silver, if his dog caused death of a man through bite (Théodorides, 1986). Aristotle, in the 4th century B.C, described rabies as a disease that drives animals mad and that animals will contract disease from such a mad dog. Man was, however, not considered to be affected by the disease. One widespread belief was that rabies was caused by a small worm, called *lytta* by the Greeks and was thought to be found at the base of the dog's tongue. A contemporary poet of Ovid (1st century B.C), Grattius Faliscus knew the mythical origin of sublingual "lyssa" of rabid dogs (from Greek word *lyssa*, meaning "rage") and also believed that extracting the worms completely cured the dogs of the disease (Wilkinson, 2002). Georg Gottfried Zinke (1804) demonstrated that rabies could be transmitted by saliva, however, there was no accurate diagnosis of the infectious agent in both men and animals at that time. The isolation of the infectious agent, rabies control (based on quarantine measures, muzzling orders or euthanasia) and human treatment were only possible in the 19th century (Baer, 2007). In 1885, the first human rabies vaccine was developed by Louis Pasteur and his co-workers, and used successfully to treat a 9-year-old boy, Joseph Meister, who had sustained severe wounds after being bitten by a rabid dog in France. The crude nervous tissue-derived preparation was used thereafter throughout the world to manage rabies infections. Since the late 1880s, the administration of rabies vaccines and post-exposure prophylaxis (PEP) have been developed the management of dog-bite cases through safe and efficacious biologics against the viral infection (McGettigan, 2010). Today, rabies vaccines are virtually 100% efficacious when used according to the recommendations of the World Health Organization (WHO) (Briggs, 2007).

1.2 Classification of lyssaviruses

Rabies virus (RABV) is the prototype species of the genus *Lyssavirus* in the family *Rhabdoviridae* (a word derived from the Greek word *rhabdos*, meaning "rod"). The family

Rhabdoviridae has been classified together with *Paramyxoviridae*, *Filoviridae* and *Bornaviridae* and they constitute the “super family” taxon, order *Mononegavirales*. All members of this order contain non-segmented, negative-sense and single-strand RNA genomes of approximately 12 kb in length (Mayo and Pringle, 1998). The morphology, chemical structure and life cycles of these members are closely related to vesicular stomatitis virus (VSV), the prototype member of the genus *Vesiculovirus*, in the same family (Schnell *et al.*, 2010; Tordo *et al.*, 2005). Classical RABV and rabies-related lyssaviruses belong to one of 12 lyssavirus species as recommended by the International Committee on Taxonomy Viruses in 2011 (<http://www.ictvonline.org>) and these members share the unique capability with RABV to produce a rabies-like encephalomyelitis. Rabies virus is a prototype member of genotype 1 virus (formerly referred to as serotype 1) and occurs globally. Other members of the lyssavirus genus include Lagos bat virus (LBV, genotype 2), Mokola virus (MOKV, genotype 3), Duvenhage virus (DUVV, genotype 4), European bat lyssavirus type-1 and type-2 [EBLV-1 (genotype 5) and EBLV-2 (genotype 6)] and Australian bat lyssavirus (ABLV, genotype 7). Several lyssaviruses also have been recovered from Chiroptera including Aravan virus (ARAV) from the mouse-eared bat (*Myotis blythii*) in southern Kyrgyzstan in 1991 (Kuzmin *et al.*, 1992), Khujand virus (KHUV) from a whiskered bat (*Myotis mystacinus*) in northern Tajikistan in 2001 (Kuzmin *et al.*, 2003), Irkut virus (IRKV) from the greater tube-nosed bat (*Murina leucogaster*) in eastern Siberia as well as West Caucasian bat virus (WCBV) from a common bent-winged bat (*Miniopterus schreibersii*) in Krasnodar, Russia (Botvinkin *et al.*, 2003). More recently, Shimoni bat virus (SHIV), recovered from a brain of a dead Commerson’s leaf-nosed bat (*Hipposideros commersoni*) in the coastal region of Kenya (Kuzmin *et al.*, 2010), has been classified as a new independent lyssavirus species by the ICTV. In addition, there are two proposed new species into lyssavirus genus, namely Ikoma lyssavirus (IKOV) (Marston *et al.*, 2012) and Bokeloh bat lyssavirus (BBLV) (Freuling *et al.*, 2011).

This virus (RABV) circulates and is maintained by carnivoran and chiropteran species. All lyssaviruses, with the exception of Mokola virus (MOKV), have been isolated from bats (Badrane and Tordo, 2001; Nel and Rupprecht, 2007). In addition, bat lyssaviruses still remain important in order to understand both virus and chiropteran host ecology and to determine the potential for spill over transmission into both humans and non-flying mammal populations (Banyard *et al.*, 2011).

Lyssaviruses have been divided into two distinct phylogroups immunopathologically and phylogenetically (Badrane *et al.*, 2001). In this classification, genotypes 1, 4, 5, 6 and 7 belong to phylogroup I. The genotype 3 and 4 (LBV and MOKV) are distributed exclusively on the African continent and are members of phylogroup II (Badrane *et al.*, 2001). The members of phylogroup I are pathogenic to mice when introduced via both intramuscular and intracerebral routes (Badrane *et al.*, 2001). In contrast, the members of phylogroup II appear to be pathogenic to mice only via the intracerebral route, although high doses (1×10^6 LD₅₀) via the intramuscular route can also cause death in mice (Markotter, 2007). According to the criteria proposed for lyssavirus phylogroup classification, West Caucasian bat virus (WCBV) could be considered as a representative of an independent phylogroup III as it is the most divergent of the lyssaviruses, with only limited relatedness to LBV and MOKV (Kuzmin *et al.*, 2003). Commercial vaccinal strains belong to RABV and the corresponding rabies vaccines are effective against all the members in phylogroup I, however, they offer only partial protection to members in phylogroup II (Badrane *et al.*, 2001; Nel, 2005).

1.3 Rabies virus structure

All rhabdoviruses are bullet-shaped with one flattened end (planar) and the other rounded (hemispherical). The viral particles are composed of protein (67-74%), lipid (20-26%), RNA (2-3%) and carbohydrate (3%) as integral components (per cent of total mass) of their structure (Wunner, 1991). The physical appearance was first described through electron microscopy (EM) (Davies *et al.*, 1963; Matsumoto, 1962, 1963). The average length of a standard-size, infectious virion is 180 nm (130-250 nm) and the average diameter is 75 nm (60-110 nm) (Davies *et al.*, 1963; Hummeler *et al.*, 1967; Sokol, 1975). The virion consists of two structural units: a central and dense cylinder formed by the helical nucleocapsid (NC) or ribonucleoprotein (RNP) core, and a thin surrounding envelope (8 nm wide) covered with spike-like projections, which are 10 nm in length and 5 nm apart. The five structural proteins of the virus particle (virion) include the nucleoprotein (N), the phosphoprotein (P), the matrix protein (M), the glycoprotein (G) and the RNA-dependent RNA polymerase (L) (Figure 1.1) (Schnell *et al.*, 1994; Tordo, 1996; Wunner *et al.*, 1988).

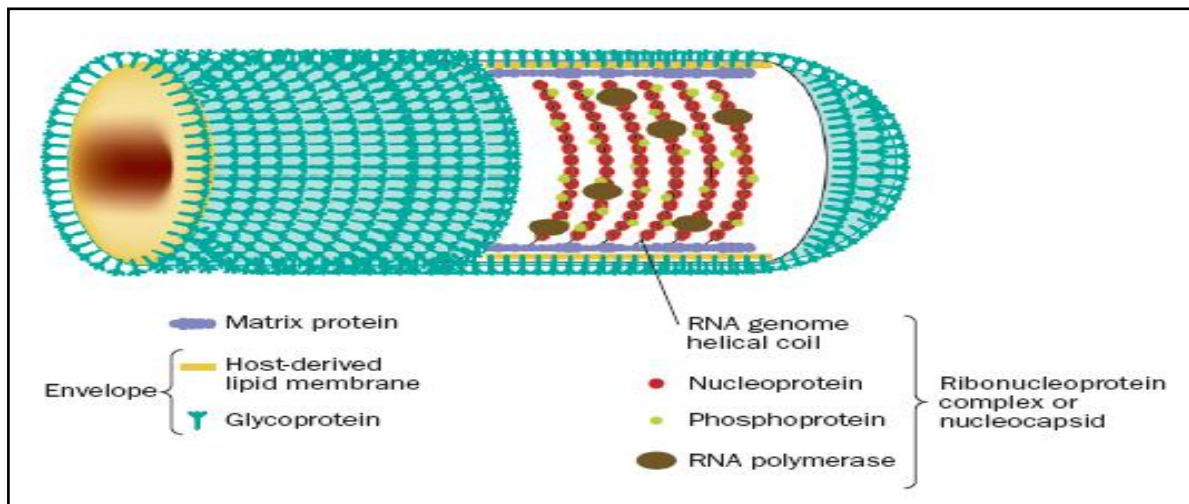


Figure 1.1 A structure of the RABV particle illustrating the arrangement of the structural proteins and the nucleocapsid with the RNA genome (Warrell and Warrell, 2004).

The viral RNA genome plus N-, P- and L-proteins form the backbone of the tightly coiled helical NC, which extends along the longitudinal axis of the bullet-shaped virus particle. The NC is associated with a significant amount of P-protein and some of which carry copies of the L-protein (Albertini *et al.*, 2011). The NC covered with M-protein is wrapped by a lipid bilayer containing G-protein derived from the host cell plasma membrane during the budding process (Albertini *et al.*, 2011). The repartition of G- and M-proteins in the envelope of the virus is not homogeneous with the planar end of the particle and this part is solely comprised of the lipid bilayer (Guichard *et al.*, 2011).

The membrane-associated proteins, M-protein and G-protein, are associated with the lipid-bilayer envelope that surrounds the helical NC core. The rabies virus M-protein is involved in virus budding, virion morphogenesis, modulation of genome replication and transcription (Finke and Conzelmann, 2003; Finke *et al.*, 2003), whereas the G-protein, which forms spikes, plays a critical role in attachment to host cells and determining the neuroinvasive pathway of the virus (Albertini *et al.*, 2011; Kucera *et al.*, 1985; Ito *et al.*, 2001; Yan *et al.*, 2002).

The lyssavirus genome is a single-stranded RNA molecule with negative sense polarity and cannot be translated directly. It implies that the negative-sense genome RNA needs to transcribe the genome RNA to produce complementary (positive-strand) monocistronic mRNAs. The non-coding leader (*Le*) sequence at the 3' end (first 58 nucleotides) of the 11,932-nucleotide genome

RNA of RABV (Pasteur virus, PV strain) is multifunctional in RABV replication, as it is in VSV (Conzelmann and Schnell, 1994; Whelan and Wertz, 1999). This particular signal initiates genome transcription and replication. Immediately downstream of the *Le*, in sequential order, are the five structural genes (N, P, M, G and L) followed by a non-coding trailer (*Tr*) sequence (last 70 nucleotides) at the 5' end. The genes are separated by short sequences including the pseudogene (ψ), which represent the intergenic regions of the genome (Figure 1.2).

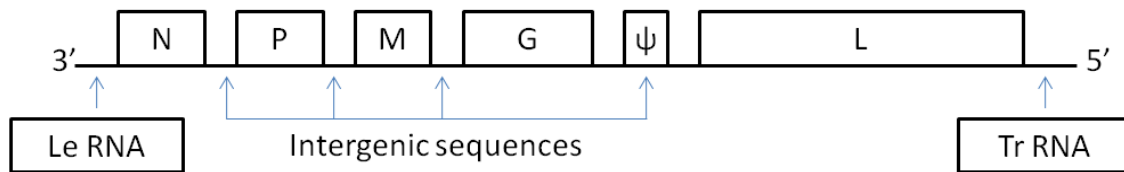


Figure 1.2 A schematic illustration of the rabies virus genome. Nucleoprotein (N), phosphoprotein (P), matrix protein (M), glycoprotein (G) and RNA-dependent RNA polymerase protein (L) genes are separated by non-coding intergenic sequences including the pseudogene (ψ). Short (58 and 70 nucleotides) non-coding sequences at the 3' and 5' ends of the genome, called leader (*Le*) and trailer (*Tr*) sequences, respectively.

1.4 Functions of rabies virus proteins

1.4.1 Nucleocapsid

The nucleocapsid is the vital component active in transcription and replication. During RNA synthesis, the P-protein binds the L-protein to the N-RNA template through an N-P interaction that involves two adjacent N-proteins in the NC. The L-P binding to the N-RNA probably triggers conformational changes that allow access of the polymerase to the RNA (Albertini *et al.*, 2011).

1.4.1.1 RNA-dependent RNA polymerase/ large protein

The RNA-dependent RNA polymerase (large protein) is the largest of the five proteins encoded by the viral genome and makes more than half (54%) of the coding potential of the RABV genome (Wunner, 2007). The L-protein is the enzymatic component of the L-P polymerase complex which, along with the non-catalytic co-factor, the P-protein, responsible for the majority of enzymatic activities involved in viral RNA transcription and replication and for the synthesis

of the cap-structure for the viral mRNAs (Albertini *et al.*, 2011; Wunner, 2007). Apart from sequence analyses, very little is known about the L-protein of RABV, because no easy system exists for reconstituting *in vitro* transcription or replication (Albertini *et al.*, 2011). Therefore, many of activities of these multifunctional enzymes such as L-protein have been identified in genetic and biochemical studies by using the polymerase of VSV and the paramyxovirus Sendai virus. Three essential activities encoded by the RNA-polymerase are involved in the binding and utilization of ATP. These are i) binding and utilization of ATP, ii) the transcriptional activity that requires binding to substrate ribonucleoside triphosphates (rNTPS) and iii) polyadenylation and protein kinase activity for specific phosphorylation of the P-protein in transcriptional activation (Banerjee and Chattopadhyay, 1990; Poch *et al.*, 1990; Sánchez *et al.*, 1985). Many of the putative functions of this multifunctional protein, including mRNA capping, methylation and polyadenylation are not fully understood yet (Wunner, 2007).

1.4.1.2 Nucleoprotein

The nucleoprotein of the RABV (450 amino acid residues) is the most conserved of the viral proteins and a major component of the internal NC (Wunner, 2007). The N-protein binds to cellular RNA and forms long helical N-RNA complexes or closed N-RNA rings, depending on the length of the encapsidated RNA (Iseni *et al.*, 1998). The N-protein is one major component of packing RNA genome and protects the viral genome against ribonuclease activity and factors which recognize foreign nucleic acids in order to start interferon production (Albertini *et al.*, 2011; Schneider *et al.*, 1973). In addition, genotype-specific epitopes on the N-protein enable the assignment of viruses to genotypes on the basis of their reactivity patterns (antigenicity) with a panel of anti-N monoclonal antibodies (mAbs) (Flamand *et al.*, 1980; Dietzschold *et al.*, 1987; Smith, 1989). Immunologically, the N-protein is a major target for T helper (Th) cells that cross-react among RABV and rabies-related viruses to induce immunological reactions (Celis *et al.*, 1988a, 1988b; Ertl *et al.*, 1989). Several T helper cell epitopes in the N-protein of RABV have been identified and mapped using a series of overlapping synthetic peptides (Ertl *et al.*, 1989). Furthermore, the NC of the RABV and N-protein in particular behave as an exogenous super antigen (SAg) (Lafon *et al.*, 1992) both in humans and mice (Lafon *et al.*, 1994), which may increase immunopathogenicity and also enhance the antibody response. This may explain the potent activation of peripheral blood lymphocytes in human vaccines and ability to increase and potentiate immune response to vaccination by the N-protein (Lafon *et al.*, 1994). In addition, N-

protein could also contribute in damping the host innate immune response favouring interferon evading strategy. The amino acids at positions 273 and 394 in the N-protein seem to be important for the host innate immune response (Masatani *et al.*, 2011; Rieder and Conzelmann, 2009).

1.4.1.3 Phosphoprotein

The Phosphoprotein of RABV is an essential component of the replication and transcription complex and acts as a co-factor for the viral RNA-dependent RNA polymerase. The P-protein of rhabdoviruses has a modular multi-domain architecture and is central to the formation of an active NC. It recruits the viral polymerase to the N-protein-bound viral RNA (N-RNA) via an interaction between its C-terminal domain and the N-RNA complex (Delmas *et al.*, 2010). The P-protein acts as a chaperone for soluble nascent N-protein and prevents its polymerization (self-assembly) and non-specific binding to cellular RNA (Mavrakis *et al.*, 2003), thus directing N-protein encapsidation of the viral RNA (Chenik *et al.*, 1994; Fu *et al.*, 1994; Gigant *et al.*, 2000). The specific interaction of a conserved domain within the P-protein and the cytoplasmic light chain (LC8), involved in the intracellular transport of organelle, had been proposed at first to play a role in the retrograde transport to the central nervous system (CNS) (McGettigan *et al.*, 2003). Nevertheless, a recent study demonstrated that the interaction between the P-protein and LC8 is not directly involved in the retrograde axonal transport from the periphery to CNS nor pathogenicity. Rather, the P-protein-LC8 has a significant role in the transcriptional activity of viral polymerase (Tan *et al.*, 2007).

In addition, the P-protein of RABV is a type I interferon (IFN) antagonist counteracting transcriptional activation of IFN and IFN-mediated JAK/STAT signaling (Brzózka *et al.*, 2005, 2006; Chelbi-Alix *et al.*, 2006). The P-protein contains two independent domains accounting for the IFN antagonistic functions: the amino acid residues 176-186 being involved in the inhibition of interferon regulatory factor (IRF) 3 and 7 phosphorylation and the C-terminal (288-297) being involved in the binding to Signal Transducer and Activator of Transcription (STATs) preventing the nuclear import of activated STATs (Rieder *et al.*, 2011). Therefore, the P-protein inhibits IFN production by impairing IRF-3 phosphorylation, IFN signaling by blocking nuclear transport of STAT1 and alters promyelocytic leukemia (PML) nuclear bodies (a part of cellular immune defense mechanism) by retaining PML in the cytoplasm (Chelbi-Alix *et al.*, 2006).

1.4.2 Envelope proteins

Viral membrane proteins, M- and G-proteins, and a mixture of lipoprotein components derived from the cell membrane form the outer envelope of virus particle (Wunner, 2007). The M-protein associates with both the NC and the viral G-protein, collaborating with G-protein in infected cells, to produce progeny virions in the budding process at the cell membrane (Nakahara *et al.*, 1999). On the other hand, the G-protein produces the trimeric spike-like projections or peplomers to facilitate the virus to bind to the receptors on the cell surface (Gaudin *et al.*, 1992).

1.4.2.1 Matrix protein

The matrix protein of RABV is small multi-functional protein of 202 amino acids (25 kDa) and is responsible for the assembly and budding of virus particles (Finke *et al.*, 2003). The M-protein binds to and condenses the nascent NC core into a tightly coiled, helical RNP-M protein complex, forming a sheath around it and producing the bullet-shaped ‘skeleton’ structure of the virion. In the mean time, the M-protein binds to the NC structure and the cytoplasmic domain of the G-protein (Cyto-G) (Mebatsion *et al.*, 1999) facilitating the binding of the viral core structure to the host membrane at the marginal region of the cytoplasm where it initiates virus budding from the cell plasma membrane (Mebatsion *et al.*, 1999). Therefore, the M-protein gives the virion its characteristic bullet-shape, regardless of whether its location is within the NC core or on the external surface of the core (Barge *et al.*, 1993; Lyles *et al.*, 1996). Apart from virus assembly, the M-protein is involved in regulating RNA synthesis, maintaining a balance between replication and transcription (Finke *et al.*, 2003).

In addition, the M-protein of RABV is known to be a determinant of pathogenicity and may contribute to host tropism (Finke *et al.*, 2010). In non-virulent RABV strains, the M-protein was found to activate host cell caspases and induce apoptosis as TRAIL dependent pathway (the tumor necrosis factor-related apoptosis-inducing ligand) (Kassis *et al.*, 2004; Larrous *et al.*, 2010). The existence of “late” or L-domains (PPEY) in the M-protein could also facilitate the viral budding by anchoring the M-NC with host cell proteins (Wirblich *et al.*, 2008). It is suggested that RABV PPEY motif possesses L-domain activity in the context of a virus infection

and may be important for the pathogenic potential of the virus in an animal model (Okumura and Harty, 2011).

1.4.2.2 Glycoprotein

The glycoprotein forms trimeric transmembrane spike structures that allow the virus to attach to neurons and then enter the host cell via a fusion event. The G-protein facilitates also the budding of the virus (Mebatsion *et al.*, 1996; Robison and Whitt, 2000). The mature G-protein of all RABV strains has 505 amino acid residues (524 amino acids are translated from a G-mRNA transcript). In contrast, a mature MOKV G has 503 amino acids (522 amino acids are encoded in the MOKV G-mRNA) (Benmansour *et al.*, 1992; Bourhy *et al.*, 1993). The G-protein of all RABV and rabies-related lyssaviruses is composed of four domains; the signal peptide domain (SP), the ectodomain (ED), the transmembrane domain (TM) as well as the cytoplasmic domain (CD) (Wunner, 2007). The G-protein of RABV plays an important role in establishing the phenotype of the virus in defining the pathogenicity of the virus (Ito *et al.*, 2001; Kucera *et al.*, 1985; Yan *et al.*, 2002). The ectodomain of G-protein (amino acid residues 1-439) is responsible for interaction of the RABV with its receptors such as nicotinic acetylcholine receptors (nAChR), neuronal cell adhesion molecule (NCAM), p75 neurotrophin receptor (p75NTR) and gangliosides (Lafon, 2005). The pathogenic or virulent phenotype of the virus correlates with a single amino acid at a specific position in the G-protein. For instance, the amino acid residue arginine (Arg) [or lysine (Lys)] at position 333 in the wild-type (normal) G-protein is responsible for the virulence phenotype of RABV. Intracerebral inoculation of RABV into adult immunocompetent mice resulted in virus variants with different amino acid residues [e.g. glutamine (Gln), isoleucine (Ile), glycine (Gly), methionine (Met) or serine (Ser)] in place of Arg-333 in the G-protein, less pathogenic or avirulent phenotypes are induced by these amino acid residue substitutions compared to the parental wild-type virus (Dietzschold *et al.*, 1983; Seif *et al.*, 1985; Tuffereau *et al.*, 1989). Mebatsion *et al.* (1996) showed that the G-protein enhances the efficiency of virus budding by up to 30-fold, suggesting that this protein has an autonomous exocytic activity (Mebatsion *et al.*, 1996; Robison and Whitt, 2000).

The carboxyl terminal portion (last 44 amino acids) of the G-protein, namely the cytoplasmic domain, extends inward from the plasma membrane into the cytoplasm of the infected cell where it interacts with the M-protein (Mebatsion *et al.*, 1999), the major structural protein involved in

virion assembly and egress (Okumura and Harty, 2011). The presence of the cytoplasmic domain augments the incorporation of spikes into the viral envelope (Mebatsion *et al.*, 1996). The cytoplasmic domain of the G-protein encodes at the C-terminal a PDZ-binding site (PDZ-BS) allowing the binding of the G-protein with the PDZ domain of peculiar host cell partners influencing RABV pathogenicity of the RABV infected neurons. The PDZ domains are globular structures, 80-100 amino acids long, that contain a groove into which the C-terminal segment of a partner protein, PDZ-BS, inserts (Lafon, 2011). The cytoplasmic tail carries a crucial determinant controlling the balance between neuronal survival and death of an infected neuron (Prehaud *et al.*, 2010). The G-protein is also pivotal for the induction of host humoral immune response to RABV infection and as the target of virus-neutralizing antibody (VNA) and for virus-specific helper and cytotoxic T cells (Celis *et al.*, 1988a; Macfarlan *et al.*, 1986). Overall, the nature of the G-protein governs the neurotropism, the speed of uptake of virus particles as well as the promotion of the survival of the infected cells (Lafon, 2011; Schnell *et al.*, 2010).

1.4.3 Non-coding regions of rabies virus

The five structural genes of the lyssavirus genome are separated by non-coding nucleotide sequences: one dinucleotide (N-P), two pentanucleotide (P-M and M-G) and one long 423 nucleotide sequence (G-L) (Figure 1.2). This non-coding region has been implicated in the shut-off of the host cell macromolecular synthesis in VSV (Grinnell and Wagner, 1985), however, protein shut off is not usually observed during infection with the RABV (Tuffereau and Martinet-Edelist, 1985). The leader RNA (*Le*) sequence, a small RNA (57-58 ribonucleotides) and very rich in alanine, is transcribed at the 3' end of the genome. The long intergenic region between the G and L genes is a remnant gene or pseudogene (ψ) lacking an open reading frame (ORF) to code for a detectable protein (Tordo *et al.*, 1986). This region is highly mutable and is the most divergent area of the RABV genome (Sacramento *et al.*, 1991).

1.5 Host species, the route of infection and life cycle

1.5.1 Host species of rabies virus and the route of infection

All terrestrial mammals are susceptible to RABV infection and this disease occurs on all continents except the Antarctica (Warrell and Warrell, 2004). Indeed, the RABV has been

isolated from nearly all mammalian orders (Rupprecht *et al.*, 2002) with Carnivora and Chiroptera, being major vectors of RABV and rabies-related lyssaviruses (Badrane and Tordo, 2001). For instance, domestic dogs are the major reservoir of the disease throughout Africa and Asia (Rupprecht *et al.*, 2002). The red fox (*Vulpes vulpes*) is the main vector species involved in rabies epidemiology in Europe (Cliquet and Aubert, 2004), whereas raccoons and skunks are the most frequently diagnosed species with RABV in the USA (Krebs *et al.*, 2005). In developing countries of Asia and Africa, dogs remain the major vectors, although wildlife species are also involved in transmission cycles (Bingham *et al.*, 1999).

The RABV is usually introduced through bites or scratches with infectious saliva, although transmission can result via licks on broken skin or mucous membrane, but not through intact skin. Airborne natural infection is possible in exceptional circumstances, for instance in caves harbouring large numbers of potential infected bats (Constantine, 1962) or in laboratory accidents by aerosolized RABV (Tillotson *et al.*, 1977; Winkler *et al.*, 1973). Contamination of other mucous membranes, such as the eyes and nose, is a potential risk, and human infections documented to date were as a result of corneal or organ transplantation (Anderson *et al.*, 1984; Centers for Disease Control and Prevention, 1999; Hellenbrand *et al.*, 2005; Srinivasan *et al.*, 2005).

1.5.2 The life cycle of rabies virus

The life cycle of RABV either in cell culture or *in vivo* can be divided into three phases. The first or early phase, which includes virus attachment to receptors on susceptible host cells, entry via direct virus fusion and uncoating of virus particles into cytoplasm followed by the second or middle phase, which includes transcription and replication of the viral genome and protein synthesis. Finally, the third or late phase comprises virus assembly and egress from the infected cells (Wunner, 2007). The schematic overview of RABV life cycle in the host cell is shown in Figure 1.3.

1.5.2.1 The first phase (attachment and entry)

The RABV enters nervous system via a motor neuron through the neuromuscular junction or a sensory nerve through nerve spindle. Infection starts with the attachment of RABV to a target

cell surface receptor. The muscle expresses the alpha nicotinic acetylcholine receptor (AChR) especially at the muscle side of neuromuscular junctions. The RABV usage of this receptor can allow virus multiplication in muscle prior to entry into the nervous system or concentration of the viral particles at the neuromuscular junction improving the probability of RABV being taken up by nervous terminal (Lafon, 2005). The neural cell adhesion molecule (NCAM) CD 56, expressed at the neural side of the neuromuscular junction and at the synaptic membrane, is a good candidate for entry into the nervous system (Lafon, 2005; Thoulouze *et al.*, 1998), whereas the low-affinity neurotrophin receptor (p75NTR) might contribute to the axonal transport of RABV (Langevin *et al.*, 2002; Tuffereau *et al.*, 1998, 2007). After entry at the neuromuscular junction or passage through the synapse, RABV particles propagate in axonal vesicles transported by a retrograde route (Klingen *et al.*, 2008). RABV replication occurs in the cell body and dendrites but not in the axon (Ugolini, 1995). Once the cell body is reached, it is likely that the vesicles liberate the NC by fusion of the G-protein with the membrane of the axonal routing vesicle. Nevertheless, no experimental evidence of this step has been brought yet. It is responsible for low pH-induced fusion of the viral envelope with plasma and endosomal membranes (Gaudin *et al.*, 1993; Roche and Gaudin, 2004) and the acidic environment of the vesicle induces a conformational change of the G-protein (Albertini *et al.*, 2011).

1.5.2.2 The second phase (virus replication)

All transcription and replication events take place in the cytoplasm (Albertini *et al.*, 2011). The L-P complex enters the nucleocapsid at the 3' end of the RNA and starts transcription with the production of a short RNA molecule, the leader RNA. Subsequently, mRNAs are produced for N-, P-, M-, G- and L-proteins, generating a gradient of amount of transcript (leader RNA > mRNA N > mRNA P > mRNA M > mRNA G > mRNA L) (Albertini *et al.*, 2011). During transcription, the mRNA is capped and methylated on its nascent 5' extremity at the end of the gene. The replication requires ongoing protein synthesis to provide a source of soluble N-protein (N⁰) necessary to encapsidate the nascent RNA. Later in infection, the activity of the polymerase P-L complex switches from transcription to replication to produce a full-length positive RNA strand complementary to the complete genome (Albertini *et al.*, 2011). These positive-stranded RNAs are also encapsidated by N-protein, bind the L-P complex and are used as templates to amplify new negative-stranded RNA genomes for new nucleocapsids (Albertini *et al.*, 2008).

1.5.2.3 The third phase (virus assembly and budding)

Once sufficient pools of viral progeny (negative strand) RNA and the viral N-, P- and L- proteins have accumulated in the infected cell, formation of rabies viral RNP complexes and assembly of virus particles begins (Wunner, 2007), starting with encapsidation of progeny (negative-strand) genome RNA and NC formation (Iseni *et al.*, 1998; Liu *et al.*, 2004; Mavrakis *et al.*, 2003).

Rabies virus infection causes the appearance of specific histopathologic changes of infected nerve cells, known as Negri bodies, which are characteristic neuronal intracytoplasmic inclusions in the infection with street RABV strains. The Negri bodies are typical perinuclear aggregates formed by viral proteins, viral nucleic acids and host proteins such as TLR3 (Lahaye *et al.*, 2009; Ménager *et al.*, 2009). In close vicinity of mitochondria and rough endoplasmic reticulum, they form assembly factories for the virus. They are pathognomical (typical feature of the infection) structures used as definite histological proof of rabies. Amongst the five encoded proteins, the viral M-protein plays a key role in virus budding and is thought to recruit host proteins to facilitate efficient virion egress. A late budding domain (L-domain) mediates the recruitment of host proteins linked to the vacuolar protein sorting (vps) pathway of the cell to facilitate virus-cell separation (Chen and Lamb, 2008; Okumura and Harty, 2011). The mature virions acquire lipid bilayer envelope and the infectious virions will be produced bearing the G molecules arranged as trimeric spike-like structures tightly packed and anchored in the viral envelope in the final stages of RABV assembly (Wunner, 2007). Eventually, the virus particles then escape from the infected cells by budding.

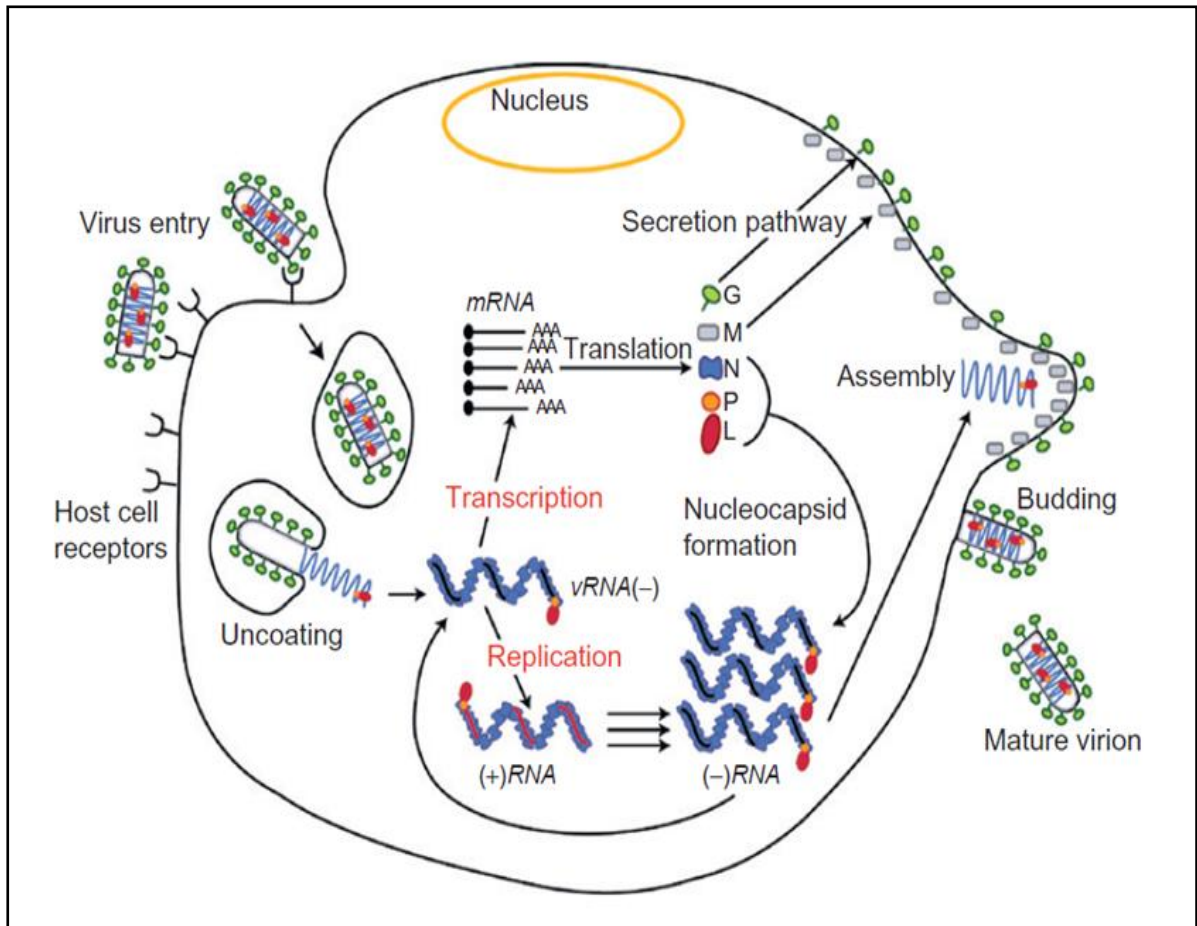


Figure 1.3 A schematic overview of RABV life cycle in host cells (Albertini *et al.*, 2011).

1.6 Infection of the nervous system by rabies virus

1.6.1 Entry into the central nervous system

The RABV is a highly neurotropic virus that spreads along the neuronal network. Once the virus enters, it then travels from the site of peripheral inoculation to the CNS by retrograde fast axonal transport. The virus multiplies first in the muscle before entry into the nervous system, it seems to depend on the nature of the strain with street RABV isolates multiplying into muscular cells (Fekadu and Shaddock, 1984; Murphy *et al.*, 1973) and laboratory RABV strains such as CVS not infecting into muscles (Coulon *et al.*, 1989; Shankar *et al.*, 1991). Whatever the route of inoculation through masseter muscle (Jackson, 1991) or intranasal route (Lafay *et al.*, 1991), the spread of virus variants within the CNS is dependent on the fast axonal transport mechanism (Jackson, 2007). Movement to the brain via the spinal cord is rapid and associated with an explosive increase in viral particles. Studies performed with G-protein gene-deficient

recombinant RABV showed limited spread in the brain of mice after intracerebral inoculation (Etessami *et al.*, 2000). It demonstrates that the G-protein of RABV is necessary for trans-synaptic from one neuron to another (Jackson, 2007). Once CNS neurons become infected, there is rapid dissemination of RABV infection along neuroanatomical pathways. The brainstem is infected first, followed by the thalamus and lastly the cortex (Tsiang, 1988). The infections are widespread and involve major regions of the CNS including the cerebral cortex, hippocampus, brainstem, cerebellum and spinal cord. It predominantly infects pyramidal neurons of the hippocampus with relative sparing of neurons in the dentate gyrus in adult mice (Jackson and Reimer, 1989).

1.6.2 Spread from the central nervous system

Spread from the CNS to peripheral sites such as various organs including the salivary glands, allows efficient transmission of the infection to its natural hosts. Widespread infection of epithelial cells of salivary gland results from viral spread along multiple terminal axons rather than spread between epithelial cells (Charlton *et al.*, 1983). In the same regard, infection was observed in the ganglion cell layer of the retina and in corneal epithelial cells, innervated by sensory afferents via the trigeminal nerve. Thus, the detection of RABV antigens in corneal impression smears has been used as a diagnostic test for human rabies (Koch *et al.*, 1975). Studies in both natural and experimental rabies have demonstrated infection in a variety of extraneural organs including the adrenal medulla, cardiac ganglia and plexuses in the luminal gastrointestinal tract, liver and exocrine pancreas (Balachandran and Charlton, 1994; Debbie and Trimarchi, 1970; Jackson *et al.*, 1999).

1.7 Diagnosis of rabies

Rabies diagnosis is most frequently performed for the post-mortem examination of animals that have had human contact (bite/lick) or have otherwise potentially caused human exposure to the disease. Nevertheless, the presence of neutralizing antibodies in the serum, the cerebrospinal fluid (CSF) and detection of viral RNA in skin nuchal biopsies can be performed in the patients alive. The results of the diagnostic test underpin disease control, prevention of the disease and management of human contact cases. Evidence of the RABV infection, based on positive diagnostic test results, needs prompt administration of rabies post-exposure prophylaxis (PEP) to

the exposed person, preventing onset of the almost invariably fatal infection (Trimarchi and Nadin-Davis, 2007).

The fluorescent antibody test (FAT) is the gold standard and one of the most accurate microscopic tests available for the diagnosis of rabies and is more sensitive compared to histopathological methods (Dean *et al.*, 1996). The presence of RABV antigen is demonstrated in acetone-fixed brain smears by means of immunofluorescence using a polyclonal anti-lyssavirus fluorescein labeled conjugate. This test is fast, comparatively inexpensive and more than 99% sensitivity in experienced hands (Dean *et al.*, 1996). Another sensitive and reliable test is the mouse inoculation test (MIT), which is applicable in the case of inconclusive or human contact cases that are negative on FAT. However, it requires a large number of mice per sample, labour-intensive and requires long periods of observation (up to 28 days). In many laboratories, the rabies tissue-culture infection test (RTCIT) has now replaced MIT. The RTCIT is considerably more sensitive to infection with low amounts of virus than are experimental mice. It is also relatively easy to perform, less expensive and results are obtained within 4 days, as compared with the MIT which takes 28 days (Webster and Casey, 1996). Current developments in PCR technology have focused on improvements in the quantitative capability of the methodology. Furthermore, real-time PCR technique is also able to offer the potential of a rapid diagnosis and an additional benefit for a significant reduction in the chance for false-positive results arising through sample contamination (Trimarchi and Nadin-Davis, 2007). Real time-qPCR is one of the most recent assays to detect minute quantities of virus in brain tissues (Szanto, 2009) and this technique allows all genes involved in the pathogenesis of RABV to be monitored (Wang *et al.*, 2005).

1.8 Role of glycoprotein in pathogenicity and neuroinvasiveness

1.8.1 Pathogenic determinants in ectodomain

Several studies have demonstrated that virus variants with a mutation from arginine to glutamate at position 333 affecting antigenic site III of the G-protein, become apathogenic, regardless of the site of infection or the dose of virus used (Coulon *et al.*, 1982, 1983; Dietzschold *et al.*, 1983; Seif *et al.*, 1985; Tuffereau *et al.*, 1989). A virulent strain with arginine at position 333 in the G-protein spreads more rapidly in the mouse brain than an attenuated strain with an amino acid

residue other than arginine, and that *in vitro* cell-to-cell spread of the virulent strain is more efficient than that of the attenuated strain (Dietzschold *et al.*, 1985). Other amino acid substitutions at different positions on the G-protein of RABV appear to confer or influence viral pathogenicity. For instance, the mutation position at 194 results in lysine replacing asparagine and is associated with increased pathogenicity in adult mice (Faber *et al.*, 2005; Prehaud *et al.*, 1988). The two substitutions, phenylalanine at position 318 substituted for by serine or valine and histidine at position 352 substituted for by arginine or tyrosine, prevent the G-protein of RABV from interacting with p75NTR (soluble or membrane-anchored form) (Langevin and Tuffereau, 2002).

1.8.2 Protein interaction domains in cytoplasmic domain

RABV carboxyl-terminus encodes a PDZ-BS allowing the cytoplasmic domain of G-protein to interact with host cell proteins expressing a PDZ domain. The PDZ domains are one of the most commonly found protein-protein interaction modules controlling main signalization pathways such as cell growth, survival and death (Sheng and Sala, 2001). The PDZ domains were first identified as regions of sequence homology found in diverse signaling proteins (Cho *et al.*, 1992; Kim *et al.*, 1995; Woods and Bryant, 1993). The name PDZ is derived from the first three proteins in which these domains were identified: PSD-95, DLG and ZO-1. These domains have also been referred to as Discs large homology region (DHR) or GLGF repeats (after the conserved Gly-Leu-Gly-Phe signature within the primary sequence).

Recently, the PDZ domains have emerged as one of the most abundant protein interaction domains in organisms as diverse as bacteria, yeast, plants, invertebrates and vertebrates (Ponting, 1997). These domains specifically recognize short C-terminal peptide motifs located in the partner protein. The PDZ target specificity is dependent on the C-terminal amino acid sequence of the interacting protein (Songyang *et al.*, 1997). Since being recognized as sequence repeats, PDZ domains have emerged in the past few years as important modular protein interaction domains found in organizing diverse cell signaling assemblies (Sheng and Sala, 2001). The residue of C-terminal is referred to as the P₀; subsequently residues termed P₋₁, P₋₂, P₋₃, etc are toward N-terminus. The PDZ domains generally show the carboxylated amino acid at the 0 position of the peptide ligand is a major determinant in the interaction and are specialized for binding of carboxyl-terminus in partner proteins, most often transmembrane receptors and

channel proteins and/or other PDZ domains (Jeleń *et al.*, 2003). The structure of a PDZ domain comprises six β -strands (β A ~ β F) and two α -helices (α A and α B), which fold into a six-stranded β -sandwich domain. Peptide binding occurs in a groove between the β B strand and the α B helix. Each PDZ domain binds a single peptide ligand. The main chain of the β B strand runs the length of the peptide-binding groove and provides important interactions with the main chain of the peptide (Figure 1.4) (Sheng and Sala, 2001).

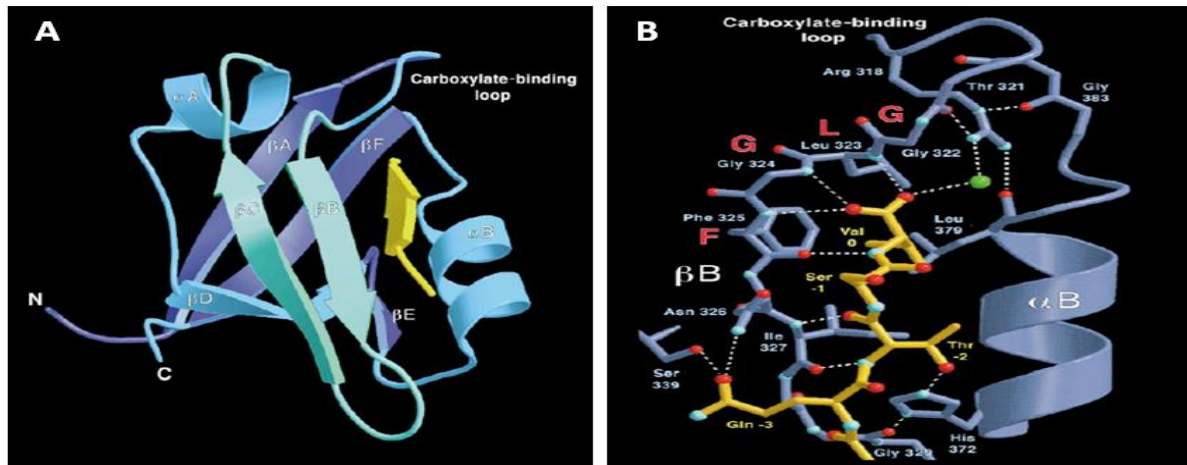


Figure 1.4 Structural diagrams of PDZ3 domain of PSD-95. (A) Ribbon representation of the PDZ3 domain; 6 β -sheets and 2 α -helices consists of the modular structure characteristic for PDZ domains. The carboxylate-binding loop involved in ligand binding is indicated. (B) Chemical interactions involved in peptide binding. Hydrogen bonds are depicted (dashed white line) between residues of the PDZ domain (blue) and the peptide ligand (orange) (Doyle *et al.*, 1996).

The inhibition or perturbation of the function of cellular PDZ proteins appears to be a widely used strategy for viruses to enhance their replication, dissemination in the host and transmission to new hosts (Javier and Rice, 2011). The RABV also has evolved mechanisms to enforce the survival of the host cells infected by targeting the PDZ domain of Microtubule Associated Serine-Threonine kinase 2 (MAST2), which is acting as an inhibitor of neuron survival (Loh *et al.*, 2008). The RABV infected human neurons may undergo either death or survival pathway whether the RABV strain is attenuated or virulent. The capacity of the RABV to promote neuronal survival (*a signature of virulence*) or death (*a marker of attenuation*) depends on the cellular partners recruited by the PDZ-BS of its envelope G-protein (Prehaud *et al.*, 2010). The result of single amino acid difference from glutamine (Q) to glutamic acid (E) at position P₋₃, relative to the last amino acid residue of the C-terminal, which is denoted as 0, displayed distinct abilities to promote the neuronal survival or apoptotic death of infected neurons *in vitro* (Prehaud

et al., 2010). Remarkably, one mutation (Q to E) in the PDZ-BS was sufficient to switch the fate of the infected cell from survival to apoptosis (Prehaud *et al.*, 2010).

In this rationale, we have decided to analyze the neurosurvival and pro-apoptotic properties by the amino acid sequences in the Cyto-G of the South African isolates.

1.9 Objectives of the study

The majority of human rabies deaths (> 90%) in South Africa is caused by the canid rabies biotype rather than the mongoose rabies biotype (wildlife) (Weyer *et al.*, 2010). This observation has led to the notion that the canid rabies biotype is more pathogenic than the mongoose biotype. The question is therefore whether high number of human deaths by canid rabies is the result of the different level of pathogenicity or caused by other factors such as high chances of contact between humans and domestic dogs. This study was therefore aimed to evaluate the difference in virulence of the two rabies biotypes commonly encountered in South Africa.

The virulence of RABV relies on the capacity of this virus to reach the nervous system and to propagate into the nervous system without killing the infected cells by premature apoptosis and without being cleared off by the immune response. This virus has evolved unique strategies to evade the host immune response and preserve the neuronal network integrity (Lafon, 2011). The objective of this project was first to sequence the entire G-protein encoding gene of the three South African RABV isolates and then to compare the properties of the C-terminal of the G-protein to trigger *in vitro* either neurite outgrowth or apoptosis. In previous study, two laboratory RABV strains were compared to demonstrate how RABV controls the fate of infected neurons: CVS-NIV and ERA-NIV. CVS-NIV causes fatal encephalitic rabies after inoculation and engages neurosurvival signaling pathway in neurons, whereas ERA-NIV strain was identified that it causes neuronal death in the infected cells (Prehaud *et al.*, 2010). The chimeric constructs were generated by grafting last 12 amino acids of the G-proteins of isolates replacing of the original residues of a virulent RABV strain CVS-NIV. After the infection of the recombinant constructs to human and rat neuronal cells, the phenotypes of neurite outgrowth and apoptotic induction were evaluated and the pathogenicity of South African isolates was determined in a recombinant lentivirus system.

The objectives of this research project were:

- i) To genetically characterize the complete G-protein encoding genes of the South African rabies virus isolates (canid, mongoose and spill over).
- ii) To compare neurosurvival and pro-apoptotic features of the last 12 amino acid residues of the Cyto-G of the 3 variants with those of canonic RABV (ERA-NIV and CVS-NIV).
 - By expressing the last 12 amino acids of the South African variants and ERA-NIV and CVS-NIV in rat and human neuronal cells infected with recombinant lentiviruses.

CHAPTER 2

Genetic characterization and identification of pathogenic determinants of genotype 1 South African rabies biotypes

2.1 Literature review

2.1.1 Host species of rabies in South Africa

Canid and mongoose rabies biotypes are independently maintained and transmitted in South Africa. The former infects carnivores of the *Canidae* family such as domestic dogs (*Canis familiaris*), jackal species (*Canis mesomelas* and *Canis adustus*) and bat-eared foxes (*Otocyon megalotis*). The latter, mongoose rabies has been present in South Africa at least 200 years before the introduction of the canid rabies lineage (King *et al.*, 1993; Swanepoel *et al.*, 1993; Van Zyl *et al.*, 2010; Von Teichman *et al.*, 1995) and small carnivores (1~5 kg; 23~75 cm) are involved in the infectious cycle (Nel *et al.*, 2005).

The first outbreak of dog rabies in South Africa occurred in 1892 in Port Elizabeth and was caused by an infected dog imported from England. This outbreak primarily involved dogs and other domestic animals such as cats and cattle. After strict control measures, however, the disease was eradicated from this area and canid rabies was only encountered in South Africa five decades later (Cluver 1927; Neitz and Thomas, 1933). In this most recent introduction of the disease, canid rabies spread from Angola into the southern African neighbouring countries (Namibia, Botswana, Zimbabwe and eventually South Africa) from the late 1940s onwards (Swanepoel *et al.*, 1993). Canid rabies became common in South Africa after 1950, when it entered the dog population in the northern Limpopo province (Alexander, 1952). Today, canid rabies is maintained by dogs and jackals in the northern Limpopo province, also in dogs in KwaZulu-Natal and Eastern Cape provinces. In the drier western regions of this country, the bat-eared fox is suggested to be a reservoir and maintain the canid rabies biotype (Bingham, 2005; Sabeta *et al.*, 2007; Swanepoel *et al.*, 1993; Thomson and Meredith, 1993). In South Africa, rabies is constantly diagnosed in domestic and wildlife carnivore species including mongooses. Whilst dogs remain the major vector of human rabies in South Africa, only few cases reported exposures to domestic cats (Weyer *et al.*, 2010).

Mongoose rabies was first identified in the 1890s and is thought to be indigenous to southern Africa (Nel *et al.*, 2005; Snyman, 1940; Swanepoel *et al.*, 1993). Since 1916, several cases of suspected rabies had been reported from different areas of the country with strong evidence

suggesting yellow mongooses and genets as vectors of the disease (Cluver, 1927). Mongoose rabies is not only endemic in South Africa, but has been reported from other parts of the world including the Caribbean, where it appears to be the main manifestation of enzootic disease (Chaparro and Esterhuysen, 1993; Zumpt, 1982). As a consequence of different habitat and distribution patterns among mongoose species, the principal vector species for the mongoose rabies biotype in South Africa is the yellow mongoose (*Cynictis penicillata*) (Swanepoel *et al.*, 1993; Taylor, 1993). The slender mongoose (*Galerella sanguinea*) was initially thought to be the maintenance host of mongoose rabies in Zimbabwe (Bingham *et al.*, 2001; Foggin, 1988), although current data seems to suggest that the African civet is possibly a key host for this variant (Sabeta *et al.*, 2008). The mongoose rabies biotype is currently reported to contribute approximately 10% of total confirmed rabies cases through monoclonal antibody typing in South Africa (Records of the Onderstepoort Veterinary Institute, 2010). The mongoose rabies biotype is thought to be well adapted to these small carnivores of southern Africa with considerable antigenic and genetic diversity in comparison to the canid rabies biotype (Bingham, 1999; King *et al.*, 1993; Von Teichman *et al.*, 1995). Previous studies have shown that these two rabies biotypes (canid and mongoose) may jump species boundaries, called “*spill over infection*”, although such events are thought to occur infrequently (Chaparro and Esterhuysen, 1993; King *et al.*, 1993; Nel *et al.*, 1997). Interestingly, the spill over of mongoose rabies biotype into dog hosts does not establish further dog to dog transmission thereby leading to dead end infections (Figure 2.1) (Ngoepe *et al.*, 2009).

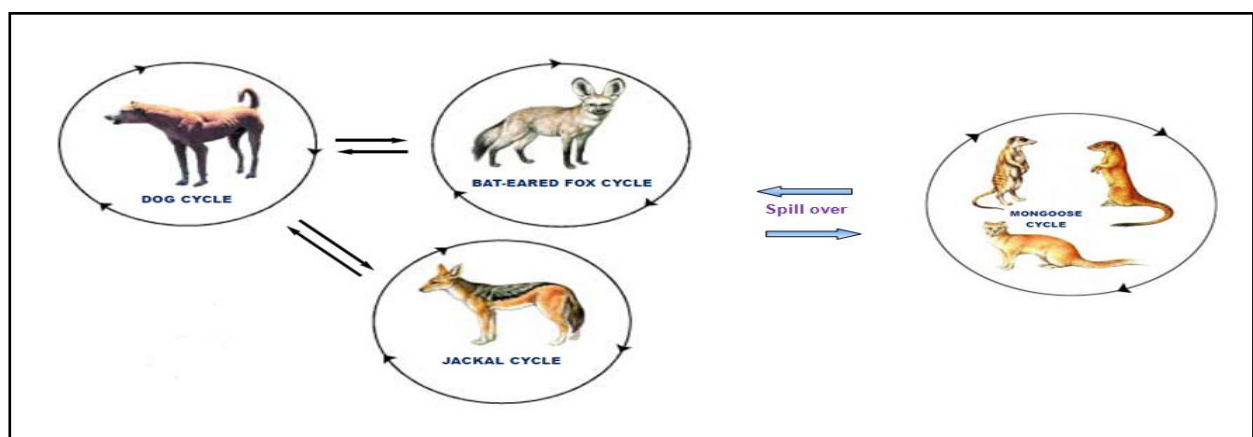


Figure 2.1 Two well-characterized RABV biotypes in South Africa, the canid and mongoose, circulate independently. The canid biotype infects carnivores of the *Canidae* family such as domestic dogs (*Canis familiaris*), jackal species (*Canis mesomelas* and *Canis adustus*) and bat-eared foxes (*Otocyon megalotis*), whereas the yellow mongoose (*Cynictis penicillata*) is the principal vector species of the mongoose rabies biotype. Occasionally, host switch events have happened between two families and are referred as spill over.

2.1.2 Objective

The objective of this set of experiments was to genetically characterize the complete G-protein encoding genes of three RABV isolates commonly encountered in South Africa.

2.2 Materials and methods

2.2.1 Selection of rabies virus isolates and diagnostic tests

2.2.1.1 Selection of rabies viruses

Three South African rabies viruses used in this study were retrieved from the archive of the O.I.E Rabies Reference Laboratory of the Agricultural Research Council-Onderstepoort Veterinary Institute (ARC-OVI) in Pretoria, South Africa. The viruses and epidemiological information (i.e. origin species, biotype, locality of origin and longitude/latitude) are shown in Table 2.1 and Figure 2.2. In addition, a mongoose rabies biotype recovered from a domestic dog will be referred as a “*spill over isolate*” in this study.

Table 2.1 Epidemiological information of RABV isolates from various localities of South Africa used in this study.

Lab ref No./ Year of isolation	Species of origin	Biotype	Locality of origin	Longitude	Latitude
22/07	Yellow mongoose (<i>Cynictis penicillata</i>)	Mongoose	Bloemfontein (Free State)	26.21	29.10
143/07	Canine (<i>Canis familiaris</i>)	Canid	Selwana village (Limpopo)	23.42	30.56
198/08	Canine (<i>Canis familiaris</i>)	Mongoose	De Aar (Northern Cape)	24.01	30.43

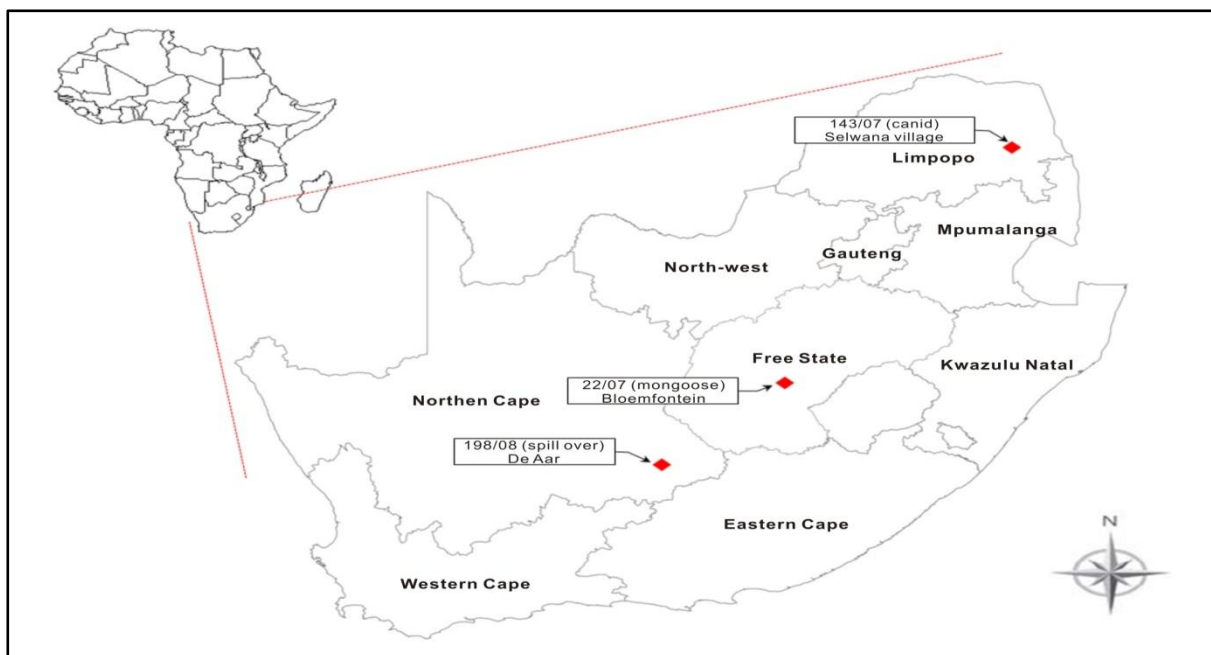


Figure 2.2 Representative map indicating geographical origins where the RABV isolates were recovered.

2.2.1.2 Fluorescent antibody test

The original brain samples for this study were tested for the presence of lyssavirus antigen with fluorescent antibody test (FAT) (Dean *et al.*, 1996). A composite brain smear was prepared on degreased clean slide glasses in a biological safety cabinet (BSC) class II, air-dried at room temperature and fixed with cold acetone for 15 minutes. The smear was stained with a polyclonal fluorescein isothiocyanate (FITC)-conjugated immunoglobulin produced in goats (goat antisera) (O.I.E Rabies Reference Laboratory, ARC-OVI) and incubated at 37°C in a humidified atmosphere for 30 minutes. After the incubation period, the slides were washed three times in 0.01 M phosphate buffered saline (pH 7.2-7.4), air-dried, mounted with mounting fluid (glycerol and PBS, 1:1) and examined using a fluorescent microscope (Axiolab-Zeiss, Germany) (Dean *et al.*, 1996).

2.2.1.3 Monoclonal antibody typing

Monoclonal antibodies (mAbs) directed against the rabies nucleocapsid (anti-N) were first described in 1978 (Wiktor *et al.*, 1978), and since then this tool has been used to identify and characterize RABV variants and thereby understand the geographical spread of rabies biotypes and their maintenance in specific hosts. The samples, positive for the lyssavirus antigen (Dean *et*

al., 1996) were further characterized using a panel of 15 anti-N monoclonal antibodies (N-mAbs) (Centre of Expertise for Rabies, Canadian Food Inspection Agency, Nepean, Ontario, Canada) (Table 2.2).

Table 2.2 Panel of 15 anti-nucleocapsid monoclonal antibodies (N-mAbs) for antigenic typing of southern African lyssaviruses and reactivity pattern of South African rabies isolates used in this study.

Monoclonal antibody	Canid biotype	Mongoose biotype	Mongoose (22/07)	Canid (143/07)	Spill over (198/08)
1C5	–	–	–	–	–
26AB7	+++	Var	+++	+++	+++
26BE2	+++	Var	+++	+++	+++
32GD12	var	Var	–	+++	–
38HF2	+++	+++	+++	+++	+++
M612	–	–	–	–	–
M837	–	–	–	–	–
M850	–	Var	+++	–	–
M853	+++	–	–	+++	–
M1001	–	–	–	–	–
M1335	–	Var	+++	–	–
M1386	–	+++	+++	–	+++
M1400	–	var	–	–	+++
M1407	+++	var	+++	+++	+++
M1412	+++	var	+++	+++	+++
M1494	–	var	+++	–	+++

Key

- +++ Highly positive
- No reaction
- var Variable (reacts with some viruses, but not with others)

2.2.1.4 Mouse inoculation test

A 10% brain suspension of the original brain tissue of each of the three samples was prepared for the mouse inoculation test (MIT) in Dulbecco's Modified Eagle's Medium (DMEM, Invitrogen) (Koprowski, 1996). In brief, fresh original brain material was homogenized in DMEM and centrifuged at $200 \times g$ at 4°C for 10 minutes. The supernatant ($\sim 20 \mu\text{l}$) was inoculated into three-day-old suckling mice ($n=8$ per family) via intracerebral route using a 1 ml syringe with 25 G needle ($0.50 \times 16 \text{ mm}$) (Terumo, Japan). Clinical signs daily were monitored for a period of 28 days. The FAT test was then undertaken on brains of mice which succumbed to RABV infection during this period to confirm the presence of antigen.

2.2.2 Recovery of viral RNA and sequences

2.2.2.1 Total viral RNA extractions

Total viral RNAs were extracted from original brain material using Trizol[®] Reagent (Sigma, USA) according to the manufacturer's guidelines. Approximately 0.1 mg of original brain tissue was homogenized by vortex mixing in 1 ml of Trizol[®] Reagent. Then 200 µl of chloroform (Sigma, USA) was added and centrifuged the homogenate at 13,000 rpm for 10 minutes. The aqueous phase was transferred to a clean 1.5 ml eppendorf tube and total RNA was extracted using the RNA Clean & Concentrator kit (Zymo research, USA) as described in the manufacturer's instruction. The membrane was then washed twice with wash buffer and the RNA eluted with 25 µl of nuclease free water (Promega, USA).

2.2.2.2 Primer sequences

Previously designed forward and reverse primers for a conserved region of G-protein encoding gene for canid and mongoose rabies biotypes were used as described by Van Zyl *et al.* (2010) (Table 2.3). The primers were synthesized without any further purification by Integrated DNA technologies (IDT, USA) and reconstituted according to manufacturer's instructions. A primer combination of ViVMF (forward primer) and L(-) (reverse primer) was used for both biotypes as an external pair of primers (2444 bp). The second pairs of primers, RabC4100F (forward primer) and RabC4203R (reverse primer) for the canid rabies biotype and ViVGF (forward primer) and ViVGR2 (reverse primer) for the mongoose rabies biotype (including spill over isolate), were designed and used for an internal pairs of primers (hemi-nesting) to increase the specificity of DNA amplification of G-protein encoding gene.

Table 2.3 Primers used in cDNA synthesis, PCR and sequences (Van Zyl *et al.*, 2010).

Primer name	Sequences (5'→3')	Annealing position	Biotype
ViVMF (+)	G A T T C C T C T C T G C T T C T A G	3099 PV	canid/ mongoose
L(-)	C A A A G G A G A G T T G A G A T T G T A G T C	5543 PV	canid/ mongoose
ViVGR2 (-)	G C A T C G C G A C C C A T G T T C C	4086 PV	mongoose
ViVGF (+)	G G A T T C G T G G A T G A A A G A G G C	4016 PV	mongoose
RabC4203R (-)	C A C T C C T C T C T C T T C T T G A C	4203 NC 001542	canid
RabC4100F (+)	T T A T G G A T G G A A C A T G G G T C G C G	4100 NC 001542	canid

2.2.2.3 Complementary DNA synthesis

Complementary DNA (cDNA) synthesis of the complete G-protein encoding gene was performed as previously described (Sacramento *et al.*, 1991; Von Teichman *et al.*, 1995). The sense primer ViVMF (10 pmol) and 200 ng of the extracted RNA were denatured at 65°C for 5 minutes on AccuBlcok™ Digital Dry Baths (Labnet International, USA) and immediately snap cooled on ice for 5 minutes. The reverse transcription reaction consisted of 2 µl of dNTP mix (2.5 mM each), 2 µl of 0.1 M DTT, 40 U of RNaseOut (Invitrogen, USA), 1 µl (200 U/µl) of SuperScript™ III Reverse Transcriptase (Invitrogen, USA), 4 µl of 5X First-Strand Buffer (250 mM Tris-HCl, 375 mM KCl and 15 mM MgCl₂, pH 8.3, Invitrogen) and nuclease free water in a total volume of 20 µl. The reaction was performed at 42°C for 50 minutes and a final inactivation at 70°C for 15 minutes.

2.2.2.4 Polymerase chain reaction

The amplification of the complete G-protein encoding gene was conducted in a 50 µl volume, and consisted of 5 µl of 10X PCR buffer, 2.5 mM each dNTP mixture, 25 mM MgCl₂ solution, 2 µl of cDNA hybrid, 2 U of Taq DNA polymerase (5 U/µl, Takara Biotechnology, Japan), 4 µl of 10 pmol of each of the forward and reverse primers (Table 2.2), and nuclease-free water. The PCR mixture was then subjected to the following cycling conditions in a Gene Amp 9700 thermocycler (Applied Biosystems, USA): an initial denaturation at 94°C for 2 minutes, followed by 30 cycles of 94°C for 30 seconds, 42°C for 30 seconds and 72°C for 90 seconds, a final extension step of 72°C for 7 minutes and then the reaction mixtures were kept at 4°C (Van Zyl *et al.*, 2010). The PCR products were assessed on 1% ethidium bromide stained agarose gel and visualized under UV transillumination.

2.2.2.5 DNA sequencing and analysis

The PCR products were purified using the Wizard® SV Gel and PCR Clean-up system (Promega, USA). For the purification, the band expected (2444 bp) was excised from the gel and purified the PCR amplicon. Then it was quantified using a spectrophotometer ND-1000 (Nanodrop Technologies, USA) and then the DNA was sequenced using the BigDye terminator kit (Applied

Biosystems, USA) according to the manufacturer's guidelines, with the same primer set that was used in the preceding RT-PCR steps. The sequencing products were analyzed on an automated ABI Prism 377 DNA sequencer (Applied Biosystems, USA). A consensus sequence was generated by editing the forward and reverse nucleotide sequences using all alignments algorithm in Molecular Evolutionary Genetics Analysis (MEGA) 4.0 (Tamura *et al.*, 2007).

2.2.2.6 Phylogenetic analysis

In order to establish and confirm the biotypes, 592 bp nucleotide sequence region, encompassing the cytoplasmic domain of the G-protein and the G-L intergenic region, was used. The nucleotide sequences were aligned using Clustal X (Higgins and Sharp, 1989) and then the multiple alignments were conducted to generate a distance matrix for reconstruction of the phylogenetic trees. The genetic distances were evaluated by Kimura's two-parameter method (Kimura, 1980) and the phylogenetic trees constructed with the neighbour-joining method. The branching order of the phylogenetic tree was evaluated by using bootstrap analysis of 1,000 bootstrap replications to evaluate the significance of the branching pattern and the phylogenetic tree was viewed with NJPlot software (Perrière and Gouy, 1996). For the generating phylogenetic tree, mongoose rabies isolates from Zimbabwe and South Africa (n=25) and canid rabies isolates (n=27) were retrieved from the GenBank (Table 2.4) (Nel *et al.*, 2005; Zulu *et al.*, 2009), with positions relative to the nucleotide sequence of Pasteur virus (PV) (GenBank Acc. Number: M13215) (Tordo *et al.*, 1986).

Table 2.4 Epidemiological information of previously characterized mongoose and canid rabies biotypes from different localities in South Africa and Zimbabwe (Nel *et al.*, 2005; Zulu *et al.*, 2009).

Virus No.	Labreference No.	Year of isolation	Species	Province	Locality	Longitude	Latitude	GenBankAcc.No
1	19518	1991	<i>Galerella sanguinea</i>	Matabeleland	Fort Rixon	29°08'	19°51'	AF304187
2	20948	1992	<i>Mellivora capensis</i>	Matabeleland	Bulawayo	28°40'	19°59'	AF304189
3	19571	1991	<i>Mellivora capensis</i>	Matabeleland	Bulawayo	29°52'	19°26'	AF304184
4	22107	1994	<i>Galerella sanguinea</i>	Manicaland	Rusape	32°08'	18°32'	AF304185
5	19671	1991	<i>Civettictis civetta</i>	Manicaland	Rusape	32°10'	18°37'	AF304188
6	759/96	1996	Feline	Mpumalanga	Belfast	29°53'	25°48'	AY353992
7	926/93	1993	<i>Suricata suricatta</i>	Mpumalanga	Carolina	30°16'	26°04'	AF079908
8	669/90	1990	<i>Cynictis penicillata</i>	Mpumalanga	Grootgewaagd	29°52'	26°42'	AF079907
9	878/92	1992	<i>Atilax paludinosus</i>	Free State	Harrismith	28°55'	27°47'	AF079918
10	420/90	1990	<i>Cynictis penicillata</i>	Northwest	Wolmaranstad	26°14'	27°13'	AF079921
11	970/93	1993	<i>Suricata suricatta</i>	Northwest	Ventersdorp	26°32'	26°23'	AF079924
12	480/90	1990	<i>Cynictis penicillata</i>	Northwest	Bloemhof	25°32'	27°25'	AF079923
13	372/96	1996	<i>Genetta genetta</i>	Free State	Ficksburg	27°54'	28°46'	AY353993
14	248/98	1998	<i>Xerus inauris</i>	Free State	Clocolan	27°30'	28°59'	AY353994
15	271/98	1998	<i>Suricata suricatta</i>	Free State	Bothaville	26°37'	27°24'	AF354013
16	28/96	1996	<i>Cynictis penicillata</i>	Northern Cape	Kimberley	24°40'	29°03'	AF304180
17	476/96	1996	<i>Suricata suricatta</i>	Northern Cape	Hopetown	24°02'	29°37'	AF304178
18	257/98	1998	<i>Cynictis penicillata</i>	Northern Cape	Victoria West	22°53'	30°35'	AF304173
19	364/96	1996	<i>Cynictis penicillata</i>	Eastern Cape	Uitenhage	25°28'	33°48'	AY354004
20	558/95	1995	<i>Suricata suricatta</i>	Mpumalanga	Middelburg	24°32'	31°29'	AY354003
21	127/91	1991	<i>Otocyon megalotis</i>	Western Cape	Malmesbury	18°25'	33°25'	AF079915
22	262/95	1995	<i>Suricata suricatta</i>	Western Cape	Piketberg	18°59'	33°08'	AY354016
23	611/92	1992	<i>Genetta genetta</i>	Northern Cape	Postmasburg	22°53'	27°43'	AF079912
24	446/92	1992	<i>Genetta genetta</i>	Northern Cape	Postmasburg	22°30'	28°12'	AF079909
25	718/98	1998	<i>Genetta genetta</i>	Northern Cape	Gordonia	20°30'	27°58'	AF304169
26	1265/80	1980	<i>Canis familiaris</i>	Northwest	Brits	27°34'	25°22'	EF686047
27	820/94	1994	<i>Canis familiaris</i>	Northwest	Vryburg	24°45'	26°08'	AF177118
28	479/96	1996	<i>Canis familiaris</i>	Limpopo	Thabazimbi	27°24'	24°43'	AF303070
29	536/96	1996	<i>Canis familiaris</i>	Mpumalanga	Carolina	30°33'	25°57'	EF686057
30	373/97	1997	<i>Canis familiaris</i>	Mpumalanga	Barberton	31°48'	25°42'	AF303069
31	224/98	1998	<i>Canis familiaris</i>	Mpumalanga	Ermelo	29°59'	26°31'	AF177098
32	208/99	1999	<i>Canis familiaris</i>	Limpopo	Waterberg	28°21'	24°35'	EF686061
33	596/99	1999	<i>Canis familiaris</i>	Mpumalanga	Piet Retief	30°45'	27°15'	AF303063
34	675/99	1999	<i>Canis familiaris</i>	Northwest	Mankwe	27°23'	25°06'	AF303071
35	733/99	1999	<i>Canis familiaris</i>	Northwest	Brits	27°33'	25°14'	AF303067
36	1004/99	1999	<i>Canis familiaris</i>	Limpopo	Polokwane	29°14'	23°43'	EF686052
37	1041/99	1999	<i>Canis familiaris</i>	Mpumalanga	Wakkerstroom	30°32'	27°04'	EF686058
38	273/00	2000	<i>Canis familiaris</i>	Limpopo	Polokwane	29°24'	24°03'	EF686065
39	572/00	2000	<i>Canis familiaris</i>	Limpopo	Potgietersrus	28°10'	22°58'	EF686066
40	582/01	2001	<i>Canis familiaris</i>	Mpumalanga	Piet Retief	30°48'	27°42'	EF686072
41	644/01	2001	<i>Canis familiaris</i>	Mpumalanga	Barberton	31°35'	25°37'	EF686078
42	42/01	2001	<i>Canis familiaris</i>	Limpopo	Musina	29°47'	22°33'	EF686067
43	224/03	2003	<i>Canis familiaris</i>	Limpopo	Ellisras	28°12'	22°42'	EF686111
44	187/04	2004	<i>Canis familiaris</i>	Mpumalanga	Nkomazi	31°40'	25°21'	EF686102
45	606/04	2004	<i>Canis familiaris</i>	Mpumalanga	Piet Retief	31°08'	27°11'	EF686131
46	729/05	2005	<i>Canis familiaris</i>	Mpumalanga	Skukuza	31°36'	24°59'	EF686120
47	757/05	2005	<i>Canis familiaris</i>	Limpopo	Ellisras	28°17'	22°47'	EF686122
48	98/06	2006	<i>Canis familiaris</i>	Mpumalanga	Ermelo	30°07'	26°05'	EF686125
49	136/06	2006	<i>Canis familiaris</i>	Limpopo	Thohoyandou	30°28'	22°58'	EF686126
50	288/06	2006	<i>Canis familiaris</i>	Limpopo	Giyani	31°8'	23°56'	EF686128
51	341/06	2006	<i>Canis familiaris</i>	Limpopo	Louis Trichardt	29°54'	23°2'	EF686150
52	197/06	2006	<i>Canis familiaris</i>	Limpopo	Sibasa	30°28'	22°58'	EF686152

Key

Virus No.	1	~	25	mongoose rabies viruses
Virus No.	26	~	52	canid rabies viruses
Virus No.	1	~	5	All from Zimbabwe (Nel <i>et al.</i> , 2005)
Virus No.	6	~	52	All from South Africa (Nel <i>et al.</i> , 2005; Zulu <i>et al.</i> , 2009)

2.3 Results

2.3.1 Viral isolation and monoclonal antibody typing

Fluorescent antibody test (FAT) was performed to confirm the presence of lyssavirus antigen considering that these isolates had been in storage at -80°C for 2~3 years. The three virus isolates showed typical bright apple-green fluorescent antigen, varying in size and in 100% fields of the smear through FAT. The reactivity of South African rabies isolates using a panel of anti-N-mAbs is shown in Table 2.2.

The median survival days were 8.5 days in canid, 7.5 days in mongoose and 6 days in spill over isolates. The mouse inoculation test was used to amplify viral antigen and the survival curve of each group was evaluated by monitoring the development and progress of clinical signs. Although MIT is not a way of evaluating pathogenicity, the mice survival curve of South African rabies viruses exhibited no significant difference by Log-rank (Mantel-Cox) test. All suckling mice deaths were observed at 17 days post infection (DPI) (canid and mongoose isolates) and 14 DPI (spill over isolate) (Figure 2.3). FAT test was performed and 23 out of 24 brains from dead mice (one negative result was from a mouse succumbed at 3 DPI in spill over group) showed positive results at the end point of experiment.

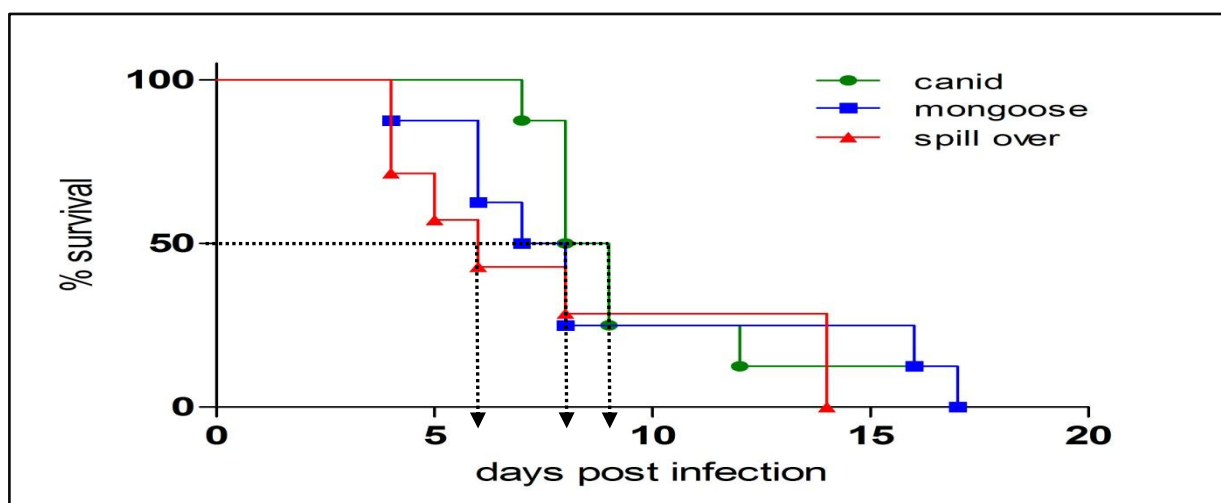


Figure 2.3 Mice mortality pattern of canid, mongoose and spill over isolates of 3-day-old outbred suckling BALB/c mice ($n=8$ per group) injected intracerebrally with 10% brain suspensions. Mortality was recorded daily basis and the Kaplan-Meier survival curves were established.

2.3.2 PCR and phylogenetic analysis

PCR amplicons were obtained with the combination of ViVMF/L(-) primer to amplify the complete G-protein encoding gene (Figure 2.4). The PCR products were sequenced and analyzed for amino acid differences in the known and described pathogenic domains as described in Materials and Methods 2.2.2.5. The nucleotide sequences obtained were edited [see Appendix 1 (1518 bp)] and the phylogenetic tree generated is shown in Figure 2.5. Both mongoose (lab ref No. 22/07) and spill over isolates (lab ref No. 198/08) belonged to a cluster of typical South African mongoose rabies (group 4), which is the most prevalent lineage identified in yellow mongooses in the Free State and Northern Cape (Nel *et al.*, 2005). The canid rabies biotype (lab ref No. 143/07) was part of a cluster of a typical canid virus from a dog-rabies endemic area, that is, 'Limpopo, Mpumalanga and North West provinces' and is the dominant canid variant encountered in this country (Zulu *et al.*, 2009).

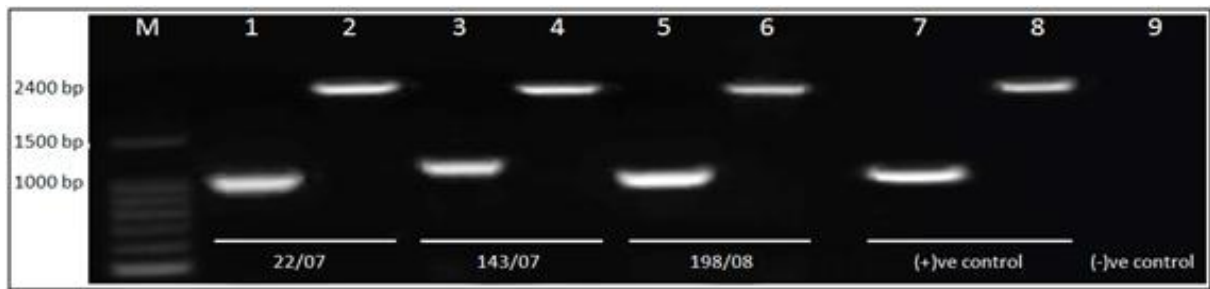


Figure 2.4 One per cent agarose gel stained with ethidium bromide and visualized by UV light. Lanes 1, 3 and 5 are hemi-nested PCR products (~ 1000 bp), whereas lane 2, 4 and 6 are the PCR products of the complete G genes (lane 7 and 8; positive controls and lane 9; negative control). Canid rabies biotype (lab reference number 77/10) and nuclease free water were used as positive and negative controls, respectively. A 100 bp DNA ladder was used for molecular weight marker (M) in lane 1.

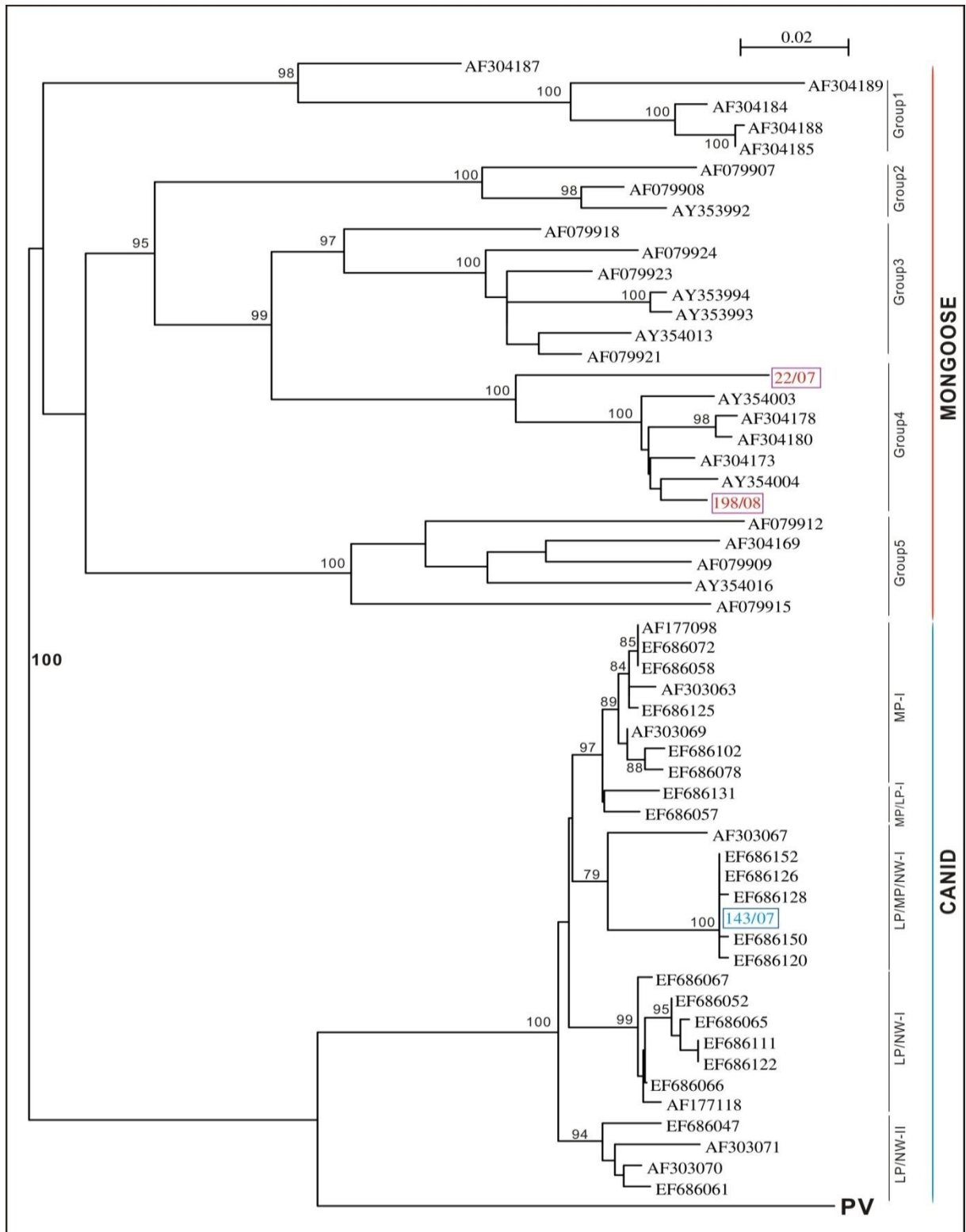


Figure 2.5 A neighbour-joining tree constructed from an alignment of 592 bp nucleotide sequences encompassing the cytoplasmic domain of the G-protein gene and the G-L intergenic region of canid and mongoose rabies biotypes from Zimbabwe and South Africa. Bootstrapping of 1,000 trials was applied and only node confidence limits of $\geq 70\%$ were considered significant. The scale bar indicates nucleotide substitutions per site.

Key–LP-Limpopo, NW-Northwest, MP-Mpumalanga

2.3.3 Comparison of pathogenic domains on glycoprotein

The complete G-protein (503 amino acids) of each virus except the signal peptide domain (19 amino acids) was used to confirm the homology of nucleotide and amino acid sequences of the G-protein amongst the three South African virus isolates. Nucleotide analyses of the complete G-protein genes demonstrated 95.19% nucleotide identity in the G-protein encoding gene between mongoose and the spill over isolates (1445/1518 nucleotide identity). The nucleotide homologies for the canid/mongoose and canid/spill over isolates were 85.90% and 86.95%, respectively (Table 2.5, Appendix 1). On the other hand, there were 17 amino acid differences (17/503, 3.38% divergence) between mongoose and spill over isolates. An amino acid identity of 91.65% (mongoose versus canid isolates) and 92.24% (canid versus spill over isolates) were shown in this analysis (Table 2.5, Appendix 2). This high homologous nucleotide and amino acid levels probably indicate that spill over isolate is originated from mongoose biotype and thus minimal changes occurring during host switch events and this was further confirmed by monoclonal antibody typing (Table 2.2). The homology was lower when canid and mongoose isolates were compared, and similar data was obtained in the comparison of canid and spill over isolates.

Table 2.5 Percentage nucleotide and amino acid identity of the complete G-protein gene of South African rabies isolates used in this study.

South African RABV isolate			Nucleotide	Amino acid
Mongoose	vs.	Spill over	95.19% (1445/1518 nucleotide)	96.62% (486/503 amino acid)
Canid	vs.	Mongoose	85.96% (1305/1518 nucleotide)	91.65% (461/503 amino acid)
Canid	vs.	Spill over	87.02% (1321/1518 nucleotide)	92.24% (464/503 amino acid)

The amino acid residues which are known as pathogenic determinants on G-protein ectodomain of the South African virus isolates and laboratory fixed RABV strains were compared in order to determine the difference of pathogenic domains in this envelope protein. Comparisons of the amino acid differences of the G-protein are shown in Table 2.6 and it is evident that no amino acid changes practically at specific positions of G-protein which are responsible for pathogenicity amongst these rabies viruses (Table 2.6).

Table 2.6 Comparisons of amino acid residues of the pathogenic determinants in the G-protein of the South African RABV and fixed laboratory strains (CVS and ERA).

Region of G-protein	South African RABV isolates			Fixed laboratory strains		Reference
	22/7 Mongoose	143/7 Canid	198/8 spill over	CVS AF406694	ERA AF406693	
Amino acid 333	Arginine	Arginine	Arginine	Arginine	Arginine	Jackson, 1991; Lafay <i>et al.</i> , 1991
Amino acid 330	Lysine	Lysine	Lysine	Lysine	Lysine	Coulon <i>et al.</i> , 1998
Amino acid 318	Phenylalanine	Phenylalanine	Phenylalanine	Phenylalanine	Phenylalanine	Langevin and Tuffereau, 2002
Amino acid 352	Histidine	Histidine	Histidine	Histidine	Histidine	Langevin and Tuffereau, 2002
Amino acid 194	Asparagine	Asparagine	Asparagine	Asparagine	Asparagine	Faber <i>et al.</i> , 2005

2.4 Discussion

This part of the study was undertaken to genetically characterize and identify pathogenic determinants in three South African rabies isolates. The presence of lyssavirus antigen of rabies biotypes (canid, mongoose and spill over), based on FAT was confirmed by MIT. The RABV biotype was confirmed through nucleotide sequence analysis and monoclonal antibody typing. The three South African isolates showed that genetic variations due to locality of origin of the samples (Nel *et al.*, 2005; Zulu *et al.*, 2009).

A recent study demonstrated that the incubation period prior to the time the mice succumbed to rabies virus infection is dependent on the dose of inoculants (Markotter, 2007). Moreover, a longer incubation period was observed when lower amounts of virus were introduced, irrespectively of the route of inoculation. The mouse inoculation test in this study was performed only via intracerebral route with crude preparation of brain material i.e. dose of virus not known. The results obtained by using Kaplan-Meier survival analysis showed that there were no statistically significant differences in survival curves amongst three RABV isolates. The early death was observed in the spill over group at 3 DPI, however, it might be due to bacterial contamination or other technical errors (Koprowski, 1996). Although, the titre of viral infection for inoculations was unknown, the data of MIT showed analogous patterns of death irrespectively of biotypes used.

The G-protein gene of the mongoose isolate and that of the spill over isolate were homologous 95.19%. At amino acid level, the genetic divergence between mongoose and spill over isolates was 3.38% (Table 2.5). This high level of homology indicated that the spill over isolate in this study is of mongoose origin and minimal changes occurred during host switch events. In contrast, the canid isolate were 14.04% and 12.98% nucleotide divergence apart from the mongoose and spill over isolates, respectively (Table 2.5). This finding was supported by the phylogenetic analysis which indicated canid and mongoose rabies biotypes are independently maintained and transmitted in South Africa.

Previous studies using the fixed laboratory CVS strain showed that reduced pathogenicity is associated with RABV G-protein and point mutations in the G-protein gene leading to the replacement of arginine at position 333 generated avirulent viruses with a restricted capacity to propagate in the CNS (Dietzschold *et al.*, 1983; Jackson, 1991; Lafay *et al.*, 1991). The double mutation of lysine at position 330 and arginine at position 333 to asparagine and methionine respectively, was apathogenic for adult mice and the double mutant was able to infect BHK and neuroblastoma cells and freshly prepared embryonic motor neurons, albeit with a lower efficiency than the CVS strain (Coulon *et al.*, 1998). Substitutions at positions at 318 or 352 in G-protein ectodomain completely abolished virus interaction with p75NTR receptor as either a soluble or membrane-anchored receptor (Langevin and Tuffereau, 2002). Although a recent study showed that the RABV, and paradoxically so, does not require p75NTR for binding or infection, indicating that p75NTR may not be essential and that other receptors could be required for virus infection (Tuffereau *et al.*, 2007). Moreover, the mutation of asparagine at position 194 in the G-protein to AAG or AAA (Lys-194) was associated with increased pathogenicity (Faber *et al.*, 2005). Therefore, specific amino acid changes of G-protein ectodomain play a crucial role in lyssavirus pathogenicity and all three South African RABV isolates exhibited the same amino acid residues at positions (arginine at 333, lysine at 330, phenylalanine at 318, histidine at 352 and asparagine at 194) which are known as pathogenic domains in lyssavirus. There were no apparent variations in pathogenicity of RABV isolates. Other pathogenic determinants which are possibly involved in the pathogenicity of South African RABV must be sought for.

CHAPTER 3

***In vitro* neurosurvival/apoptotic properties of
COOH terminus of G-protein of South African
RABV isolates as assessed in
a recombinant lentiviral system**

3.1 Objective

The objective of the experiment was to evaluate the neuroprotective properties of Cyto-G of the South African isolates expressed in neuronal cells by recombinant lentiviruses.

This was achieved by grafting the carboxyl terminal of the cytoplasmic domain in a virulent RABV CVS backbone, the characterization of the expressed chimeric genes and phenotypes (neurosurvival or apoptosis) driven by these chimeric constructs were evaluated to determine the pathogenicity of South African isolates in a recombinant lentivirus system.

3.2 Materials and methods

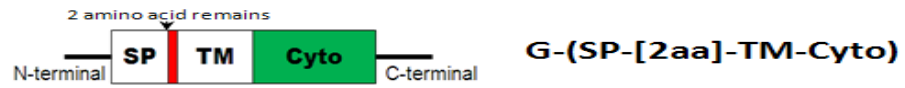
3.2.1 Design of plasmid and oligonucleotides

3.2.1.1 Plasmid

The plasmid used for the study is based on the cytoplasmic domain of G-protein of a virulent laboratory fixed rabies strain (CVS). The nucleotide sequence of the laboratory RABV CVS strain (GenBank Acc. number: AF406694), a pathogenic RABV strain causing fatal encephalitis in mice, was previously cloned and its ectodomain was deleted. The plasmid with the deleted ectodomain resulted in delta EC (Δ EC), for the evaluation of neuroprotective properties (European Patent WO 10/116258A1). Subsequently, the construct of G-protein delta EC (G- Δ EC) was delivered in a lentivirus vector plasmid (pLenti 6.3/V5-TOPO) using pLenti 6.3/V5-TOPO TA cloning kit (Invitrogen, USA), namely AF5, for the neuroprotection assay (courtesy of Dr. Z. Khan, Unité de Neuroimmunologie Virale, Institut Pasteur). This plasmid system has a neurite outgrowth promoting effect and provides a means for inducing and/or stimulating neurite outgrowth, following RABV G construct expression (Figure 3.1).

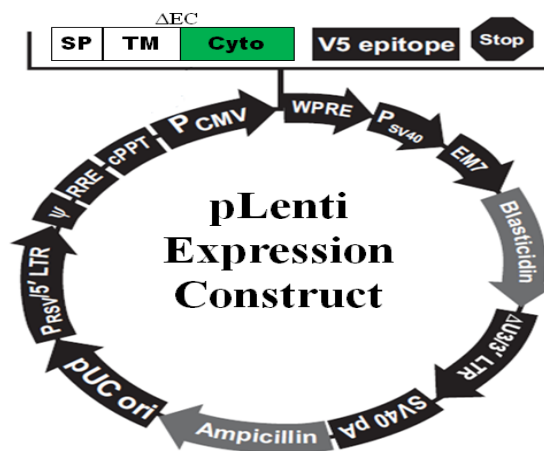


(A) G survival



(B) G survival-ΔEC

SP: Signal Peptide EC: Ectodomain
 TM: Transmembrane domain Cyto: Cytoplasmic domain



(C) pLenti expression construct containing ΔEC

Figure 3.1 Schematic diagrams of the complete G-protein and RABV G gene construct. (A) Complete G-protein (524 amino acids are translated including signal peptide domain) of RABV CVS strain which contains the signal peptide domain, ectodomain, transmembrane domain and cytoplasmic domain. (B) The structure of G survival ΔEC, derived from complete G-protein, 437 amino acid residues of ectodomain were deleted and the cytoplasmic tail of the G-protein is the neurovirulent RABV (CVS strain) genetic back ground. (C) pLenti expression construct containing G-survival ΔEC, based on pLenti6.3/V5-TOPO vector (Invitrogen, USA).

3.2.1.2 Oligonucleotides for mutagenesis

The mutagenic oligonucleotide primers based on sequences of the cytoplasmic domains of G-proteins (Table 3.1) and the synthetic 46-base oligonucleotides were synthesized by Eurogentec Co. (Belgium) and used without further purification. For the mutant strand synthesis, 125 ng per each primer was used. The sequences of mutagenic oligonucleotide primers for this study, were based on the sequence of the cytoplasmic domain of virulent laboratory RABV strain (CVS-NIV) (GenBank Acc. number: AF406694), whereas the sequence of the ERA-NIV strain (attenuated

laboratory strain, GenBank Acc. No. AF406693) was used to generate G construct for a negative control of neurite outgrowth and a positive control of apoptotic assay (Table 3.2).

Table 3.1 Last 12 amino acid residues and nucleotide sequences of the cytoplasmic domain of laboratory RABV strains (CVS-NIV and ERA-NIV) and South African RABV isolates (canid, mongoose and spill over).

RABV CVS-NIV (GenBank Acc. No. AF406694)												
TGG	GAA	TCA	CAC	AAG	AGT	GGG	GGT	GGT	ACC	AGA	CTG	TGA
W	E	S	H	K	S	G	G	Q	T	R	L	stop
RABV ERA-NIV (GenBank Acc. No. AF406693)												
TGG	GAA	TCA	CAC	AAG	AGT	GGG	GGT	GAG	ACC	AGA	CTG	TGA
W	E	S	H	K	S	G	G	E	T	R	L	stop
South African canid rabies isolate (Lab ref No.143/07)												
TGG	GAA	TCA	TAC	AAG	AGT	GGG	GGT	GAG	ACC	AGA	CTG	TGA
W	E	S	Y	K	S	G	G	E	T	R	L	stop
South African mongoose rabies isolate (Lab ref No. 22/07)												
TGG	GAA	TCA	TAC	AAG	AAT	GGG	GAG	GAG	ACC	AGA	ATG	TGA
W	E	S	Y	K	N	G	E	E	T	R	M	stop
South African spillover rabies isolate (Lab ref No. 198/08)												
TGG	GAA	TCA	TAC	AAG	AAT	GGG	GGT	GAG	ACC	AGA	ATG	TGA
W	E	S	Y	K	N	G	G	E	T	R	M	stop

Table 3.2 Sequences of two complementary oligonucleotide primers containing the desired mutation for mutagenesis. The underlined and bold sequences (letters) represent the target region to be mutated.

Construct	Mutagenic oligonucleotide	Sequence
ERA	ERA1	5'- <u>TGGGAATCACACAAGAGTGGGGGTG</u> AACCAGACTGTGAGGCCAAG-3'
	ERA2	3'- <u>ACCCTTAGTGTGTTCTCACCCCACT</u> CTGGTCTGACACTCCGGTTC-5'
Canid	canid1	5'- <u>TGGGAATCATAACAAGAGTGGGGGTG</u> AACCAGACTGTGAGGCCAAG-3'
	canid2	3'- <u>ACCCTTAGTATGTTCTCACCCCACT</u> CTGGTCTGACACTCCGGTTC-5'
Mongoose	mongoose1	5'- <u>TGGGAATCATAACAAGAATGGGGAGGAGACCAGAATGTGA</u> GGCCAAG-3'
	mongoose2	3'- <u>ACCCTTAGTATGTTCTTACCCCTCCTCTGGTCTTACACT</u> CCGGTTC-5'
Spill over	spill over1	5'- <u>TGGGAATCATAACAAGAATGGGGGTGAGACCAGAATGTGA</u> GGCCAAG-3'
	spill over2	3'- <u>ACCCTTAGTATGTTCTTACCCCACTCTGGTCTTACACT</u> CCGGTTC-5'

3.2.2 Recovery of recombinant viruses and viral characterization

3.2.2.1 Mutagenesis

The QuikChange Lightning Site-Directed Mutagenesis Kit (Stratagene, La Jolla, CA, USA) was utilized to construct the plasmid mutation. The mutant clones are generated by amino acid substitutions using the enzyme technology, called *pfuUltra* high-fidelity DNA polymerase for mutagenic primer-directed replication of plasmid strands and *Dpn* I endonuclease is used to digest the parental DNA template. In this assay, a reaction was set up to include: 5 µl of 10X reaction buffer, 50 ng of pLenti TOPO expression construct (AF5) as a backbone of vector, 125 ng of oligonucleotide primers for both directions, 1 µl of dNTP mix, 1.5 µl of QuikSolution reagent and 1 µl of QuikChange Lightning Enzyme, which is a derivative of *PfuUltra*, high-fidelity DNA polymerase for mutagenic primer-directed replication of both plasmid strands and made up to 50 µl with nuclease free water. The mutant strand synthesis reaction mixture was subjected to the following parameters in a thermocycler; an initial denaturation at 95°C for 2 minutes, and 30 cycles of 95°C for 20 seconds, 60°C for 10 seconds and 68°C for 30 seconds with a final extension step at 68°C for 12 minutes, and incubated at 4°C.

A volume of 2 µl of *Dpn* I restriction enzyme was added to each reaction to digest parental methylated (hemi-methylated) DNA and mixed thoroughly. Then, the reaction mixture was spun down briefly and incubated at 37°C for 5 minutes for the digestion of the parental supercoiled double-stranded DNA. The ligation reaction was transformed into XL10-Gold ultracompetent cells (Stratagene, La Jolla, CA, USA). The transformation was performed with 45 µl of XL10-Gold competent cells and 2 µl of the ligation reaction, and then gently swirled and incubated on ice for 30 minutes. Heat-shock treatment was subjected to the transformants at 42°C for 30 seconds in a water bath. Then, 500 µl of preheated super optimal broth (S.O.C medium) (Appendix 4) was added and the tube was incubated at 37°C for 1 hour with shaking at 225~250 rpm. The transformants were then spread on trypticase-yeast extract-maltose medium (T.Y.M medium) (Appendix 4) with Ampicillin (100 µg/ml) agar plates and incubated overnight at 37°C. The colonies grown on the plate were collected and resuspended in T.Y.M with Ampicillin (200 µg/ml) liquid broth medium and further incubated overnight at 37°C with shaking at 180 rpm. The plasmid DNA was applied to QIAprep[®] Spin Miniprep column system, which uses silica membrane technology as described in the Qiagen Spin Miniprep protocol to obtain high-copy

plasmid DNA from overnight *E.coli* cultures in medium. Then, PCR reactions were performed to confirm whether the gene of interest is in the frame with the C-terminal tag or not. Moreover, four clones (ERA, canid, mongoose and spill over) were sequenced to confirm their identities and ensure the absence of any aberrant lentiviral vector recombination (Appendix 3).

3.2.2.2 Re-transformation

The plasmids recovered through Miniprep procedures were retransformed into Stbl3 *E.coli* (Invitrogen, USA) to isolate plasmid DNA for the production of a recombinant lentivirus. The extracted Miniprep plasmid (1 μ l) was added into 5 μ l of Stbl3 chemically competent *E.coli*. It was incubated on ice for 30 minutes and treated heat-shock at 42°C for 30 seconds. Pre-warmed S.O.C medium (250 μ l) was added into the competent cell mixture and shaken at 37°C for an hour. Then, the cell mixture was spread on T.Y.M-Ampicillin agar plates. Highly purified plasmids were extracted using PureLink HiPure Plasmid filter MaxiPrep (Invitrogen, USA), which is by anion-exchange resin to purify plasmid DNA and provides high-quality plasmid DNA for transfection of eukaryotic cells, according to the manufacturer's manual. Once purified plasmids were obtained, genes encoding G-protein were sequenced by Eurofins MWG (France) to confirm the sequences prior to lentivirus isolation.

3.2.2.3 Lentiviral vectors and expression of the chimeric glycoprotein

Lentivirus vectors are commonly generated in human embryonic kidney (HEK) 293 T-cells, which are a highly transfectable cell line (Cockrell and Kafri, 2007). Therefore, vectors were produced by transient transfection, a technique for an introduction of DNA into mammalian cells, with the following modifications. A total of 5×10^6 cells were seeded in 10 cm diameter Cell⁺ dishes (Sarstedt, Germany) using Dulbecco's Modified Eagle Medium with Glutamax-1 (DMEM+Glutamax, Invitrogen) with 10% fetal calf serum and the penicillin (10,000 IU/ml) and streptomycin (10 mg/ml) mixture at 37°C with 5% CO₂. The culture medium was replaced 3~4 hours prior to transfection (70~80% confluent) and the transfection was conducted by using the calcium phosphate method, the common chemical-based transfection via the formation of a calcium phosphate-DNA precipitate. A total of 13 μ g highly purified plasmid DNA obtained through MaxiPrep step was used for transfection of one plate: 13 μ g of pMDL gag/pol RRE plasmid, 3 μ g of pRSV-Rev plasmid for viral producing and 3.75 μ g of pMD-VSVG which is

the envelope G-protein expression plasmid. Then, 125 μ l of 1 M CaCl_2 (Sigma, USA) and nuclease free water were added to make final volume of 500 μ l. The mixture was transferred to a 15 ml plastic tube, which contained 500 μ l of 2X HEPES buffered saline (Sigma, USA) in a drop wise manner to form a fine precipitation with air-bubble and the medium was replenished after 14~16 hours of the precipitation. In the mean time, the level of transfection was evaluated by using GFP (Green Fluorescent protein) through flow cytometry and assayed using the CellQuest™ Pro (BD Biosciences) software.

The HEK 293 T-cells, which contained vector particles, were collected 48 hour post transfection and the debris (impurities) were removed by centrifugation and filtration using 0.45 micron filter. Then, the concentrated vector particles were collected by ultracentrifugation at 4°C and 22,000 rpm for 90 minutes. After the ultracentrifugation, the pellet was resuspended in 50 μ l, 1% bovine serum albumin (BSA) containing PBS (PBS/BSA). It was incubated on ice for 1 hour, aliquoted into siliconized 1.5 ml plastic tubes and stored at -80°C for long term storage. The titre of lentiviral vectors were calculated by using an HIV-1 P24 ELISA Kit (Perkin-Elmer Life Science Inc., Boston, MA, USA).

3.2.3 Characterization of the expressed chimeric genes

3.2.3.1 Quantitative real-time polymerase chain reaction

Neuroscreen-1(Cellomics, USA), a subclone of PC 12 and a widely used cell line derived from rat pheochromocytoma that serves as a standard model system for neurons, was harvested for 48 hours after the infection of recombinant lentiviruses (250 ng/well). Then, total RNA was extracted using the RNeasy Mini Kit (Quiagen) as described in the manufacturer's guideline. Neuroscreen-1 cells were washed with 3 ml of warm PBS and lysed by adding 350 μ l of lysis buffer. The isolated viscous lysate was collected and homogenized by using the QIAshredder spin columns (Quiagen). Then, 50 μ l of RNase-free water was directly added to the spin column membrane and the concentration of RNA was measured using a spectrophotometer ND-1000 (NanoDrop Technologies, USA). The complementary DNA was synthesized from the 500 ng of extracted RNA using oligo dT primer, 200 IU of SuperScript II (Invitrogen) and subjected to cDNA synthesis with the following cycling parameters: 25°C for 10 minutes, 42°C for 95 minutes and 70°C for 15 minutes and 2 IU/ μ l of RNaseH (Invitrogen) was added to purify

cDNA products. The PCR amplicons were carried out in a total volume of 25 μ l with 12.5 μ l of Power SYBR Green PCR master mix (Applied Biosystems), 10 μ l of nuclease free water, 2 μ l of template cDNA and 2.5 μ l of each forward and reverse primer (0.1 μ g/ μ l), which is shown in Table 3.3. Amplification of target DNA and detection of PCR products were performed with 7500 Fast Real-Time PCR system (Applied Biosystems, USA); 10 minutes at 95°C, 40 cycles of 95°C for 15 seconds and 60°C for 60 seconds. The RNA quantification was normalized to 18S rRNA as a reference gene (housekeeping gene) and the amplification of the target sequence was detected by an increase of fluorescence above a baseline with no or little change in fluorescence.

Table 3.3 Gene-specific primers for lentivirus vectors transcription analysis.

primer	Sequence	Remark
qPCRLenti (Forward)	AGACGCCATCCACGCTGTTTTGACCTCCATAG	In plasmid sequence after transcription start site
qPCRLenti (Reverse)	GTGTTGCGTAGGTTCTGATCGATTGACTCTTC	In RABV G cytoplasmic domain

3.2.3.2 Protein concentration and Western blotting

The recombinant lentivirus infected Neuroscreen-1 cells were lysed individually in 300 μ l of RIPA buffer (50 mM Tris-HCl, pH 8.0, containing 150 mM sodium chloride, 1.0% Igepal[®] CA-630 (NP-40), 0.5% sodium deoxycholate, 0.1% sodium dodecyl sulfate, Sigma) and Protease Inhibitor Cocktail and Phosphatase Inhibitor Cocktail Tablets (Roche, Germany), and 25 units of endonuclease (Benzonase[®] Nuclease, Novagen) per microliter were added to degrade all forms of DNA and RNA. Protein concentrations generally are determined and reported with reference to standards of a common protein such as BSA. A series of dilutions of known concentration were prepared to determine standard curve, bicinchoninic acid (BCA) protein assay was used to detect and quantitation of total protein using Micro BCA[™] protein assay kit (Pierce Biotechnology, USA) according to the manufacturer's instruction. A standard curve was established to quantify the protein from the lysate reactions. After 2 hours incubation at 37°C, the resultant purple colour was measured at 562 nm absorbance with an optical reader.

All these extracts were subjected to detect the G-protein expression level by immuno blotting. One hundred microliters of lysate was mixed with 33 μ l of 4X lithium dodecyl sulfate sample buffer (LDS, Invitrogen) and 15 μ l of 10X NuPAGE[®] sample reducing agent (final conc. 1X),

which contained 500 mM dithiothreitol (Invitrogen). The reaction mixture was then boiled at 100°C for 5 minutes and cooled down on ice immediately. Proteins were separated on precast 4%~20% gradient polyacrylamide gels (Pierce Biotechnology, Rockford, IL, USA) for protein electrophoresis in BupH Tris-HEPES-SDS running buffer dissolved in 500 ml of deionized water at 120 volt for an hour. Polyvinylidene difluoride membranes (PVDF, Hybond-P; GE HealthCare) used widely in immunoblotting applications were rinsed with absolute ethanol and soaked in 1X NuPAGE® Transfer Buffer (Invitrogen). The gel, which was sandwiched between a sheet of the PVDF membrane, several sheets of blotting papers and blotting pads, was assembled on to a blotting module (XCell™ II Blot Module, Invitrogen). Then, the transferring module was electroeluted at 50 volt for 1 hour on ice. The membrane was blocked with 5% BSA in PBS -0.1% Tween buffer (PBST). The membrane was then incubated overnight at 4°C with non-commercial primary antibody purchased from Proteogenix, France (Table 3.4) in PBST on the bidirectional rotator. The primary antibody was decanted and washed 10 times with PBST buffer for every 5 minutes at room temperature on the shaker. The membrane was incubated with Donkey Anti-Mouse IgG horseradish peroxidase conjugate as a secondary antibody (Jackson Immuno Research, Code No. 715-036-150) for an hour and washed 10 times again with PBST as described above. The expressed protein was developed with Super Signal West Femto kit (Pierce Biotechnology, Rockford, IL, USA), which is a sensitive enhanced chemo luminescent substrate for detecting horseradish peroxidase (HRP) on immunoblots, and subjected to G:Box gel documentation and analysis system (Syngene, Cambridge, UK).

Table 3.4 Antibodies specific for peptides encoded by the cytoplasmic domain of G-protein used in Western blotting.

Antibody	Peptides used for immunization	Species
V17	N H 2 - G K I I S S W E S H K S - C O O H	Mouse monoclonal antibody
V18	N H 2 - G K I I S S W E S H K S - C O O H	Mouse monoclonal antibody
V9	N H 2 - T G R E V S V T P Q S G K I - C O O H	Rabbit polyclonal antibody

3.2.3.3 Immunocytochemistry assay

Infected Neuroscreen-1 cells (60 ng/well) were grown in RPMI 1640 medium supplemented with 5% heat-inactivated fetal calf serum (FCS), penicillin (10,000 IU/ml), streptomycin (10 mg/ml) and 200 mM L-glutamine (100X, Invitrogen) on coverslips. After reaching confluence (~70%), Neuroscreen-1 cells were fixed in 4% paraformaldehyde in PBS for 20 minutes at room temperature and washed with PBS at 48 hours post infection. The samples were incubated for 20

minutes at room temperature in 0.3% Triton X-100-PBS and washed once with PBS. A volume of 500 μ l of MS blocking buffer (1X PBS, 2% of BSA and 5% of fetal calf serum) was added to the reaction mixture and then incubated at room temperature. The blocking buffer was replaced by 300 μ l of antibody (polyclonal antibody V9 (1/50 dilution)) with MS blocking buffer and incubated overnight at 4°C. The antibody was washed three times with PBS and the fluorescence was detected by incubation for 2 hours with 300 μ l of goat-anti mouse antibody labeled with Alexa 488 (1/500 dilution) and goat-anti rabbit labeled with Alexa 488 (1/500 dilution) with 5% CO₂ at 37°C. A volume of 300 μ l of Hoescht 33342 (1/200 dilution) was added to cells to stain nucleus and incubate another 20 minutes. The plate was washed with PBS and mounted on the slide glass and examined the distribution of G-protein with Leica DM5000B microscope.

3.2.4 Neuroprotection assay

3.2.4.1 Neurite outgrowth assay

Neurons (also called *nerve cells*) are highly specialized cells for the processing and transmission of cellular signals via chemical and electrical means by using different components; nucleus, soma, dendrites, axon and synapses. Neurites are referred any projections from the cell body of neurons either an axon or a dendrite. Neurite outgrowth contributes a complex wiring network, which are branched, it allows each neuron to have the ability to establish connections with multiple targets (Fig 3.2) (Mingorance-Le Meur and O'Connor, 2009).

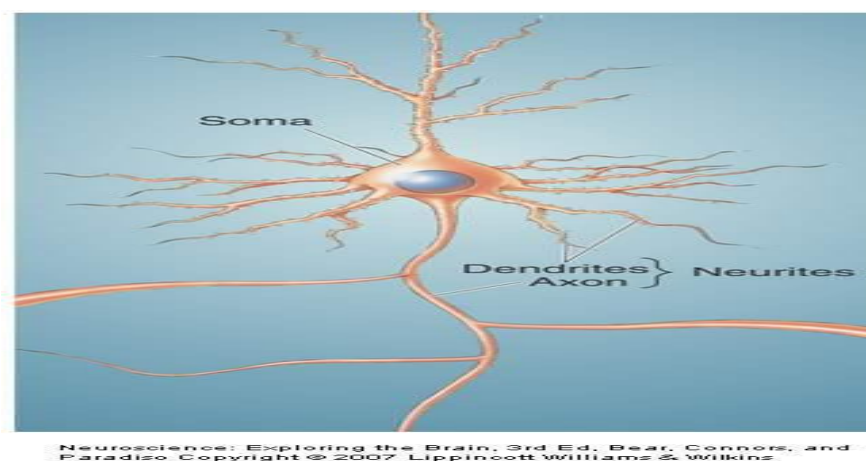


Figure 3.2 A representative of a typical neuron indicating the basic part; including soma, dendrites and axon (Bear *et al.*, 2007). Neurite refers to any filamentous or pointed outgrowth, which is either an axon or a dendrite, from the cell body of neurons. Neurite outgrowth is a fundamental process in the differentiation of neurons (Meldolesi, 2011).

Neuroscreen-1 cells were seeded in 24 well poly-D-lysine-coated tissue culture dishes (Cell Bind, Corning). The cultures were incubated at 37°C in a humidified atmosphere of 5% CO₂. After an overnight incubation, the growth media was replaced with treatment medium, which contains culture medium and 200 ng/ml of neuronal growth factor (NGF). Six hours post treatment with NGF, 60 ng of recombinant lentiviral stocks were added into each well. Cells were fixed with 4% paraformaldehyde in PBS and incubated for 30 minutes with crystal violet to visualize neurite processes at 72 hours post infections. Images were taken from cells with a Leica DM 5000B UV microscope equipped with a DC 300FX camera and analyzed data with ImageJ 1.44p, Neuron J plug in (W. Rasband, National Institutes of Health, USA; <http://imagej.nih.gov/ij>). The assay was repeated to establish reliability, and the significance of the differences between means was evaluated statistically by using GraphPad™ Prism 5 (GraphPad Software, Inc.).

3.2.4.2 Measurement of apoptosis

Early in the apoptosis process, phosphatidylserine becomes exposed on the cell surface by flipping from the inner to outer leaflet of the cytoplasmic membrane. Plasma membrane binding of Annexin V in unfixed conditions was used to detect and quantify apoptotic cells. Whilst Propidium Iodide (PI) staining is a marker of membrane permeability alteration, measuring all types of cell death including early, late apoptosis and necrosis. Apoptosis was measured by flow cytometric using the infected SK-N-SH human neuroblastoma cells. These cells (SK-N-SH) were propagated in Dulbecco modified Eagle medium (Invitrogen, USA) containing 2 mM of L-glutamine, 1 mM of Na pyruvate, 10% of fetal calf serum, 2% of bicarbonate, 100 IU/ml (penicillin) and 100 µg of streptomycin/ml at 37°C with 5% CO₂. The harvested cells were infected with 60 ng of each recombinant lentivirus stock. The infected cells were trypsinized and incubated with Annexin V conjugate (Annexin V-FITC, Trevigen) in binding buffer for 15 minutes or with PI at room temperature at 96 hours post infection. A volume of 300 µl of 1X Binding Buffer was added and centrifuged at 1000 rpm and 20°C for 5 minutes. After the centrifugation, the supernatant was aspirated with a vacuum pump and cells were resuspended in 400 µl of 1X Binding buffer and 50 µl of CellFix (BD Biosciences) prior to direct analysis by flow cytometry with a FACSCalibur (BD Biosciences). The results were analyzed using the CellQuest™ Pro (BD Biosciences) software.

3.3 Results

Part 1: Characterization of recombinant rabies viruses

3.3.1 Quantitative monitoring of gene expression level

Real-time qPCR is a reliable detection and measurement of products generated during each cycle of the polymerase chain reaction process which are directly proportionate to the amount of template prior to the start of the PCR process (Ginzinger, 2002). Quantitative gene analysis was utilized for this study to determine the genome quantity of chimeric constructs. All methods used for analysis are based on determining the threshold cycle (Ct), the fractional cycle number at which a fixed amount of mRNA is formed through PCR cycling. The threshold cycle values provide accurate measurements over a very large range of relative starting target quantities. Thus, the relative levels of mRNA transcription were measured as shown in Figure 3.3. The level of mRNA of G-spill over showed the lowest value (2.139×10^5) amongst three South African constructs, followed by G-canid (3.177×10^5) and G-mongoose chimeric constructs (3.179×10^5). The level of mRNA transcription of G-CVS construct was expressed (6.367×10^5) on average 2-fold more than that of G-canid and G-mongoose constructs.

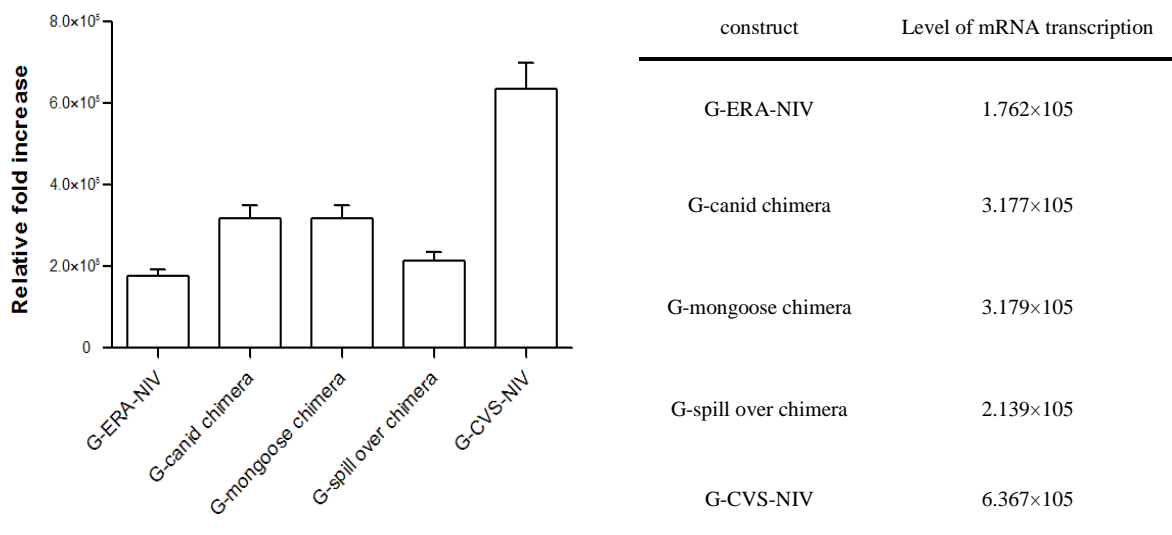


Figure 3.3 Variations in the relative abundance of mRNA transcription level in a recombinant lentivirus system by relative RT quantitative PCR at 48 hours post infection.

3.3.2 Concentration of total protein

The quantity of total protein was evaluated using micro BCA protein assay with BSA for the quantification of total protein concentration obtained. G-CVS-NIV showed the highest level of total protein concentration (3.4 $\mu\text{g}/\mu\text{l}$), on the other hand, the total concentration of protein in chimeric G-ERA-NIV was 2.1469 $\mu\text{g}/\mu\text{l}$. The chimeric mongoose construct indicated the highest level of the concentration of protein (2.63 $\mu\text{g}/\mu\text{l}$) amongst the three South African constructs followed by G-spill over (2.47 $\mu\text{g}/\mu\text{l}$) and G-canid (1.98 $\mu\text{g}/\mu\text{l}$) constructs (Figure 3.4).

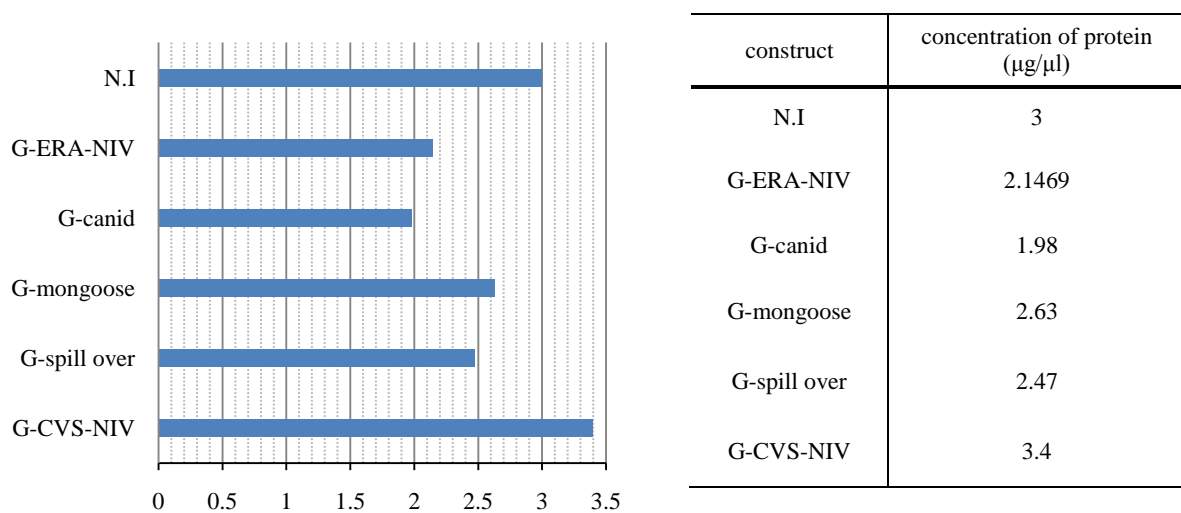


Figure 3.4 Concentrations of total protein determined using Micro BCA Protein assay Kit, which is a detergent-compatible bicinchoninic acid formulation for the colorimetric detection and evaluation of total protein. Representative results of protein contents of cellular lysates. N.I., not infected.

3.3.3 Western blotting for protein expression

The protein lysates were separated by SDS-PAGE in 4~20% gradient gel to verify the G-protein expression level by Western blotting techniques. All chimeric constructs exhibited the protein expression in lentivirus infected Neuroscreen-1 cells using the non-commercial polyclonal antibody (V9), from an immunized rabbit, directly against (or recognizes) the peptide $\text{NH}_2\text{-TGREVSVTPQSGKI-COOH}$ (Figure 3.5A). The prototype chimeric laboratory rabies strains (G-CVS-NIV and G-ERA-NIV) which have no mutations of monoclonal antibody binding sites, however, 1 or 2 amino acid residue changes on the peptides where monoclonal antibodies recognized were in South African chimeric constructs (Figure 3.5A). South African G-constructs

exhibited lower level of protein expression with non-commercial monoclonal mouse antibodies (V17 and V18) compared to G-CVS-NIV and G-ERA-NIV (data not shown). On the other hand, the homologous protein expression patterns in Neuroscreen-1 cells were presented with the polyclonal antibody (V9) (Figure 3.5B). Therefore, the homologous expression level by using the polyclonal rabbit antibody might be explained that it recognized the epitope upstream which had no mutations for binding amongst all G-constructs compared with monoclonal antibodies in this study.

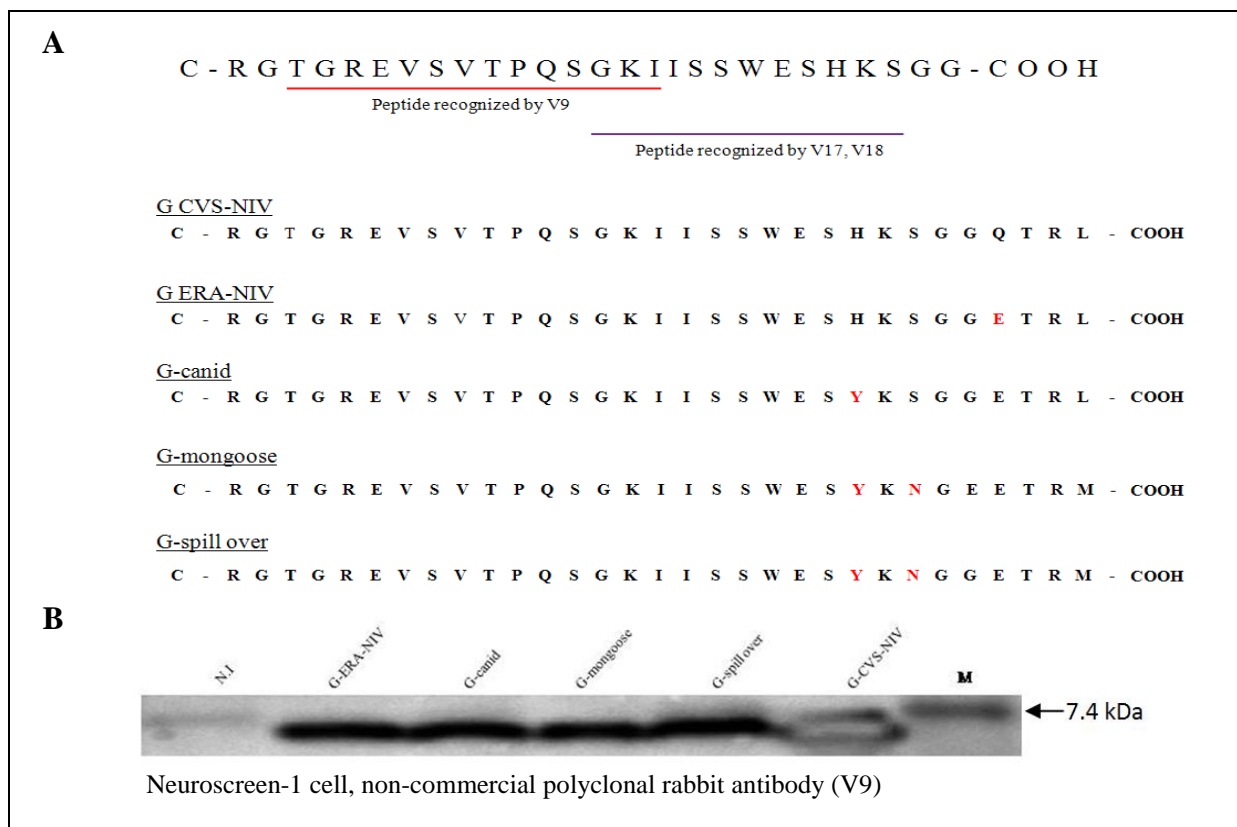


Figure 3.5 Immunoblotting analysis of G-constructs expressing recombinant lentiviruses. Proteins were separated electrophoretically on a 4~20% gel SDS-polyacrylamide gel, transferred to a PVDF membrane and detected with a specific anti-RABV G cytoplasmic domain antibody (V9). (A) Peptides which antibodies were recognized to express proteins. Polyclonal antibody (V9) recognizes NH₂-TGREVSVTPQSGKI-COOH and monoclonal antibodies (V17 and V18) recognize NH₂-GKIISWESHKS-COOH. No amino acid residue mutations in G-ERA-NIV and G-CVS-NIV on the peptides against monoclonal antibodies (V17 or V18). (B) Detection by Western blotting of cytoplasmic domain, RABV G-protein with polyclonal antibody (V9). The signal obtained for G-CVS-NIV was at saturated level. N.I., not infected.

3.3.4 Immunocytochemistry

The cellular distributions of RABV G-protein expressed were analyzed using double immunofluorescence assay in infected cells (including non-infected cells as a negative control). Nucleus was detected by Hoescht 33342 staining and G-protein expression was detected by using the polyclonal rabbit antibody used in Western blotting. After the infection with the chimeric G expressing recombinant lentiviruses, all infected cells exhibited the uniform cytoplasmic expression of G-protein (Figure 3.6).

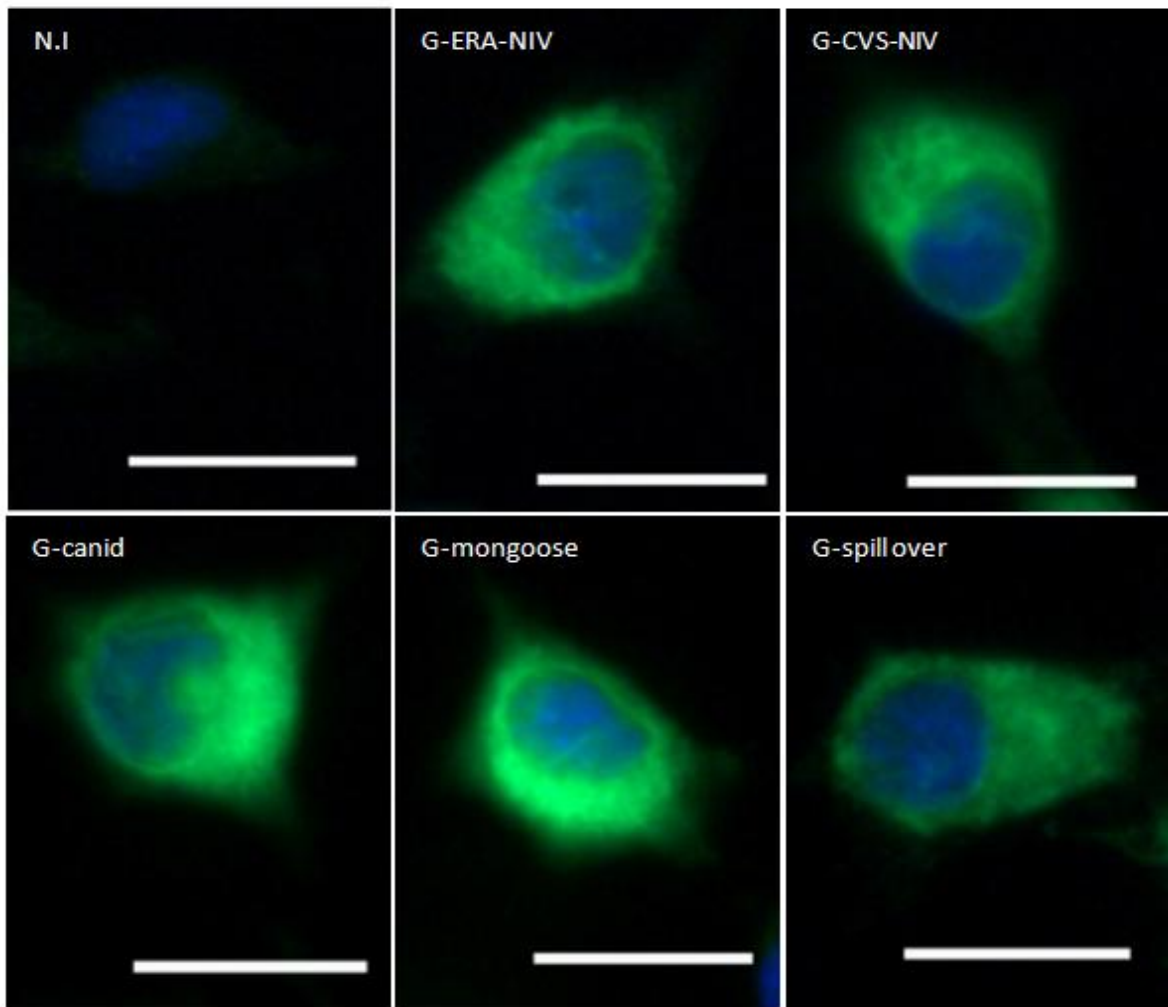


Figure 3.6 Expression of G-protein distribution of a recombinant lentivirus expressing each G-construct was detected after the infection of recombinant viruses. The cellular RABV G distribution (green) was detected by UV microscopy. The nucleus was shown in blue by Hoescht 33342 staining. N.I., not infected. Scale bars, 20 μm .

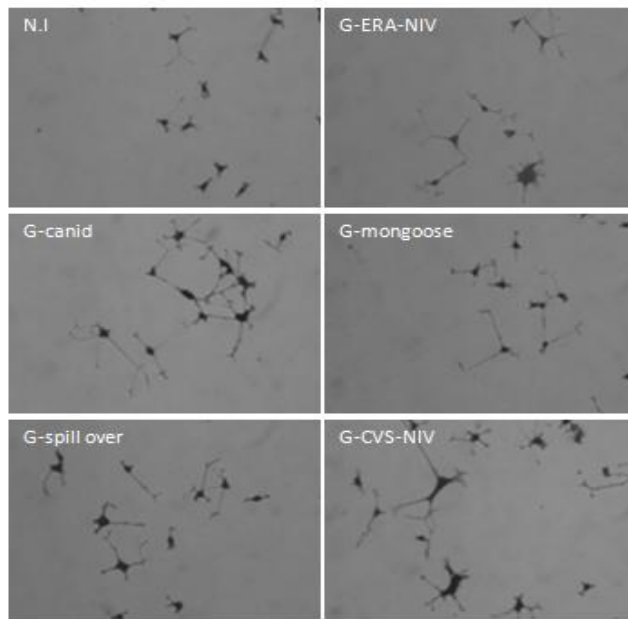
Part 2: Neuroprotection of G construct chimeras delivered by a recombinant lentivirus

3.3.5 Neurite outgrowth assay

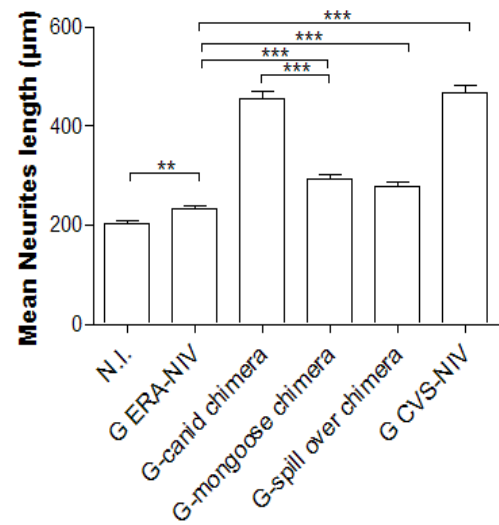
Viral vector particles based on lentivirus were generated by plasmid transfection system as described Materials and Methods 3.2.2.3. According to a previous study, virulent rabies strain induces neurite elongation (Prehaud *et al.*, 2010). Neuroscreen-1 cells exhibited a wide range of phenotypic patterns depending on the chimeric strains infected at 72 hours post infection of recombinant constructs. The average length of neurite per neuron of chimeric virulent CVS-NIV construct was 468.127 μm , a two-fold increased, compare to that of chimeric G-ERA-NIV construct (232.182 μm). The G-canid chimeric construct showed the highest neurite outgrowth (455.782 μm) amongst three South African rabies chimeric constructs, followed by G-mongoose (293.927 μm) and G-spill over constructs (277.4 μm) (Figure 3.7).

GraphPadTM Prism software was used to determine the values statistically and the threshold significance level (P value: 0.05) was defined. (If the P value is less than the threshold, the difference is ‘*statistically significant*’. If the P value is greater than the threshold, the difference is ‘*not statistically significant*’). The data indicated that there were no significant differences of the mean neurite outgrowth in the comparisons of “G-mongoose / G-spill over (P value: 0.1702)” and “G-canid / G-CVS-NIV (P value: 0.5389)”. On the other hand, statistically significant differences (P value < 0.05) were observed in other P value comparisons amongst G-constructs (Table 3.5).

A



B



C

Mean value of neurites length (µm)					
N.I	G-ERA	G-canid	G-mongoose	G-spillover	G-CVS
201.6±7.886	232.2±7.438	455.8±13.77	293.9±7.832	277.4±9.052	468.1±14.54

Figure 3.7 Neurite outgrowth of RABV infected cells. Neuroscreen-1 cells (72 hour post infection). (A) Variable different patterns of neurite outgrowth depending on the expression of the different G constructs. (B) Sustained neurite outgrowth was measured for average length of neurite with ImageJ 1.44p, Neuron J plug in. (C) The mean value of neurite length. The data shown are representative of duplicate experiments. N.I., not infected.

Table 3.5 Pairwise comparisons and statistical analysis of neurite outgrowth of G-constructs.

Pairwise comparisons of constructs		P value	Presence ^a
G-CVS	: N.I	<0.0001	+
G-ERA	: N.I	0.0057	+
G-ERA	: G-spill over	0.0002	+
G-ERA	: G-canid	<0.0001	+
G-ERA	: G-mongoose	<0.0001	+
G-ERA	: G-CVS	<0.0001	+
G-canid	: G-CVS	0.5389	-
G-canid	: N.I	<0.0001	+
G-canid	: G-mongoose	<0.0001	+
G-canid	: G-spill over	<0.0001	+
G-mongoose	: G-spill over	0.1702	-
G-mongoose	: N.I	<0.0001	+
G-mongoose	: G-CVS	<0.0001	+
G-spill over	: N.I	<0.0001	+
G-spill over	: G-CVS	<0.0001	+

^a Presence (+) of P value is indicated that P value is less than 0.05 and the presence (-) of P value is higher than 0.05.

3.3.6 Apoptosis assay

Lentivirus infected SK-N-SH human neuroblastoma cells were analyzed for the induction of cell death and apoptosis by Propidium Iodide and Annexin V staining. The mean value of apoptosis and cell death were determined statistically by using GraphPadTM Prism software (P value: 0.05). The high-level Annexin V expression was noted in cells expressing the G-construct derived from the attenuated strain G-ERA-NIV (13.94%) at 96 hours post infection. In the same condition, the level of apoptosis by cells expressing the G construct derived from the virulent strain G-CVS-NIV was 7.38%. These two constructs constituted the positive and negative controls, respectively. Amongst South African RABV G-constructs, G-canid chimeric (4.51%) and G-spill over chimeric (5.55%) constructs showed low level of apoptosis, whereas G-mongoose construct showed relatively higher level of apoptosis (11.14%) (Figure 3.9).

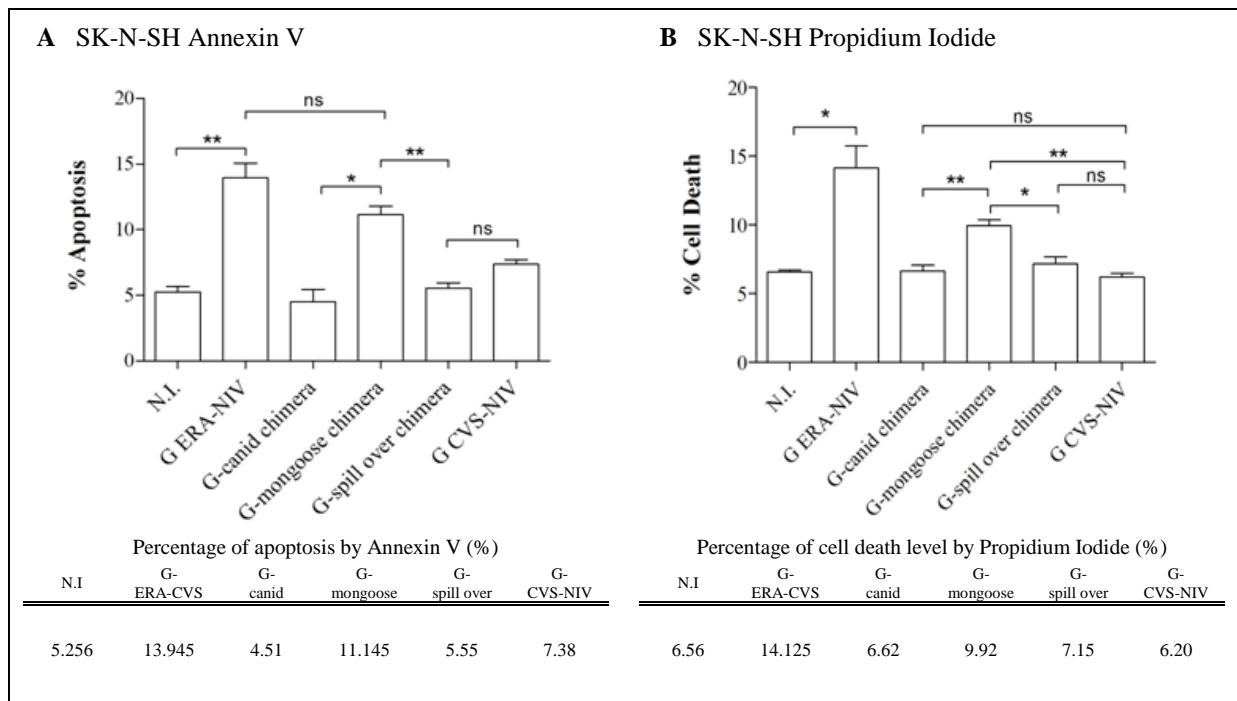


Figure 3.8 Analysis of the level of apoptosis using Annexin V-FITC (A) and membrane permeability using propidium Iodide (B) were analyzed at 96 hours post infection and the relative percentage values of apoptosis/cell death levels N.I., not infected. ns, not significant.

Table 3.6 Significant differences by GraphPad™ Prism 5 and the percentage value of apoptosis and cell death by Annexin V and Propidium Iodide (PI) analyses to indicate the level of cell surface changes during the apoptotic process. Statistical significance (P value < 0.05) is denoted as (+) and ‘not statistical significance’ is shown as (-) (P value > 0.05).

Pairwise comparison of constructs			Annexin-V		Propidium Iodide	
			P value	significance	P value	Significance
G-ERA	:	N.I	0.0032	+	0.0420	+
G-ERA	:	G-canid	0.0079	+	0.0106	+
G-ERA	:	G-mongoose	0.1599	-	0.0501	-
G-ERA	:	G-spill over	0.0034	+	0.0142	+
G-ERA	:	G-CVS	0.0301	+	0.0078	+
G-canid	:	N.I	0.5154	-	0.9174	-
G-canid	:	G-mongoose	0.0151	+	0.0060	+
G-canid	:	G-spill over	0.3724	-	0.4705	-
G-canid	:	G-CVS	0.1071	-	0.4557	-
G-mongoose	:	N.I	0.0039	+	0.0106	+
G-mongoose	:	G-spill over	0.0042	+	0.0148	+
G-mongoose	:	G-CVS	0.0339	+	0.0021	+
G-spill over	:	N.I	0.6426	-	0.4371	-
G-spill over	:	G-CVS	0.0524	-	0.1751	-
G-CVS	:	N.I	0.0398	+	0.4077	-

Part 3: Summary of phenotypes observed

The recombinant lentivirus G-CVS-NIV construct exhibits the property of triggering neurite outgrowth without the induction of apoptosis, while the recombinant lentivirus G-ERA-NIV does not trigger neurite outgrowth but apoptosis instead. These features are consistent with previous data collected by using recombinant RABV expressing entire G-proteins, with the virulence of CVS-NIV and the absence of virulence of ERA-NIV (Prehaud *et al.*, 2010). Successful RABV propagation in the nervous system requires that neuronal cell bodies are not damaged by premature apoptosis and that the integrity of axons and dendrites is preserved and propagated (Lafon, 2011). Using this rough guideline, it can be hypothesized that G-canid construct could be virulent since the expression of the chimeric G-protein construct triggered neurite outgrowth and did not trigger apoptosis. With the same regards, the G-spill over construct could also be virulent, negative induction of apoptosis and neurite outgrowth was less stringent than those obtained by G-protein construct of the canid isolate.

In contrast, G-mongoose construct triggered apoptosis and low neurite outgrowth *in vitro*, it could be expected that G-mongoose construct has the lowest virulence than G-canid and G-spill

over constructs through phenotypic observations. The summary of phenotypes observed is presented below (Figure 3.9).

-11	-10	-9	-8	-7	-6	-5	-4	-3	-2	-1	0				
<u>Virulent positive control according to Prehaud <i>et al.</i>, 2010</u>												apoptosis	Neurite outgrowth	rRABV virulence	
TGG	GAA	TCA	CAC	AAG	AGT	GGG	GGT	GGT	ACC	AGA	CTG	TGA	Negative	Positive	Positive
W	E	S	H	K	S	G	G	Q	T	R	L	STOP			
<u>Virulent negative control according to Prehaud <i>et al.</i>, 2010</u>															
TGG	GAA	TCA	CAC	AAG	AGT	GGG	GGT	GAG	ACC	AGA	CTG	TGA	Positive	Negative	Negative
W	E	S	H	K	S	G	G	E	T	R	L	STOP			
<u>RABV G-canid construct</u>												apoptosis	Neurite outgrowth	Hypothetical virulence	
TGG	GAA	TCA	TAC	AAG	AGT	GGG	GGT	GAG	ACC	AGA	CTG	TGA	Negative	Positive	Positive
W	E	S	Y	K	S	G	G	E	T	R	L	STOP			
<u>RABV G-mongoose construct</u>															
TGG	GAA	TCA	TAC	AAG	AAT	GGG	GAG	GAG	ACC	AGA	ATG	TGA	Positive	Positive /Negative	Intermediate
W	E	S	Y	K	N	G	E	E	T	R	M	STOP			
<u>RABV G-spill over construct</u>															
TGG	GAA	TCA	TAC	AAG	AAT	GGG	GGT	GAG	ACC	AGA	ATG	TGA	Negative	Positive /Negative	Intermediate
W	E	S	Y	K	N	G	G	E	T	R	M	STOP			

Figure 3.9 Summary of the phenotypic observation through the level of apoptosis and neurite outgrowth and hypothetical virulence of recombinant viruses. The mutations of amino acid residues are indicated as underlined bold letters.

3.4 Discussion

The role of the cytoplasmic domain of the RABV G-protein *in vitro* neurite outgrowth or apoptosis has been previously studied by using recombinant RABVs (Prehaud *et al.*, 2010). By this means, it has been established that the control of death or neurite outgrowth relies on the nature of the C-terminal of 4 amino acid residues in a recombinant lentivirus system and one single mutation (Q to E at -3) in the PDZ-BS is sufficient to switch the fate of the infected cells from neuronal survival to apoptosis. By using a chimeric expression of the C-terminus of the Cyto-G delivered by a lentivirus, it was demonstrated that the expression of the 12 amino acid triggers cell death when the C-terminus is terminated by amino acid sequences ETRL (G-ERA-NIV construct), whereas expression of QTRL-COOH (G-CVS-NIV construct) triggers the cell

survival phenotype as measured by neurite outgrowth. These observations validated our experimental model.

When the properties of the three South Africa chimeras were compared to the prototype chimeric CVS and ERA (G-CVS-NIV and G-ERA-NIV), it appeared that the G-canid chimeric construct showed dominant feature of neurite outgrowth phenotype and low apoptotic level. On the other hand, the chimeric G-spill over construct exhibited intermediate level of neuronal outgrowth and negative apoptotic phenotype, whereas chimeric G-mongoose exhibited a remarkable apoptotic phenotype and low capacity to trigger neurite outgrowth. Although the induction of apoptosis was suggested to correlate with high level of G-protein expression (Yan *et al.*, 2001), no significant G-protein expression level difference was observed through immune blotting and immunocytochemistry assay in this study.

Therefore, the results obtained in this study indicate the hypothetical virulence of three South African rabies isolates: G-mongoose can be regarded as less virulent compared to G-canid construct, and G-spill over construct showed intermediate virulent phenotype. It is important to note that these results obtained are only forecasts. Animal experiments are now necessary to strongly validate these conclusions and it will allow us to get more insight about RABV pathogenicity comparing morbidity and progression of clinical signs after animals have received the same amount of infectious viral particles of the three South African isolates.

Intriguingly, despite the expression of PDZ-BS ETRL as does ERA-NIV chimera which triggers apoptosis, the G-canid chimera did not trigger apoptosis in this study. The chimeric G-ERA-NIV and G-canid constructs were different by only one amino acid where the histidine at position -8 (G-ERA-NIV was replaced by tyrosine at the same locus in G-canid construct). Our observation leads to conclude that this amino acid replacement at -8 may be important to abrogate death phenotype. A similar situation can be found in a virulent CVS strain [PDZ-BS ETRL and tyrosine at -8] (GenBank Acc. AJ506997.1). In contrast, an attenuated SAD-B19 strain [PDZ-BS ETRL and the expression of histidine at position -8 in cytoplasmic domain] (GenBank Acc. M31046.1) showed the same amino acid sequences as ERA-NIV strain has. Our result suggests that the insertion of tyrosine at position -8 modifies the induction of apoptosis.

A previous study (Prehaud *et al.*, 2010) showed that apoptosis induction was associated with an increase of the cellular partners fished by the PDZ-BS ETRL, whereas the number of interactors remains low with the PDZ-BS QTRL. It can therefore be proposed that the replacement of histidine by tyrosine at position -8 has modified the number of cellular partners. This is supported by previous reports indicating that formation of the complex between the PDZ and the PDZ-BS is dependent not only on the last 4 amino acids of C-terminal but also on the nature of the residues as far back as position 8 from the 5' end of cytoplasmic domain (Songyang *et al.*, 1997) and also by Drs Nicolas Wolff and Elouan Terrien (Unit of Nuclear Magnetic Resonance of Biomolecules headed by Muriel Delepierre) who have observed that amino acid residues up to position -13 were indeed involved in the formation of the complex between MAST2 PDZ and the RABV G peptide (Dr Elouan Terrien, personal communication).

Furthermore, the mutation from glycine (G) to glutamic acid (E) at position -4 from the 5' end of the cytoplasmic domain leads to an increase in apoptosis induction. This observation suggests that amino acids outside the canonical PDZ-BS (4 amino acids) may also be involved in the virulence/attenuation phenotype.

This hypothesis deserves further investigations to determine whether the constants of dissociation of the complex and the number of cellular partners have been modified by the replacement at position -8 (H/Y) and by the replacement at position -4 (G/E). With these findings, it would be easier to understand why some ETRL strains can be considered as virulent and why ETRM strains have lost their virulence. Nowadays, these new results emphasize the critical role of the cytoplasmic domain in controlling commitment to survival or death and open new avenues to identify unconventional PDZ-BS/PDZ interactions.

CHAPTER 4

**Concluding remarks and
future directions**

The neurotropic rabies virus spreads along neuronal pathways and invades the central nervous system. Successful invasion of the nervous system by RABV requires that neuronal cell bodies are not damaged by premature apoptosis and the integrity of axons and dendrites is preserved. Cumulative evidence indicates that the rabies virus G-protein, the surface spike protein involved in attachment to host cells, plays a pivotal role in the pathogenicity of the virus. Amongst four distinct domains of G-protein, the cytoplasmic domain has been identified as a critical element for the neurosurvival and apoptotic phenotypes (Lafon, 2011). The tissue culture-adapted rabies virus strains such as ERA, HEP and CVS have been shown to correlate with the presences of pathogenic determinants, however, the pathogenicity of South African street rabies virus has not been undertaken. This study provides the first insight into pathogenicity of typical South African rabies biotypes (canid and mongoose rabies biotypes) through genetic characterization and neuroprotection properties.

The major purpose of this study was to elucidate the virulence of typical South African rabies isolates from different localities (canid, mongoose and spill over). The genetic characterization through phylogenetic analysis confirmed that mongoose and spill over isolates belonged to the same cluster and the canid isolate represented a typical canid rabies variant in South Africa. In addition, the three South African rabies virus isolates showed identical amino acid residues at specific positions which are responsible for the interaction of the RABV with specific receptors. Given this development, other factors responsible for the virulence in the G-protein were further investigated.

Following investigations through *in vitro* analysis of the phenotypic properties carried by the carboxyl terminus of the G-protein of the chimeric constructs, the recombinant G chimeras expressed in a lentivirus system demonstrated different phenotypes regarding neurite outgrowth and apoptosis. In brief, the canid chimeric construct showed the highest virulence amongst chimeric constructs followed by the spill over and lastly the mongoose constructs. These hypothetical conclusions of virulence were derived from the phenotypic observations through neuroprotection assays. However, the pathogenicity from the recombinant constructs may not reflect the real pathogenicity of the original RABV isolates. Therefore, animal experimentation is hereby proposed for a further study by using a dog model. Overall, the animal experiments will monitor progressively the clinical signs and assess immunologic parameters such as inflammatory mediator interleukin (IL-6), Type 1 interferons (IFN- α and - β), proinflammatory

chemokines (CXCL10) and interferon signaling genes (STATs) as markers of immunopathogenesis. This set of animal model experiments will provide more precise data for the pathogenicity in a natural host species of rabies and complement the pathogenicity data we obtained. During this investigation, it is expected that more informative data will be obtained for the dead-end infection, while host switching events and actual pathogenicity levels of South African rabies biotypes will be established through the proposed experiments.

In conclusion, this study is the first attempt to investigate the role of G-protein in the pathogenicity of the South African canid and mongoose rabies biotypes. Indeed, there is a critical involvement of the cellular signalling interactions (PDZ-BS/PDZ domains) for the different phenotypic inductions. These findings alone though are not able to explain fully the RABV pathogenicity, however, the series of the proposed experiments will contribute to generate new information on the pathogenicity of canid and mongoose rabies variants and further studies including animal experiments are able to lead to advances in the treatment of rabies and other viral diseases.

REFERENCES

Albertini, A. A. V., Schoehn, G., Weissenhorn, W. and Ruigrok, R. W. H. (2008). Structural aspects of rabies virus replication. *Cellular and Molecular Life Sciences* **65**, 282-294.

Albertini, A. A. V., Ruigrok, R. W. H. and Blondel, D. (2011). Rabies virus transcription and replication. *Advances in Virus Research* **79**, 1-22.

Alexander, R. A. (1952). Rabies in South Africa: a review of the present position. *Journal of the South African Veterinary Medical Association* **23**, 135-139.

Anderson, L. J., Williams, L. P. Jr., Layde, J. B., Dixon, F. R. and Winkler, W. G. (1984). Nosocomial rabies: investigation of contacts of human rabies cases associated with a corneal transplant. *American Journal of Public Health* **74**, 370-372.

Badrane, H., Bahloul, C., Perrin, P. and Tordo, N. (2001). Evidence of two *lyssavirus* phylogroups with distinct pathogenicity and immunogenicity. *Journal of Virology* **75**, 3268-3276.

Badrane, H. and Tordo, N. (2001). Host switching in *Lyssavirus* history from the Chiroptera to the Carnivora orders. *Journal of Virology* **75**, 8096-8104.

Baer, G. M. (2007). The History of Rabies. In: *Rabies* (A.C. Jackson and W.H. Wunner, eds). pp. 1-22. London: Elsevier Academic Press.

Balachandran, A. and Charlton, K. (1994). Experimental rabies infection of non-nervous tissues in skunks (*Mephitis mephitis*) and foxes (*Vulpes vulpes*). *Veterinary Pathology* **31**, 93-102.

Banerjee, A. K. and Chattopadhyay, D. (1990). Structure and function of the RNA polymerase of vesicular stomatitis virus. *Advances in Virus Research* **38**, 99-124.

Banyard, A. C., Hayman, D., Johnson, N., McElhinney, L. and Fooks, A. R. (2011). Bats and lyssaviruses. *Advances in Virus Research* **79**, 239-289.

Barge, A., Gaudin, Y., Coulin, P. and Ruigrok, R. W. H. (1993). Vesicular stomatitis virus M protein may be inside the ribonucleocapsid coil. *Journal of Virology* **67**, 7246-7253.

Bear, M. F., Connors, B. W. and Paradiso, M. A. (2007). Neurons and glia In: *Neuroscience: exploring the brain – 3rd ed.* (M.F. Bear, B.W. Connors and M.A. Paradiso, eds). pp. 23-50. Baltimore Philadelphia: Lippincott Williams & Wilkins.

Benmansour, A., Brahim, M., Tuffereau, C., Coulon, P., Lafay, F. and Flamand, A. (1992). Rapid sequence evolution of street rabies glycoprotein is related to the highly heterogeneous nature of the viral population. *Virology* **187**, 33-45.

Bingham, J. (1999). *The Control of Rabies in Jackals in Zimbabwe*. PhD thesis. University of Zimbabwe.

Bingham, J. (2005). Canine rabies ecology in southern Africa. *Emerging Infectious Diseases* **11**, 1337-1342.

Bingham, J., Foggin, C. M., Wandeler, A. I. and Hill, F. W. (1999). The epidemiology of rabies in Zimbabwe. 1. Rabies in dogs (*Canis familiaris*). *Onderstepoort Journal of Veterinary Research* **66**, 1-10.

Bingham, J., Javangwe, S., Sabet, C. T., Wandeler, A. I. and Nel, L. H. (2001). Report of isolations of unusual lyssaviruses (rabies and Mokola virus) identified retrospectively from Zimbabwe. *Journal of the South African Veterinary Association* **72**, 92-94.

Bishop, G. C., Durrheim, D. N., Kloock, P. E., Godlonton, J. D., Bingham, J., Speare, R. and the Rabies Advisory Group. (2002). Rabies - Guide for the medical, veterinary and allied professions. Department of Agriculture, South Africa.

Botvinkin, A. D., Poleschuk, E. M., Kuzmin, I. V., Borisova, T. I., Gazaryan, S. V., Yager, P. and Rupprecht, C. E. (2003). Novel lyssaviruses isolated from bats in Russia. *Emerging Infectious Disease* **9**, 1623-1625.

Bourhy, H., Kissi, B. and Tordo, N. (1993). Molecular diversity of the *lyssavirus* genus. *Virology* **194**, 70-81.

Briggs, D. J. (2007). Human rabies vaccines. In: *Rabies* (A.C. Jackson and W.H. Wunner, eds). pp. 505-515. London: Elsevier Academic Press.

Brzózka, K., Finke, S. and Conzelmann, K. K. (2005). Identification of the rabies virus alpha/beta interferon antagonist: Phosphoprotein P interferes with phosphorylation of Interferon Regulatory Factor 3. *Journal of Virology* **79**, 7673-7681.

Brzózka, K., Finke, S. and Conzelmann, K. K. (2006). Inhibition of interferon signaling by rabies virus phosphoprotein P: Activation-dependent binding of STAT1 and STAT2. *Journal of Virology* **80**, 2675-2683.

Celis, E., Karr, R. W., Dietzschold, B., Wunner, W. H. and Koprowski, H. (1988a). Genetic restriction and fine specificity of human T cell clones reactive with rabies virus. *Journal of Immunology* **141**, 2721-2728.

Celis, E., Ou, D., Dietzschold, B. and Koprowski, H. (1988b). Recognition of rabies and rabies-related viruses by T cells derived from human vaccine recipients. *Journal of virology* **62**, 3128-3134.

Centers for Disease Control and Prevention (1999). Human rabies prevention - United States, 1999: recommendations of the Advisory Committee on Immunization Practices (ACIP). *Morbidity Mortality Weekly Report* **48**, 1-22.

Chaparro, F. and Esterhuysen, J. J. (1993). The role of the yellow mongoose (*Cynictis penicillata*) in the epidemiology of rabies in South Africa-preliminary results. *Onderstepoort Journal of Veterinary Research* **60**, 373-377.

Charlton, K. M., Casey, G. A. and Campbell, J. B. (1983). Experimental rabies in skunks: mechanisms of infection of the salivary glands. *Canadian Journal of Comparative Medicine* **47**, 363-369.

Chelbi-Alix, M. K., Vidy, A., El Bougrini, J. and Blondel, D. (2006). Rabies viral mechanisms to escape the IFN system: The viral protein P interferes with IRF-3, STAT1 and PML nuclear bodies. *Journal of Interferon & Cytokine Research* **26**, 271-280.

Chen, B. J. and Lamb, R. A. (2008). Mechanisms for enveloped virus budding: Can some viruses do without an ESCRT? *Virology* **372**, 221-232.

Chenik, M., Chebli, K., Gaudin, Y. and Blondel, D. (1994). In vivo interaction of rabies virus phosphoprotein (P) and nucleoprotein (N): existence of two N-binding sites on P protein. *Journal of General Virology* **75**, 2889-2896.

Cho, K. O., Hunt, C. A. and Kennedy, M. B. (1992). The rat brain postsynaptic density fraction contains a homolog of the drosophila discs-large tumor suppressor protein. *Neuron* **9**, 929-942.

Cliquet, F. and Aubert, M. (2004). Elimination of terrestrial rabies in Western European countries. *Developments in biologicals* **119**, 185-204.

Cluver, E. (1927). Rabies in South Africa. *Journal of the Medical Association of South Africa* **1**, 247-253.

Cockrell, A.S. and Kafri, T. (2007). Gene delivery by lentivirus vectors. *Molecular biotechnology* **36**, 184-204.

Constantine, D. G. (1962). Rabies transmission by non-bite route. *Public Health Reports* **77**, 287-289.

Conzelmann, K. K. and Schnell, M. J. (1994). Rescue of synthetic genomic RNA analogs of rabies virus by plasmid-encoded proteins. *Journal of Virology* **68**, 713-719.

Coulon, P., Rollin, P. E., Aubert, M. and Flamand, A. (1982). Molecular basis of rabies virus virulence. I. Selection of avirulent mutants of the CVS strain with anti-G monoclonal antibodies. *Journal of General Virology* **61**, 97-100.

Coulon, P., Rollin, P. E. and Flamand, A. (1983). Molecular basis of rabies virus virulence. II. Identification of a site on the CVS glycoprotein associated with virulence. *Journal of General Virology* **64**, 693-696.

Coulon, P., Derbin, C., Kucera, P., Lafay, F., Prehaud, C. and Flamand, A. (1989). Invasion of the peripheral nervous systems of adult mice by the CVS strain of rabies virus and its avirulent derivative AvO1. *Journal of Virology* **63**, 3550-3554.

Coulon, P., Ternaux, J. P., Flamand, A and Tuffereau, C. (1998). An avirulent mutant of rabies virus is unable to infect motoneurons *in vivo* and *in vitro*. *Journal of Virology* **72**, 273-278.

Davies, M. C., Englert, M. E., Sharpless, G. R. and Cabasso, V. J. (1963). The electron microscopy of rabies virus in cultures of chicken embryo tissues. *Virology* **21**, 642-651.

Dean, D. J., Abelseth, M. K. and Atanasiu, P. (1996). The fluorescent antibody test. In: *Laboratory Techniques in Rabies* (F.-X. Meslin, M.M. Kaplan and H. Koprowski, eds). pp. 88-95. Geneva: World Health Organization.

Debbie, J. G. and Trimarchi, C. V. (1970). Pantropism of rabies virus in free-ranging rabid red fox *Vulpes fulva*. *Journal of Wildlife Diseases* **6**, 500-506.

Delmas, O., Assenberg, R., Grimes, J. M. and Bourhy, H. (2010). The structure of the nucleoprotein binding domain of lyssavirus phosphoprotein reveals a structural relationship between the N-RNA binding domains of Rhabdoviridae and Paramyxoviridae. *RNA Biology* **7**, 322-327.

Dietzschold, B., Wunner, W. H., Wiktor, T. J., Lopes, A. D., Lafon, M., Smith, C. L. and Koprowski, H. (1983). Characterization of an antigenic determinant of the glycoprotein that correlates with pathogenicity of rabies virus. *Proceedings of the National Academy of Sciences of the United States of America* **80**, 70-74.

Dietzschold, B., Wiktor, T. J., Trojanowski, J. Q., Macfarlan, R. I., Wunner, W. H., Torres-Anjel, M. J. and Koprowski, H. (1985). Differences in cell-to-cell spread of pathogenic and apathogenic rabies virus *in vivo* and *in vitro*. *Journal of Virology* **56**, 12-18.

Dietzschold, B., Lafon, M., Wang, H., Otvos, L. Jr., Celis, E., Wunner, W. H. and Koprowski, H. (1987). Localization and immunological characterization of antigenic domains of the rabies virus internal N and NS proteins. *Virus Research* **8**, 103-125.

Doyle, D. A., Lee, A., Lewis, J., Kim, E., Sheng, M. and MacKinnon, R. (1996). Crystal structures of a complexed and peptide-free membrane protein-binding domain: molecular basis of peptide recognition by PDZ. *Cell* **85**, 1067-1076.

Ertl, H. C. J., Dietzschold, B., Gore, M., Otvos, L. Jr., Larson, J. K., Wunner, W. H. and Koprowski, H. (1989). Induction of rabies virus-specific T-helper cells by synthetic peptides that carry dominant T-helper cell epitopes of viral ribonucleoprotein. *Journal of Virology* **63**, 2885-2892.

Etessami, R., Conzelmann, K. K., Fadai-Ghotbi, B., Natelson, B., Tsiang, H. and Ceccaldi, P. E. (2000). Spread and pathogenic characteristics of a G-deficient rabies virus recombinant: an *in vitro* and *in vivo* study. *Journal of General Virology* **81**, 2147-2153.

Faber, M., Faber, M. L., Papaneri, A., Bette, M., Weihe, E., Dietzschold, B. and Schnell, M. J. (2005). A single amino acid change in rabies virus glycoprotein increases virus spread and enhances virus pathogenicity. *Journal of Virology* **79**, 14141-14148.

Fekadu, M. and Shaddock, J. H. (1984). Peripheral distribution of virus in dogs inoculated with two strains of rabies virus. *American Journal of Veterinary Research* **45**, 724-729.

Finke, S. and Conzelmann, K. K. (2003). Dissociation of rabies virus matrix protein functions in regulation of viral RNA synthesis and virus assembly. *Journal of Virology* **77**, 12074-12082.

Finke, S., Mueller-Waldeck, R. and Conzelmann, K. K. (2003). Rabies virus matrix protein regulates the balance of virus transcription and replication. *Journal of General Virology* **84**, 1613-1621.

Finke, S., Granzow, H., Hurst, J., Pollin, R. and Mettenleiter, T. C. (2010). Intergenotypic replacement of lyssavirus matrix proteins demonstrates the role of lyssavirus M proteins in intracellular virus accumulation. *Journal of Virology* **84**, 1816-1827.

Flamand, A., Wiktor, T. J. and Koprowski, H. (1980). Use of hybridoma monoclonal antibodies in the detection of antigenic differences between rabies and rabies-related virus proteins. I. The nucleocapsid protein. *Journal of General Virology* **48**, 97-104.

Foggin, C. M. (1988). *Rabies and rabies-related viruses in Zimbabwe: Historical, virological and ecological aspects*. PhD thesis. University of Zimbabwe.

Freuling, C. M., Beer, M., Conraths, F. J., Finke, S., Hoffmann, B., Keller, B., Kliemt, J., Mettenleiter, T. C., Mühlbach, E., Teifke, J. P., Wohlsein, P. and Mülle, T. (2011). Novel lyssavirus in Natterer's bat, Germany. *Emerging Infectious Diseases* **17**, 1519-1522.

Fu, Z. F., Zheng, Y., Wunner, W. H., Koprowski, H. and Dietzschold, B. (1994). Both the N- and the C-terminal domains of the nominal phosphoprotein of rabies virus are involved in binding to the nucleoprotein. *Virology* **200**, 590-597.

Gaudin, Y., Ruigrok, R. W. H., Tuffereau, C., Knossow, M. and Flamand, A. (1992). Rabies virus glycoprotein is a trimer. *Virology* **187**, 627-632.

Gaudin, Y., Ruigrok, R. W. H., Knossow, M. and Flamand, A. (1993). Low-pH conformational changes of rabies virus glycoprotein and their role in membrane fusion. *Journal of Virology* **67**, 1365-1372.

Gigant, B., Iseni, F., Gaudin, Y., Knossow, M. and Blondel, D. (2000). Neither phosphorylation nor the amino-terminal part of rabies virus phosphoprotein is required for its oligomerization. *Journal of General Virology* **81**, 1757-1761.

Grinnell, B. W. and Wagner, R. R. (1985). Inhibition of DNA-dependent transcription by the leader RNA of vesicular stomatitis virus: role of specific nucleotide sequences and cell protein binding. *Molecular and Cellular Biology* **5**, 2502-2513.

Guichard, P., Krell, T., Chevalier, M., Vaysse, C., Adam, O., Ronzon, F. and Marco, S. (2011). Three dimensional morphology of rabies virus studied by cryo-electron tomography. *Journal of Structural Biology* **176**, 32-40.

Hellenbrand, W., Meyer, C., Rasch, G., Steffens, I. and Ammon, A. (2005). Cases of rabies in Germany following organ transplantation. *Euro Surveillance* **10**, E050224.6.

Higgins, D. G. and Sharp, P. M. (1989). Fast and sensitive multiple sequence alignments on a microcomputer. *Computer Applications in the Biosciences* **5**, 151-153.

Hummeler, K., Koprowski, H. and Wiktor, T. J. (1967). Structure and development of rabies virus in tissue culture. *Journal of Virology* **1**, 152-170.

Izeni, F., Barge, A., Baudin, F., Blondel, D. and Ruigrok, R. W. H. (1998). Characterization of rabies virus nucleocapsids and recombinant nucleocapsid-like structures. *Journal of General Virology* **79**, 2909-2919.

Ito, N., Takayama, M., Yamada, K., Sugiyama, M. and Minamoto, N. (2001). Rescue of rabies virus from cloned cDNA and identification of the pathogenicity-related gene: glycoprotein gene is associated with virulence for adult mice. *Journal of Virology* **75**, 9121-9128.

Jackson, A. C. (1991). Biological basis of rabies virus neurovirulence in mice: Comparative pathogenesis study using the immunoperoxidase technique. *Journal of Virology* **65**, 537-540.

Jackson, A. C. (2007). Pathogenesis. In: *Rabies* (A.C. Jackson and W.H. Wunner, eds). pp. 341-381. London: Elsevier Academic Press.

Jackson, A. C. and Reimer, D. L. (1989). Pathogenesis of experimental rabies in mice: an immunohistochemical study. *Acta Neuropathologica* **78**, 159-165.

Jackson, A. C., Ye, H., Phelan, C. C., Ridaura-Sanz, C., Zheng, Q., Li, Z., Wan, X. and Lopez-Corella, E. (1999). Extraneural organ involvement in human rabies. *Laboratory Investigation* **79**, 945-951.

Javier, R. T. and Rice, A. P. (2011). Emerging theme: Cellular PDZ proteins as common targets of pathogenic viruses. *Journal of Virology* **85**, 11544-11556.

Jeleń, F., Oleksy, A., Śmietana, K. and Otlewski, J. (2003). PDZ domains – common players in the cell signaling. *Acta Biochimica Polonica* **50**, 985-1017.

Kassis, M., Larrous, F., Estaquier, J. and Bourhy, H. (2004). Lyssavirus matrix protein induces apoptosis by a TRAIL-dependent mechanism involving caspase-8 activation. *Journal of Virology* **78**, 6543-6555.

Kim, E., Niethammer, M., Rothschild, A., Jan, Y. N. and Sheng, M. (1995). Clustering of Shaker-type K⁺ channels by interaction with a family of membrane-associated guanylate kinases. *Nature* **378**, 85-88.

Kimura, M. (1980). A simple method for estimating evolutionary rates of base substitutions through comparative studies of nucleotide sequences. *Journal of Molecular Evolution* **16**, 111-120.

King, A. A., Meredith, C. D. and Thomson, G. R. (1993). Canid and viverrid viruses in South Africa. *Onderstepoort Journal of Veterinary Research* **60**, 295-299.

Klingen, Y., Conzelmann, K. K. and Finke, S. (2008). Double-labeled rabies virus: Live tracking of enveloped virus transport. *Journal of Virology* **82**, 237-245.

Koch, F. J., Sagartz, J. W., Davidson, D. E. and Lawhaswasdi, K. (1975). Diagnosis of human rabies by the cornea test. *American Journal of Clinical Pathology* **63**, 509-515.

Koprowski, H. (1996). The mouse inoculation test In: *Laboratory Techniques in Rabies* (F.-X. Meslin, M.M. Kaplan and H. Koprowski, eds). pp. 80-87. Geneva: World Health Organization.

Krebs, J. W., Mandel, E. J., Swerdlow, D. L. and Rupprecht, C. E. (2005). Rabies surveillance in the United States during 2004. *Journal of the American Veterinary Medical Association* **227**, 1912-1925.

Kucera, P., Dolivo, M., Coulon, P. and Flamand, A. (1985). Pathways of the early propagation of virulent and avirulent rabies strains from the eye to the brain. *Journal of Virology* **55**, 158-162.

Kuzmin, I. V., Botvinkin, A. D., Rybin, S. N. and Baialiev, A. B. (1992). A lyssavirus with an unusual antigenic structure isolated from a bat in southern Kyrgyzstan. *Voprosy Virusologii* **37**, 256-259.

Kuzmin, I. V., Orciari, L. A., Arai, Y. T., Smith, J. S., Hanlon, C. A., Kameoka, Y. and Rupprecht, C. E. (2003). Bat lyssaviruses (Aravan and Khujand) from central Asia: phylogenetic relationships according to N, P and G gene sequences. *Virus Research* **97**, 65-79.

Kuzmin, I. V., Mayer, A. E., Niezgoda, M., Markotter, W., Agwanda, B., Breiman, R. F. and Rupprecht, C. E. (2010). Shimoni bat virus, a new representative of the *Lyssavirus* genus. *Virus Research* **149**, 197-210.

Lafay, F., Coulon, P., Astic, L., Saucier, D., Riche, D., Holley, A. and Flamand, A. (1991). Spread of the CVS strain of rabies strain of rabies virus and of the avirulent mutant AvO1 along the olfactory pathways of the mouse after intranasal inoculation. *Virology* **183**, 320-330.

Lahaye, X., Vidy, A., Pomier, C., Obiang, L., Harper, F., Gaudin, Y. and Blondel, D. (2009). Functional characterization of Negri bodies (NBs) in rabies virus-infected cells: Evidence that NBs are sites of viral transcription and replication. *Journal of Virology* **83**, 7948-7958.

Lafon, M. (2005). Rabies virus receptors. *Journal of Neurovirology* **11**, 82-87.

Lafon, M. (2011). Evasive strategies in rabies virus infection. *Advances in Virus Research* **79**, 33-53.

Lafon, M., Lafage, M., Martinez-Arends, A., Ramirez, R., Vuillier, F., Charron, D., Lotteau, V. and Scott-Algara, D. (1992). Evidence for a viral superantigen in humans. *Nature* **358**, 507-510.

Lafon, M., Scott-Algara, D., Marche, P. N., Cazenave, P. A. and Jouvin-Marche, E. (1994). Neonatal deletion and selective expansion of mouse T cells by exposure to rabies virus nucleocapsid superantigen. *The Journal of Experimental Medicine* **180**, 1207-1215.

Langevin, C., Jaaro, H., Bressanelli, S., Fainzilber, M. and Tuffereau, C. (2002). Rabies virus glycoprotein (RVG) is a trimeric ligand for the N-terminal cysteine-rich domain of the mammalian p75 neurotrophin receptor. *The Journal of Biological Chemistry* **277**, 37655-37662.

Langevin, C. and Tuffereau, C. (2002). Mutations conferring resistance to neutralization by a soluble form of the neurotrophin receptor (p75NTR) map outside of the known antigenic sites of the rabies virus glycoprotein. *Journal of Virology* **76**, 10756-10765.

Larrous, F., Gholami, A., Mouhamad, S., Estaquier, J. and Bourhy, H. (2010). Two overlapping domains of a lyssavirus matrix protein that acts on different cell death pathways. *Journal of Virology* **84**, 9897-9906.

Liu, P., Yang, J., Wu, X. and Fu, Z. F. (2004). Interactions amongst rabies virus nucleoprotein, phosphoprotein and genomic RNA in virus-infected and transfected cells. *Journal of General Virology* **85**, 3725-3734.

Loh, S. H. Y., Francescut, L., Lingor, P., Bähr, M. and Nicotera, P. (2008). Identification of new kinase clusters required for neurite outgrowth and retraction by a loss-of-function RNA interference screen. *Cell Death and Differentiation* **15**, 283-298.

Lyles, D. S., McKenzie, M. O., Kaptur, P. E., Grant, K. W. and Jerome, W. G. (1996). Complementation of M gene mutants of vesicular stomatitis virus by plasmid-derived M protein converts spherical extracellular particles into native bullet shapes. *Virology* **217**, 76-87.

Macfarlan, R. I., Dietzschold, B. and Koprowski, H. (1986). Stimulation of cytotoxic T-lymphocyte responses by rabies virus glycoprotein and identification of an immunodominant domain. *Molecular Immunology* **23**, 733-741.

Markotter, W. (2007). *Molecular epidemiology and pathogenesis of Lagos bat virus, a rabies-related virus specific to Africa*. PhD thesis. University of Pretoria.

Marston, D. A., Horton, D. L., Ngeleja, C., Hampson, K., McElhinney, L. M., Banyard, A. C., Haydon, D., Cleaveland, S., Rupprecht, C. E., Bigambo, M., Fooks, A. R. and Lembo, T. (2012). Ikoma lyssavirus, highly divergent novel lyssavirus in an African civet. *Emerging Infectious Diseases* **18**, 664-667.

Masatani, T., Ito, N., Shimizu, K., Ito, Y., Nakagawa, K., Abe, M., Yamaoka, S. and Sugiyama, M. (2011). Amino acids at positions 273 and 394 in rabies virus nucleoprotein are important for both evasion of host RIG-I-mediated antiviral response and pathogenicity. *Virus Research* **155**, 168-174.

Matsumoto, S. (1962). Electron microscopy of nerve cells infected with street rabies virus. *Virology* **17**, 198-202.

Matsumoto, S. (1963). Electron microscope studies of rabies virus in mouse brain. *The Journal of Cell Biology* **19**, 565-591.

Mavrakis, M., Iseni, F., Mazza, C., Schoehn, G., Ebel, C., Gentzel, M., Franz, T. and Ruigrok, R. W. H. (2003). Isolation and characterisation of the rabies virus N^o-P complex produced in insect cells. *Virology* **305**, 406-414.

Mayo, M. A. and Pringle, C. R. (1998). Virus Taxonomy-1997. *Journal of General Virology* **79**, 649-657.

McGettigan, J. P. (2010). Experimental rabies vaccines for humans. *Expert Review of Vaccines* **9**, 1177-1186.

McGettigan, J. P., Pomerantz, R. J., Siler, C. A., McKenna, P. M., Foley, H. D., Dietzschold, B. and Schnell, M. J. (2003). Second-generation rabies virus-based vaccine vectors expressing Human Immunodeficiency Virus Type 1 Gag have greatly reduced pathogenicity but are highly immunogenic. *Journal of Virology* **77**, 237-244.

Mebatsion, T., König, M. and Conzelmann, K. K. (1996). Budding of rabies virus particles in the absence of the spike glycoprotein. *Cell* **84**, 941-951.

Mebatsion, T., Weiland, F. and Conzelmann, K. K. (1999). Matrix protein of rabies virus is responsible for the assembly and budding of bullet-shaped particles and interacts with the transmembrane spike glycoprotein G. *Journal of Virology* **73**, 242-250.

Meldolesi, J. (2011). Neurite outgrowth: This process, first discovered by Santiago Ramon y Cajal, is sustained by the exocytosis of two distinct types of vesicles. *Brain Research Reviews* **66**, 246-255.

Ménager, P., Roux, P., Mégret, F., Bourgeois, J-P., Le Sourd, A-M., Danckaert, A., Lafage, M., Prehaud, C. and Lafon, M. (2009). Toll-Like Receptor 3 (TLR3) plays a major role in the formation of rabies virus Negri bodies. *PLoS Pathogens* **5**, e1000315.

Mingorance-Le Meur, A. and O'Connor, T. P. (2009). Neurite consolidation is an active process requiring constant repression of protrusive activity. *The EMBO journal* **28**, 248-260.

Murphy, F. A., Bauer, S. P., Harrison, A. K. and Winn, W. C. Jr. (1973). Comparative pathogenesis of rabies and rabies-like viruses. Viral infection and transit from inoculation site to the central nervous system. *Laboratory Investigation* **28**, 361-376.

Nakahara, K., Ohnuma, H., Sugita, S., Yasuoka, K., Nakahara, T., Tochikura, T. S. and Kawai, A. (1999). Intracellular behavior of rabies virus matrix protein (M) is determined by the viral glycoprotein (G). *Microbiology and Immunology* **43**, 259-270.

Neitz, W. O. and Thomas, A. D. (1933). Rabies in South Africa: Occurrence and distribution of cases during 1932. *Onderstepoort Journal of Veterinary Science and Animal Industry* **1**, 51-54.

Nel, L. H. (2005). Vaccines for lyssaviruses other than rabies. *Expert Review of Vaccines* **4**, 533-540.

Nel, L. H., Jacobs, J. A., Jaftha, J. B and Meredith, C. D. (1997). Natural spillover of a distinctly canidae-associated biotype of rabies virus into an expanded wildlife host range in southern Africa. *Virus Genes* **15**, 79-82.

Nel, L. H., Sabetta, C. T., Von Teichman, B. F., Jaftha, J. B., Rupprecht, C. E. and Bingham, J. (2005). Mongoose rabies in southern Africa: a re-evaluation based on molecular epidemiology. *Virus Research* **109**, 165-173.

Nel, L. H. and Rupprecht, C. E. (2007). Emergence of lyssaviruses in the Old World: The case of Africa. *Current Topics in Microbiology and Immunology* **315**, 161-193.

Ngoepe, C. E., Sabetta, C. T. and Nel, L. H. (2009). The spread of canine rabies into Free State province of South Africa: A molecular epidemiological characterization. *Virus Research* **142**, 175-180.

Okumura, A. and Harty, R. N. (2011). Rabies virus assembly and budding. *Advances in virus research* **79**, 23-32.

Perrière, G. and Gouy, M. (1996). WWW-query: An on-line retrieval system for biological sequence banks. *Biochimie* **78**, 364-369.

Poch, O., Blumberg, B. M., Bougueleret, L. and Tordo, N. (1990). Sequence comparison of five polymerases (L proteins) of unsegmented negative-strand RNA viruses: theoretical assignment of functional domains. *Journal of General Virology* **71**, 1153-1162.

Ponting, C. P. (1997). Evidence for PDZ domains in bacteria, yeast, and plants. *Protein Science* **6**, 464-468.

Prehaud, C., Coulon, P., Lafay, F., Thiers, C. and Flamand, A. (1988). Antigenic site II of the rabies virus glycoprotein: structure and role in viral virulence. *Journal of Virology* **62**, 1-7.

Prehaud, C., Wolff, N., Terrien, E., Lafage, M., Mégret, F., Babault, N., Cordier, F., Tan, G. S., Maitrepierre, E., Ménager, P., Chopy, D., Hoos, S., England, P., Delepierre, M., Schnell, M. J., Buc, H. and Lafon, M. (2010). Attenuation of rabies virulence: Takeover by the cytoplasmic domain of its envelope protein. *Science signaling* **3**, ra5.

Rieder, M. and Conzelmann, K. K. (2009). Rhabdovirus evasion of the interferon system. *Journal of Interferon & Cytokine Research* **29**, 499-510.

Rieder, M., Brzózka, K., Pfaller, C. K., Cox, J. H., Stitz, L. and Conzelmann, K. K. (2011). Genetic dissection of Interferon-Antagonistic functions of rabies virus phosphoprotein: Inhibition of Interferon Regulatory Factor 3 activation is important for pathogenicity. *Journal of Virology* **85**, 842-852.

Robison, C. S. and Whitt, M. A. (2000). The membrane-proximal stem region of vesicular stomatitis virus G protein confers efficient virus assembly. *Journal of Virology* **74**, 2239-2246.

Roche, S. and Gaudin, Y. (2004). Evidence that rabies virus forms different kinds of fusion machines with different pH thresholds for fusion. *Journal of Virology* **78**, 8746-8752.

Rupprecht, C. E., Hanlon, C. A. and Hemachudha, T. (2002). Rabies re-examined. *The Lancet Infectious Diseases* **2**, 327-343.

Sabeta, C. T., Mansfield, K. L., McElhinney, L. M., Fooks, A. R. and Nel, L. H. (2007). Molecular epidemiology of rabies in bat-eared foxes (*Otocyon megalotis*) in South Africa. *Virus research* **129**, 1-10.

Sabeta, C. T., Shumba, W., Mohale, D. K., Miyen, J. M., Wandeler, A. I. and Nel, L. H. (2008). Mongoose rabies and the African civet in Zimbabwe. *Veterinary Record* **163**, 580.

Sacramento, D., Bourhy, H. and Tordo, N. (1991). PCR technique as an alternative method for diagnosis and molecular epidemiology of rabies virus. *Molecular and Cellular Probes* **5**, 229-240.

Sánchez, Á., De, B. P. and Banerjee, A. K. (1985). *In vitro* phosphorylation of NS protein by the L protein of vesicular stomatitis virus. *Journal of General Virology* **66**, 1025-1036.

Schneider, L. G., Dietzschold, B., Dierks, R. E., Matthaeus, W., Enzmann, P.-J. and Strohmaier, K. (1973). Rabies group-specific ribonucleoprotein antigen and a test system for grouping and typing Rhabdoviruses. *Journal of Virology* **11**, 748-755.

Schnell, M. J., Mebatsion, T. and Conzelmann, K. K. (1994). Infectious rabies viruses from cloned cDNA. *The EMBO Journal* **13**, 4195-4203.

Schnell, M. J., McGettigan, J. P., Wirblich, C. and Papaneri, A. (2010). The cell biology of rabies virus: using stealth to reach the brain. *Nature Reviews Microbiology* **8**, 51-61.

Seif, I., Coulon, P., Rollin, P. E. and Flamand, A. (1985). Rabies virulence: effect on pathogenicity and sequence characterization of rabies virus mutations affecting antigenic site III of the glycoprotein. *Journal of Virology* **53**, 926-934.

Shankar, V., Dietzschold, B. and Koprowski, H. (1991). Direct entry of rabies virus into the central nervous system without prior local replication. *Journal of Virology* **65**, 2736-2738.

Sheng, M. and Sala, C. (2001). PDZ domains and the organization of supramolecular complexes. *Annual Review of Neuroscience* **24**, 1-29.

Smith, J. S. (1989). Rabies virus epitopic variation: Use in ecological studies. *Advances in Virus Research* **36**, 215-253.

Snyman, P. S. (1940). The study and control of vectors of rabies in South Africa. *Onderstepoort Journal of Veterinary Science and Animal Husbandry* **15**, 9-44.

Sokol, F. (1975). Chemical composition and structure of rabies virus. In: *The Natural History of Rabies, Volume I* (G.M. Baer, ed.). pp. 79-102. New York: Academic Press.

Songyang, Z., Fanning, A. S., Fu, C., Xu, J., Marfatia, S. M., Chishti, A. H., Crompton, A., Chan, A. C., Anderson, J. M. and Cantley, L. C. (1997). Recognition of unique carboxyl-terminal motifs by distinct PDZ domains. *Science* **275**, 73-77.

Srinivasan, A., Burton, E. C., Kuehnert, M. J. *et al.* (2005). Transmission of rabies virus from an organ donor to four transplant recipients. *New England Journal of Medicine* **352**, 1103-1111.

Swanepoel, R., Barnard, B. J. H., Meredith, C. D., Bishop, G. C., Brückner, G. K., Foggin, C. M. and Hübschle, O. J. (1993). Rabies in Southern Africa. *Onderstepoort Journal of Veterinary Research* **60**, 325-346.

Szanto, A. (2009). *Molecular genetics of the raccoon rabies virus Control*. PhD thesis. Trent University.

Tamura, K., Dudley, J., Nei, M. and Kumar, S. (2007). MEGA4: Molecular Evolutionary Genetics Analysis (MEGA) software Version 4.0. *Molecular Biology and Evolution* **24**, 1596-1599.

Tan, G. S., Preuss, M. A. R., Williams, J. C. and Schnell, M. J. (2007). The dynein light chain 8 binding motif of rabies virus phosphoprotein promotes efficient viral transcription. *Proceedings of the National Academy of Sciences of the United States of America* **104**, 7229-7234.

Taylor, P. J. (1993). A systematic and population genetic approach to the rabies problem in the yellow mongoose (*Cynictis Penicillata*). *Onderstepoort Journal of Veterinary Research* **60**, 379-387.

Théodorides, (1986). *Histoire de la Rage*. Paris: Masson.

Thomson, G. R. and Meredith, C. D. (1993). Rabies in bat-eared foxes in South Africa. *Onderstepoort Journal of Veterinary Research* **60**, 399-403.

Thoulouze, M. I., Lafage, M., Schachner, M., Hartmann, U., Cremer, H. and Lafon, M. (1998). The neural cell adhesion molecule is a receptor for rabies virus. *Journal of Virology* **72**, 7181-7190.

Tillotson, J. R., Axelrod, D. and Lyman, D. O. (1977). Rabies in a laboratory worker - New York. *Morbidity and Mortality Weekly Report* **26**, 183-184.

Tordo, N. (1996). Characteristics and molecular biology of the rabies virus. In: *Laboratory Techniques in Rabies* (F.-X. Meslin, M.M. Kaplan and H. Koprowski, eds). pp. 28-51. Geneva: World Health Organization.

Tordo, N., Poch, O., Ermine, A., Keith, G. and Rougeon, F. (1986). Walking along the rabies genome: is the large G-L intergenic region a remnant gene? *Proceedings of the National Academy of Sciences of the United States of America* **83**, 3914-3918.

Tordo, N., Benmansour, A., Calisher, C., Dietzgen R. G., Fang, R. X., Jackson, A. O., Kurath, G., Nadin-Davis, S., Tesh, R. B. and Walker, P. J. (2005). In: *Virus Taxonomy – Classification and Nomenclature of Viruses*. Eighth Report of the International Committee on the Taxonomy of Viruses (C.M. Fauquet, M.A. Mayo, J. Maniloff, U. Desselberger and L.A. Ball, eds). pp. 623-644. Boston: Elsevier Academic Press.

Trimarchi, C. V. and Nadin-Davis, S. A. (2007). Diagnostic evaluation. In: *Rabies* (A.C. Jackson and W.H. Wunner, eds.). pp. 411-469. London: Elsevier Academic Press.

Tsiang, H. (1988). Interactions of rabies virus and host cells. In: *Rabies* (J.B. Campbell and K.M. Charlton, eds). pp. 67-100. Boston: Kluwer Academic Publishers.

Tuffereau, C. and Martinet-Edelist, C. (1985). Effects of rabies infection on the metabolism of the host-cell: does inhibition of cellular RNA synthesis take place? *Comptes rendus de l'Academie des sciences, Série III, Sciences de la vie* **300**, 597-600.

Tuffereau, C., Leblois, H., Bénéjean, J., Coulon, P., Lafay, F. and Flamand, A. (1989). Arginine or lysine in position 333 of ERA and CVS glycoprotein is necessary for rabies virulence in adult mice. *Virology* **172**, 206-212.

Tuffereau, C., Bénéjean, J., Blondel, D., Kieffer, B. and Flamand, A. (1998). Low-affinity nerve-growth factor receptor (P75NTR) can serve as a receptor for rabies virus. *The EMBO Journal* **17**, 7250-7259.

Tuffereau, C., Schmidt, K., Langevin, C., Lafay, F., Dechant, G. and Koltzenburg, M. (2007). The rabies virus glycoprotein receptor p75 is not essential for rabies virus infection. *Journal of Virology* **81**, 13622-13630.

Ugolini, G. (1995). Specificity of rabies virus as a transneuronal tracer of motor networks: Transfer from hypoglossal motor neurons to connected second-order and higher order central nervous system cell groups. *The Journal of Comparative Neurology* **356**, 457-480.

Van Zyl, N., Markotter, W. and Nel, L. H. (2010). Evolutionary history of African mongoose rabies. *Virus Research* **150**, 93-102.

Von Teichman, B. F., Thomson, G. R., Meredith, C. D. and Nel, L. H. (1995). Molecular epidemiology of rabies virus in South Africa: evidence for two distinct virus groups. *Journal of General Virology* **76**, 73-82.

Wang, Z. W., Sarmiento, L., Wang, Y., Li, X., Dhingra, V., Tsegai, T., Jiang, B. and Fu, Z. F. (2005). Attenuated rabies virus activates, while pathogenic rabies virus evades, the host innate immune responses in the central nervous system. *Journal of Virology* **79**, 12554-12565.

Warrell, M. J. and Warrell, D. A. (2004). Rabies and other lyssavirus diseases. *The Lancet* **363**, 959-969.

Webster, W. A. and Casey, G. A. (1996). Virus isolation in neuroblastoma cell culture. In: *Laboratory Techniques in Rabies* (F.-X. Meslin, M.M. Kaplan and H. Koprowski, eds). pp. 96-104. Geneva: World Health Organization.

Weyer, J., Szmyd-Potapczuk, A. V., Blumberg, L. H., Leman, P.A., Markotter, W., Swanepoel, R., Paweska, J. T. and Nel, L. H. (2010). Epidemiology of human rabies in South Africa, 1983-2007. *Virus Research* **155**, 283-290.

Whelan, S. P. J. and Wertz, G. W. (1999). Regulation of RNA synthesis by the genomic termini of vesicular stomatitis virus: Identification of distinct sequences essential for transcription but not replication. *Journal of Virology* **73**, 297-306.

Wiktor, T. J. and Koprowski, H. (1978). Monoclonal antibodies against rabies virus produced by somatic cell hybridization: detection of antigenic variants. *Proceedings of the National Academy of Sciences of the United States of America* **75**, 3938-3942.

Wilkinson, L. (1988). Understanding the nature of rabies: A historical perspective. In: *Rabies* (J.B. Campbell and K.M. Charlton, eds). pp. 1-23. Boston: Kluwer Academic Publishers.

Wilkinson, L. (2002). History. In: *Rabies* (A.C. Jackson and W.H. Wunner, eds). pp. 1-22. San Diego: Academic Press.

Winkler, W. G., Fashinell, T. R., Leffingwell, L., Howard, P. and Conomy, J. P. (1973). Airborne rabies transmission in a laboratory worker. *The Journal of the American Medical Association* **226**, 1219-1221.

Wirblich, C., Tan, G. S., Papaneri, A., Godlewski, P. J., Orenstein, J. M., Harty, R. N. and Schnell, M. J. (2008). PPEY motif within the rabies virus (RV) matrix protein is essential for efficient virion release and RV pathogenicity. *Journal of Virology* **82**, 9730-9738.

Woods, D. F. and Bryant, P. J. (1993). ZO-1, DlgA and PSD-95/SAP90: homologous proteins in tight, septate and synaptic cell junctions. *Mechanisms of development* **44**, 85-89.

Wunner, W. H. (1991). The chemical composition and molecular structure of rabies viruses. In: *The Natural History of Rabies* (G.M. Baer, ed.). pp. 31-67. Boca Raton: CRC Press.

Wunner, W. H. (2007). Rabies virus. In: *Rabies* (A.C. Jackson and W.H. Wunner, eds). pp. 23-68. London: Elsevier Academic Press.

Wunner, W. H., Larson, J. K., Dietzschold, B. and Smith, C. L. (1988). The molecular biology of rabies viruses. *Clinical Infectious Diseases* **10** (supplement 4), S771-S784.

Yan, X., Prosnik, M., Curtis, M. T., Weiss, M. L., Faber, M., Dietzschold, B. and Fu, Z. F. (2001). Silver-haired bat rabies virus variant does not induce apoptosis in the brain of experimentally infected mice. *Journal of Neurovirology* **7**, 518-527.

Yan, X., Mohankumar, P. S., Dietzschold, B., Schnell, M. J. and Fu, Z. F. (2002). The rabies virus glycoprotein determines the distribution of different rabies virus strains in the brain. *Journal of Neurovirology* **8**, 345-352.

Zulu, G. C., Sabeta, C. T. and Nel, L. H. (2009). Molecular epidemiology of rabies: Focus on domestic dogs (*Canis familiaris*) and black-backed jackals (*Canis mesomelas*) from northern South Africa. *Virus Research* **140**, 71-78.

Zumpt, I. (1982). The yellow mongoose as a rabies vector of the central plateau of South Africa (*Cynictis penicillata*). *South African Journal of Science* **78**, 417-418.

Other references

Patent document

Prehaud, C., Lafon, M. and Schnell, M. J. (2010). Neuron generation, regeneration and protection. World Intellectual Property Organization, WO 2010/116258 A1.

Websites

<http://www.ictvonline.org> (International Committee on Taxonomy of viruses)

<http://imagej.nih.gov/ij> (ImageJ 1.44p)

APPENDICES

Appendix 1. Multiple sequence alignment of a 1518-bp nucleotide sequence region of the G-protein gene and South African rabies isolates; mongoose (22/07), canid (143/07) and spill over (198/08). The dots indicate positions of identity amongst the aligned sequences and reference sequences (ERA, GenBank Acc No. AF406693).

ERA	AAA	TTC	CCT	ATT	TAC	ACG	ATA	CCA	GAC	AAG	CTT	GGT	CCC	TGG	AGC	CCG
mongoose	..GCTT	..A
canid	.G.CAA
spill overCT	..A
ERA	ATT	GAC	ATA	CAT	CAC	CTC	AGC	TGC	CCA	AAC	AAT	TTG	ATA	GTG	GAG	GAC
mongooseTTT	..TA	G.C
canidT	G.T
spill overTTT	..TA	G.CT
ERA	GAA	GGA	TGC	ACC	AAC	CTG	TCA	GGG	TTC	TCC	TAC	ATG	GAA	CTT	AAA	GTT
mongoose	..GAATCG
canidC
spill overAAG
ERA	GGA	TAC	ATC	TTA	GCC	ATA	AAA	ATG	AAC	GGG	TTC	ACT	TGC	ACA	GGC	GTT
mongooseC.G.	G.A	.GTT	..G	..TT	..G
canidC.G	G..A
spill overC.	G.A	..TT	..G	..TT	..G
ERA	GTG	ACG	GAG	GCT	GAA	ACC	TAC	ACT	AAC	TTC	GTT	GGT	TAT	GTC	ACA	ACC
mongooseAATT	..CC	...
canidTT	..AC	...
spill overAATT	..C	..CT	...
ERA	ACG	TTC	AAA	AGA	AAG	CAT	TTC	CGC	CCA	ACA	CCA	GAT	GCA	TGT	AGA	GCC
mongoose	..AGTGGCT
canidGTC
spill over	..AG.TG	...	T.GTT
ERA	GCG	TAC	AAC	TGG	AAG	ATG	GCC	GGT	GAC	CCC	AGA	TAT	GAA	GAG	TCT	CTA
mongoose	C..TAG
canid	..A
spill over	..A	...	C..TAG
ERA	CAC	AAT	CCG	TAC	CCT	GAC	TAC	CGC	TGG	CTT	CGA	ACT	GTA	AAA	ACC	ACC
mongooseAA.C
canidA.
spill overA.
ERA	AAG	GAG	TCT	CTC	GTT	ATC	ATA	TCT	CCA	AGT	GTG	GCA	GAT	TTG	GAC	CCA

mongooseA	..C	...	A.CC	..T
canidCG
spill overA	..CCC	..TG
ERA	TAT	GAC	AGA	TCC	CTT	CAC	TCG	AGG	GTC	TTC	CCT	AGC	GGG	AAG	TGC	TCA
mongooseA.	..T	..CAT	...	T..	.A.
canidA.C
spill overA.A.
ERA	GGA	GTA	GCG	GTG	TCT	TCT	ACC	TAC	TGC	TCC	ACT	AAC	CAC	GAT	TAC	ACC
mongoose	..G	T..	A.T	..A	..CTG
canid	...	A..	A..TA
spill over	..G	C..	A.T	..A	..C	..CGT
ERA	ATT	TGG	ATG	CCC	GAG	AAT	CCG	AGA	CTA	GGG	ATG	TCT	TGT	GAC	ATT	TTT
mongoose	..CTGCAC	...
canidT	..AGC.CC	...
spill over	..CTGCAC	...
ERA	ACC	AAT	AGT	AGA	GGG	AAG	AGA	GTA	TCC	AAA	GGG	AGT	GAG	ACT	TGC	GGC
mongooseCC.G.A.	A.AA
canid	G..C.	..T	G..	A..	..C
spill overCC.G.	..A	.A.	A.AA
ERA	TTT	GTA	GAT	GAA	AGA	GGC	CTA	TAT	AAG	TCT	TTA	AAA	GGA	GCA	TGC	AAA
mongoose	..C	..G	T.G	C..G	..T	...
canidG	C..	..G
spill over	..C	..G	T.G	C.....
ERA	CTC	AAG	TTA	TGT	GGA	GTT	CTA	GGA	CTT	AGA	CTT	ATG	GAT	GGA	ACA	TGG
mongooseAGTGTG	...
canidCC
spill overAGTT	..C
ERA	GTC	GCG	ATG	CAA	ACA	TCA	AAT	GAA	ACC	AAA	TGG	TGC	CCT	CCC	GAT	CAG
mongoose	..T	..AG	G.CC	..T
canid	G..	..GT	..C	..T	..C	...
spill overAG	..G	G.CC	..T
ERA	TTG	GTG	AAC	CTG	CAC	GAC	TTT	CGC	TCA	GAC	GAA	ATT	GAG	CAC	CTT	GTT
mongooseAA	..TCGA	..T	..C	...
canidA	..T	A.AG	..TT
spill overA	..T	..A	..TCG	..C	..A	..T	..C	...
ERA	GTA	GAG	GAG	TTG	GTC	AGG	AAG	AGA	GAG	GAG	TGT	CTG	GAT	GCA	CTA	GAG
mongoose	..GA.	..A	T..	...
canid	..GA	..T	.A.	..A
spill over	..GA.	..A	T..	...

ERA	TCC	ATC	ATG	ACA	ACC	AAG	TCA	GTG	AGT	TTC	AGA	CGT	CTC	AGT	CAT	TTA
mongooseCC	..G
canidCC	..G
spill overCC	..G
ERA	AGA	AAA	CTT	GTC	CCT	GGG	TTT	GGA	AAA	GCA	TAT	ACC	ATA	TTC	AAC	AAG
mongooseC	..A	..CCA
canidCC
spill overCCA
ERA	ACC	TTG	ATG	GAA	GCC	GAT	GCT	CAC	TAC	AAG	TCA	GTC	AGA	ACT	TGG	AAT
mongoose	A.T	C.G	..C	...	G..
canidG	..TG	...	C.G
spill overTG	A..	C.G	..C	...	G..	...
ERA	GAG	ATC	CTC	CCT	TCA	AAA	GGG	TGT	TTA	AGA	GTT	GGG	GGG	AGG	TGT	CAT
mongooseT	G..	..CG	..GAC
canid	A..	..CA
spill over	G..	..CGG	..GA
ERA	CCT	CAT	GTG	AAC	GGG	GTG	TTT	TTC	AAT	GGT	ATA	ATA	TTA	GGA	CCT	GAC
mongoose	..GTAC	C..	..G	T..	..T
canid	..CACG	..C	...
spill over	..GA	..TC	C..	..G	T..	..T
ERA	GGC	AAT	GTC	TTA	ATC	CCA	GAG	ATG	CAA	TCA	TCC	CTC	CTC	CAG	CAA	CAT
mongoose	...	C..	..TC
canid	...	C..	..T	C.GCT
spill over	...	C..	..TG
ERA	ATG	GAG	TTG	TTG	GAA	TCC	TCG	GTT	ATC	CCC	CTT	GTG	CAC	CCC	CTG	GCA
mongoose	G..	..A	C..	C..A	...	G.T	...	T.G	A..T	T.A	...
canidAATG	A..T
spill over	..A	C..A	...	G.T	...	T.G	A..T	T.A	...
ERA	GAC	CCG	TCT	ACC	GTT	TTC	AAG	GAC	GGT	GAC	GAG	GCT	GAG	GAT	TTT	GTT
mongooseA	..CA	A.T	..AA
canidC	..ATA
spill overA	..CA	A.T	..AA
ERA	GAA	GTT	CAC	CTT	CCC	GAT	GTG	CAC	AAT	CAG	GTC	TCA	GGA	GTT	GAC	TTG
mongoose	..GCAGG	C..
canid	..GTAG	..G	C.A
spill over	..GCAAAA	..AG	C..
ERA	GGT	CTC	CCG	AAC	TGG	GGG	AAG	TAT	GTA	TTA	CTG	AGT	GCA	GGG	GCC	CTG
mongooseAA	.G.	...	A.T	C..	G..A
canidA	...	A..	A..	...
spill overT	..AA	...	A.T	C..	G..A

ERA ACT GCC TTG ATG TTG ATA ATT TTC CTG ATG ACA TGT TGT AGA AGA GTC
 mongoose .T.C. .C.A T.. ..CCC ...
 canid .T.T ..ACCCC ...
 spill over .T.AC. ... C.. ..A ..A ..C ..C ..CC ...

ERA AAT CGA TCA GAA CCT ACG CAA CTC AAT CTC AGA GGG ACA GGG AGG GAG
 mongoose C.. ... C..C .AAA. CGCA. AA.A. ... A..
 canid C.. ..G T.. ..T G.. .G. .G. ... G..CC ...
 spill over C.. ... C..C .A.A. CTCCCC ...

ERA GTG TCA GTC ACT CCC CAA AGC GGG AAG ATC ATA TCT TCA TGG GAA TCA
 mongoose ... G..C T..A ..A GC.CCG ...
 canidG T..A ... G..CCG ...
 spill over ... G.GC T..A ..A GC.CCG ...

ERA CAC AAG AGT GGG GGT GAG ACC AGA CTG TGA
 mongoose T..ACAG ..AAA ...
 canid T.T ..AT ... T.. .A.
 spill over T..ACAA ...

Appendix 2. Multiple sequence alignment of a 503 amino acid region of the G protein of South African rabies isolates; mongoose (22/07), canid (143/07) and spill over (198/08). The dots indicate identical positions amongst the aligned sequences and reference sequences (ERA, GenBank Acc No. AF406693).

```

ERA      K F P I Y T I P D K L G P W S P I D I H H L S C P N N L I V E D E G C T N L S G F S Y M E L K V G Y
mongoose . . . . . V . . . . .
canid    R . . . . . V . . . . .
spill over . . . . . V . . . . .

ERA      I L A I K M N G F T C T G V V T E A E T Y T N F V G Y V T T T F K R K H F R P T P D A C R A A Y N W
mongoose . S . . R V S . . . . . H .
canid    . S . . . V . . . . . I . . . . .
spill over . S . . . V . . . . . R . . . . . S . . . . . H .

ERA      K M A G D P R Y E E S L H N P Y P D Y R W L R T V K T T K E S L V I I S P S V A D L D P Y D R S L H
mongoose . . . . . H . . . . . I . . . . . K . . . .
canid    . . . . . H . . . . . K . . . . .
spill over . . . . . H . . . . . K . . . . .

ERA      S R V F P S G K C S G V A V S S T Y C S T N H D Y T I W M P E N P R L G M S C D I F T N S R G K R V
mongoose . . . . S N . . . . L T . . . . . T . . . . . A
canid    . . . . . I T . . . . F . . . . . T . . . . . A . . . . . A
spill over . . . . . N . . . . L T . . . . . T . . . . . A

ERA      S K G S E T C G F V D E R G L Y K S L K G A C K L K L C G V L G L R L M D G T W V A M Q T S N E T K
mongoose . R . N K . . . . . I . . . . . D . . . .
canid    . . . G K . . . . . D . . . . .
spill over . R . N K . . . . . I . . . . . D . . . .

ERA      W C P P D Q L V N L H D F R S D E I E H L V V E E L V R K R E E C L D A L E S I M T T K S V S F R R
mongoose . . . . . K . . . . .
canid    . . . . . I . . . . . K . . . . .
spill over . . . . . K . . . . .

ERA      L S H L R K L V P G F G K A Y T I F N K T L M E A D A H Y K S V R T W N E I L P S K G C L R V G G R
mongoose . . . . . I . . . . . D . . . . . V . . . . .
canid    . . . . . I . . . . . I . . . . .
spill over . . . . . I . . . . . D . . . . . V . . . . .

ERA      C H P H V N G V F F N G I I L G P D G N V L I P E M Q S S L L Q Q H M E L L E S S V I P L V H P L A
mongoose . . . . . S . . . . . H . . . . . V . . . . . V . . . . . M . . . .
canid    . . . . . H . . . . . M . . . . .
spill over . . . . . S . . . . . H . . . . . I . . . . . V . . . . . M . . . .

ERA      D P S T V F K D G D E A E D F V E V H L P D V H N Q V S G V D L G L P N W G K Y V L L S A G A L T A
mongoose . . . . . N . . . . . K . . . . . R . I . V . . . . . I .
canid    . . . . . K . . . . . I . . . . . T . I .
spill over . . . . . N . . . . . K . . . . . E . . . . . I . V . . . . . I .

ERA      L M L I I F L M T C C R R V N R S E P T Q L N L R G T G R E V S V T P Q S G K I I S S W E S H K S G
mongoose . . . . T T . . L . . . . H . P . . K . H R . K K . E . K . A . . S . . . . A . . . . . Y . N .
canid    . . . . . P . S . E R S . G . . . . K . . . . S . . . . V . . . . . Y . . . .
spill over . . . . I . T . L . I . . . . H . P . . K . H L . . . . E . K . A . . S . . . . A . . . . . Y . N .

```

ERA G E T R L *
mongoose E . . . M .
canid
spill over M .

Appendix 3. Multiple sequence alignment of delta EC (ectodomain deleted)-South African isolates and laboratory strains (ERA and CVS); delta EC-mongoose, delta EC-canid and delta EC-spill over.

```

canid ΔEC      ATGGTTCCTCAGGCTCTCCTGTTTGTACCCCTTCTGGTTTTTCCATTGTGTTTTGGGGGG
mongoose ΔEC  ATGGTTCCTCAGGCTCTCCTGTTTGTACCCCTTCTGGTTTTTCCATTGTGTTTTGGGGGG
spilloverΔEC  ATGGTTCCTCAGGCTCTCCTGTTTGTACCCCTTCTGGTTTTTCCATTGTGTTTTGGGGGG
ERA ΔEC       ATGGTTCCTCAGGCTCTCCTGTTTGTACCCCTTCTGGTTTTTCCATTGTGTTTTGGGGGG
CVSG ΔEClenti ATGGTTCCTCAGGCTCTCCTGTTTGTACCCCTTCTGGTTTTTCCATTGTGTTTTGGGGGG
*****

```

```

canid ΔEC      AAGTATGTATTACTGAGTGCAGGGGCCCTGACTGCCTTGATGTTGATAATTTTCCTGATG
mongoose ΔEC  AAGTATGTATTACTGAGTGCAGGGGCCCTGACTGCCTTGATGTTGATAATTTTCCTGATG
spilloverΔEC  AAGTATGTATTACTGAGTGCAGGGGCCCTGACTGCCTTGATGTTGATAATTTTCCTGATG
ERA ΔEC       AAGTATGTATTACTGAGTGCAGGGGCCCTGACTGCCTTGATGTTGATAATTTTCCTGATG
CVSG ΔEClenti AAGTATGTATTACTGAGTGCAGGGGCCCTGACTGCCTTGATGTTGATAATTTTCCTGATG
*****

```

```

canid ΔEC      ACATGTTGTAGAAGAGTCAATCGATCAGAACCTACGCAACACAATCTCAGAGGGACAGGG
mongoose ΔEC  ACATGTTGTAGAAGAGTCAATCGATCAGAACCTACGCAACACAATCTCAGAGGGACAGGG
spilloverΔEC  ACATGTTGTAGAAGAGTCAATCGATCAGAACCTACGCAACACAATCTCAGAGGGACAGGG
ERA ΔEC       ACATGTTGTAGAAGAGTCAATCGATCAGAACCTACGCAACACAATCTCAGAGGGACAGGG
CVSG ΔEClenti ACATGTTGTAGAAGAGTCAATCGATCAGAACCTACGCAACACAATCTCAGAGGGACAGGG
*****

```

```

canid ΔEC      AGGGAGGTGTCAGTCACTCCCCAAAGCGGGAAGATCATATCTTCATGGGAATCATAACAAG
mongoose ΔEC  AGGGAGGTGTCAGTCACTCCCCAAAGCGGGAAGATCATATCTTCATGGGAATCATAACAAG
spilloverΔEC  AGGGAGGTGTCAGTCACTCCCCAAAGCGGGAAGATCATATCTTCATGGGAATCATAACAAG
ERA ΔEC       AGGGAGGTGTCAGTCACTCCCCAAAGCGGGAAGATCATATCTTCATGGGAATCACAACAAG
CVSG ΔEClenti AGGGAGGTGTCAGTCACTCCCCAAAGCGGGAAGATCATATCTTCATGGGAATCACAACAAG
*****

```

```

canid ΔEC      AGTGGGGGTCAGACCAGACTGTGA
mongoose ΔEC  AATGGGGAGCAGACCAGAAATGTGA
spilloverΔEC  AATGGGGGTCAGACCAGAAATGTGA
ERA ΔEC       AGTGGGGGTCAGACCAGACTGTGA
CVSG ΔEClenti AGTGGGGGTCAGACCAGACTGTGA
*****

```

Appendix 4. Formula for media used in mutagenesis.

Super optimal broth (S.O.C) medium

Bactotryptone 20 g
Yeast extract 5.0 g
5 M NaCl 2 ml
1 M KCl 2.5 ml
1 M MgCl₂ 10 ml
1 M MgSO₄ 10 ml
1 M Glucose 20 ml
Deionized water 1 liter

Trypticase-Yeast extract-Maltose (T.Y.M) medium

Bactotryptone 20 g
Yeast extract 5.0 g
Glucose 1.0 g
10 mM MgSO₄ (2.46 g, 7H₂O)
NaCl 5.0 g
Deionized water 1 liter

COMMUNICATIONS

Poster presentation

Seo, W., Jenkins, A. and Sabeta, C. The pathogenesis of rabies virus (RABV) in canid strain and mongoose strain in South Africa. The faculty of Veterinary Science, University of Pretoria, South Africa. 2 September 2010.

Seo, W., Jenkins, A., Prehaud, C., Lafon, M. and Sabeta, C. Molecular basis of virulence of typical South African canid and mongoose rabies biotypes. OIE Global Conference on Rabies control: Towards sustainable prevention at the source, Republic of Korea, 7-9 September 2011.

Publications

Article is preparation

Seo, W., Prehaud, C., Khan, Z., Akinbowale, J. Lafon, M. and Sabeta, C. The molecular basis of virulence of typical South African canid and mongoose rabies biotypes. *To be submitted to **Journal of NeuroVirology**.*